Anthelmintic resistance in *Dirofilaria immitis*: Mechanisms and molecular markers

Emily Curry

Institute of Parasitology

McGill University, Montreal Canada

International Cotutelle with Université Toulouse III : Paul Sabatier

December 2022

A thesis submitted to McGill University in partial fulfillment of the requirements of the degree of Doctor of Philosophy

Table of Content

Abstract

Dirofilaria immitis is a parasitic filarial nematode of veterinary importance. It is the causative agent of dirofilariosis, a potentially fatal pulmonary infection of canids and felines. Dirofilariosis can be prevented with macrocyclic lactone (ML)-based chemoprophylaxis. The MLs are potent parasiticides which target the invertebrate specific glutamate gated chloride channels (GluCls). The MLs bind pseudo-irreversibly to the GluCls opening the pore leading to hyperpolarization and paralysis of the neuromuscular system, impacting alimentation, locomotion, and mediation of sensory input and response. The MLs are a class of generally safe drugs and have been used as dirofilariosis chemoprophylaxis since the mid 1980s. Unfortunately, the continuous use of ML-based chemoprophylactics over the last four decades has led to the development of drug resistance. These ML-resistant *D. immitis* isolates are phenotypically and genotypically distinct from the wildtype susceptible populations.

The aim of the thesis was to characterize potential mechanisms and molecular markers of ML resistance in *D. immitis*. For the first objective I developed of an *in vitro* colorimetric enzymatic activity assay based on the concept that MLs act on the microfilariae (mf) by paralyzing the excretory pore muscle, inhibiting the release of enzymes, metabolites, and immunomodulatory molecules. I demonstrated that the secretion of the metabolic enzyme triosephosphate isomerase (TPI) via the excretory-secretory pore (ESP) was unaffected by ivermectin (IVM) exposure in ML-resistant isolates. For the second objective I characterized *D. immitis* P-glycoprotein 11 (*Dim*Pgp-11), a gene strongly linked to the ML-resistant phenotype. I measured the level of genetic polymorphism, constitutive expression, and demonstrated, for the first time, that *Dim*Pgp-11 is strategically located surrounding the ESP in the mf lifestage. Lastly, I assessed the tryptophan catabolism enzyme, kynureninase (*Dim*KYNU-1), a gene with newly identified genetic changes associated with ML resistance. I validated the genetic polymorphism

and measured its potential impact of the constitutive expression of *Dim*KYNU-1 and its downstream product 3-hydroxyanthranilic acid (3HA). Ultimately, the thesis provides a novel perspective on the phenotypic and genotypic consequences of the development of multigenic ML resistance in *D. immitis* for the possible future development of anti-filarial pharmaceuticals.

Abrégé

Dirofilaria immitis est un nématode parasite d'importance en santé vétérinaire. Il est l'agent causal de la dirofilariose, une infection pulmonaire potentiellement mortelle des canidés et des félins. La chimioprophylaxie est à base de lactone macrocyclique anthelminthiques (LM), notamment l'ivermectine autorisée depuis 1987 pour éviter l'infection. Les LM sont de puissants antiparasitaires à large spectre qui ciblent les canaux chlore glutamate-dépendants (GluCl) spécifiques aux invertébrés. Les LM se lient de manière pseudo-irréversible aux GluCl ouvrant le canal, ce qui provoque une hyperpolarisation et une paralysie du système neuromusculaire, altérant des processus vitaux des vers comme l'alimentation, la locomotion et les réponses sensorielles. Malheureusement, l'utilisation continue des LM a conduit au développement d'une chimiorésistance. L'existence des isolats de *D. immitis* résistants aux LM phénotypiquement et génotypiquement distincts des populations sensibles, met en péril l'efficacité des traitements de la dirofilariose.

L'objectif de la thèse était d'étudier les mécanismes et de rechercher les marqueurs moléculaires de la résistance aux LM chez *D. immitis*. Dans un premier temps, j'ai développé un test enzymatique *in vitro* basé sur la notion que les LM en paralysant le muscle des pores excréteurs des microfilaires (mf) inhibent la sécrétion d'enzymes, de métabolites et de molécules immunomodulatrices. J'ai montré que l'excrétion de l'enzyme métabolique triosephoshate isomérase (TPI) par le pore excréteur-sécréteur (ESP) n'est pas affectée par l'exposition à l'ivermectine (IVM) chez les isolats résistants aux LM. Ensuite, j'ai étudié l'impact de la résistance sur la P-glycoprotéine-11 (*Dim*Pgp-11), en détaillant les polymorphismes génétiques, l'expression constitutive, et en montrant pour la première fois la localisation stratégique du transporteur sur les pores sécréteurs / excréteurs chez les mfs. Finalement, j'ai identifié un nouveau gène associé à la résistance aux LM codant pour la kynureninase (*Dim*KYNU-1), une

enzyme du catabolisme de tryptophane. J'ai confirmé le polymorphisme génétique et l'augmentation d'expression constitutive de *Dim*KYNU-1et l'impact de la résistance sur son produit en aval l'acide 3-hydroxyanthranilique (A3H). Ce travail nous permettra de mieux comprendre l'origine de la résistance au LM et d'identifier de nouvelles cibles pour le développement futur de produits anthelminthiques. La thèse offre une nouvelle perspective sur les implications phénotypiques et génotypiques du développement de la résistance multigénique à les LM chez *D. immitis*.

Acknowledgements

I would first like to sincerely thank my supervisors Dr. Roger Prichard (McGill) and Dr. Anne Lespine (UPS) for their continuous patience, guidance, and wisdom over the last five years. I am indebted to you both for the learning opportunities and life experiences I have had as an international cotutelle student. I would also like to acknowledge my committee members. Thank you to Dr. Timothy Geary for your insightful questions and encouragement. Thank you to Dr. Mélanie Alberich for teaching me the ins and outs of *C. elegans* culture and for making me feel so welcome when I arrived in Toulouse. Thank you to the past and present members of the McGill and INTHERES labs for all our conversations and coffee breaks. A particular shout out Kathy Keller, thank you for your support and your knowledge of the McGill billing systems, without your help I would need another five years to finish my PhD. Thank you to all the past and present students, postdocs, and staff of the Institute of Parasitology for making my time at McGill so memorable. I am grateful for the funding I have receive from the Natural Sciences and Engineering Research Council of Canada (NSERC), the Burroughs-Wellcome Collaborative Research Travel award, and the McGill University GREAT and Graduate Mobility awards. I would like to thank my family and friends for their unwavering support and encouraging me to keep going even when it felt like an uphill battle. Lastly, a special thank you to my parents, you have always been my biggest supporters and loudest cheerleaders. I would not be the researcher or person I am today without you.

Contributions to Original Knowledge

I have made the following novel contributions, throughout my PhD, to the understanding of macrocyclic lactone (ML) resistance in the parasitic filarial nematode, *Dirofilaria immitis*, an important parasite in the field of veterinary parasitology and a model for filarial nematodes that infect humans.

1. **Development of a rapid *in vitro* colorimetric enzymatic activity assay to differentiate macrocyclic lactone susceptible and resistant *Dirofilaria immitis* isolates.**

   It is becoming increasingly rare to find *D. immitis* isolates whose ancestors are truly naïve to ML-based chemoprophylaxis in North America. The *in vitro* biological assay I developed in Chapter 2 was designed based on the concept that MLs act on the microfilariae (mf) lifestage by paralyzing the excretory-secretory pore (ESP), inhibiting the release of molecules, including potential immunomodulators. The metabolic enzyme triosephosphate isomerase (TPI) was analyzed due to its abundance in the *D. immitis* secretome. Interestingly, the phenotypic data collected corroborates increasing genotypic evidence of genetically mixed *D. immitis* populations and was consistent with concurrently published genetic analysis of ML resistance. The measurement of enzymatic activity via the excretory secretory pore (ESP) and the *in vitro* triosephosphate isomerase (TPI) colorimetric enzymatic activity assay developed in Chapter 2 may have utility for detecting isolates that remain truly susceptible for use in academic and pharmaceutical research.

2. **Genetic polymorphism, constitutive expression, and tissue localization of *Dirofilaria immitis* P-glycoprotein 11: a putative marker of macrocyclic lactone resistance.**

   The *D. immitis* P-glycoprotein 11 (*Dim*Pgp-11) gene was among the first identified with genetic changes linked to the ML-resistant phenotype; however, its expression and localization have remained unexamined. In Chapter 3, I provide an extensive study on the

genetic polymorphism, constitutive expression, and localization of *Dim*Pgp-11 in the *D. immitis* mf lifestage. The *Dim*Pgp-11 single nucleotide polymorphism (SNP) continued to be associated with ML resistance in USA laboratory-maintained isolates. A link between *Dim*Pgp-11 and ML resistance was further supported by its lower constitutive expression in the ML-resistant JYD-34 isolate. Lastly, I demonstrated for the first time that *Dim*Pgp-11 is strategically located surrounding the ESP where it could play a role in ML efflux.

3. **Genetic polymorphism and differential expression of the integral tryptophan catabolism component kynureninase in *Dirofilaria immitis*.**

   D. immitis kynureninase (*Dim*KYNU-1) is a key component of tryptophan catabolism and a necessary precursor to the biosynthesis of rhodoquinone (RQ), an electron carrier essential to anaerobic metabolism in helminths. In Chapter 4, I describe a new SNP molecular marker on *Dim*KYNU-1. I demonstrated the difference in the frequency of the alternate allele between ML-susceptible and ML-resistant USA laboratory-maintained isolates. A link between the *Dim*KYNU-1 SNP and the altered expression of kynureninase is further corroborated by the differential constitutive expression of *Dim*KYNU-1 and its downstream product 3-hydroxyanthranilic acid (3HA) in *D. immitis* adults. *Dim*KYNU-1 could have importance as a nematode specific biological marker and upstream target for the development of future anti-filarial pharmaceuticals.

Contribution of Authors

The thesis is written by Emily Curry and comprises three original manuscripts: two manuscripts which have been accepted for publication in a peer-reviewed journals and one manuscript in preparation. The candidate is the first author of all three manuscripts. The following authors contributed to one or more of the manuscripts:

Emily Curry (E.C.)

Roger Prichard (R.P.)

Anne Lespine (A.L.)

Cristina Ballesteros (C.B.)

Manuscript 1: Experiments were conceived and designed by E.C. and R.P. Investigation and formal analyses were performed by E.C. The manuscript was written by E.C. and revised by R.P. Both authors read and approved the final manuscript.

Manuscript 2: Experiments were conceived and designed by E.C., R.P., and A.L. Investigation and formal analyses were performed by E.C. The manuscript was written by E.C. and revised by R.P., and A.L. All authors read and approved the final manuscript.

Manuscript 3: Experiments were conceived and designed by E.C., C.B., R.P., and A.L. Investigation and formal analyses were performed by E.C. The manuscript was written by E.C. and revised by C.B., R.P., and A.L. All authors read and approved the final manuscript.

List of Tables

Appendix 1.

List of Figures

Chapter 1.

Chapter 2.

Chapter 3.

List of Abbreviations

AA: Anthranilic acid

A3H: acide 3-hydroxyanthranilique

AbD: Antibody diluent

BAM: Binary Alignment

BP: base pair

BSC: Biological safety cabinet

cDNA: Complementary DNA

***Cel*Pgp-11:** *Caenorhabditis elegans* P-glycoprotein 11

CFIA: Canadian Food Inspection Agency

***Con*Pgp-11:** *Cooperia oncophora* P-glycoprotein 11

ddPCR: Droplet digital PCR

***Dim*Actin:** *Dirofilaria immitis* Actin

***Dim*amfd:** arylformamidase

***Dim*GAPDH:** *Dirofilaria immitis* GAPDH

***Dim*KYNU-1:** *Dirofilaria immitis* kynureninase

***Dim*nkat:** nematode kynurenine aminotransferase

***Dim*Pgp-3:** *Dirofilaria immitis* P-glycoprotein 3

***Dim*Pgp-10:** *Dirofilaria immitis* P-glycoprotein 10

***Dim*Pgp-11:** *Dirofilaria immitis* P-glycoprotein 11

***Dim*pmp-3:** *Dirofilaria immitis* pmp-3

***Dim*tatn:** *Dirofilaria immitis* tyrosine aminotransferase

***Dim*tph-1:** *Dirofilaria immitis* tryptophan hydrolase

dpi : days post-infection

ELISA: enzyme-linked immunosorbent assay

EMA: European Medicines Agency

ES: excretory-secretory

ESP: Excretory-secretory pore

ETC: Electron transport chain

FDA / CVM: Federal Drug Administration / Center for Veterinary Medicine

FR3: Filariasis Research Reagent Resource Center

gDNA: Genomic DNA

GluCl: Glutamate gated chloride channel

GO: Gene ontology

IFA: immunofluorescence assay.

IVM: Ivermectin

KYN: L-kynurenine

KYNU-1: kynureninase

LM: Lactone macrocylique

LOE: Loss of efficacy

mf: microfilariae

ML: Macrocyclic Lactones

mRNA: messenger RNA

NBD: Nucleotide binding domain

NEB: New England Biolabs

OD: optical density

PBS: Phosphate buffered saline

PBST: phosphate buffered saline with Triton - X 100

PCA: Principal component analysis

***Peq*Pgp-11:** *Parascaris equorum* P-glycoprotein 11

Pgp: P-glycoprotein

qPCR: Quantitative PCR

RQ: Rhodoquinone

SNP: Single nucleotide polymorphism

T_M: Melting temperature

TMB: 3,3',5,5'-Tetramethylbenzidine

TMD: Transmembrane domain

TPI: Triosphosphate Isomerase

UQ: Ubiquinone

3HA: 3-Hydroxyanthranilic acid

3HKYN: 3-Hydroxykynurenine

Chapter 1.

Introduction and Literature Review

Introduction

The filarial parasitic nematode *Dirofilaria immitis* causes dirofilariosis, a potentially fatal pulmonary infection of companion animals, with humans acting as incidental hosts. *Dirofilaria* infections can be prevented with a macrocyclic lactone (ML)-based chemoprophylactic regimen (Prichard 2021). It has recently been confirmed that some *D. immitis* isolates are resistant to MLs and these isolates are genetically distinct from wildtype populations (Bourguinat et al. 2011a, 2011b, 2011c, Pulaski et al. 2014, Wolstenholme et al. 2015, Ballesteros et al. 2018, Prichard 2021). Genetic markers which can differentiate ML-susceptible and ML-resistant *D. immitis* isolates have been identified. Despite being strongly link to the ML-resistant phenotype many of these genetic markers have gone uncharacterized. Additionally, there is a need for *in vitro* phenotypic assays to differentiate these ML-susceptible and ML-resistant populations. Phenotypic analysis and characterization of these genetic markers is required to better understand the complex interplay of phenotype and genotype in the development and modulation of multigenic ML resistance in *D. immitis*.

Dirofilaria immitis

Dirofilaria immitis is a parasitic filarial nematode which belongs to the order *Spirurida*, class *Chromadorea*, and family *Onchocercidae*. It is closely related to the human parasitic filarial nematodes *Brugia malayi* and *Onchocerca volvulus*. *D. immitis* is a dioecious species. The adult males range from 12 – 20 cm in length and 0.7 – 0.9 mm in diameter, with a coiled posterior end. The females range from 25 – 31 cm in length and 1.0 – 1.3 mm in diameter (Platzer 2009). *D. immitis* is predominantly found in warm or sub-tropic environments, such as the southeastern

USA and the Mediterranean (Genchi et al. 2005, Pulaski et al. 2014, Genchi and Kramer, 2020). The prevalence and geographic distribution of *D. immitis* is expanding, likely the result of increased temperatures due to climate change and increased movement of companion animals across borders. This allows *Dirofilaria* infections to encroach on regions previously untouched by naturally occurring infections (Genchi et al. 2005, Traversa et al. 2010, Genchi and Kramer, 2020, Jacobson et al. 2020, Norman et al. 2020).

***Dirofilaria immitis* lifecycle**

D. immitis undergoes an indirect lifecycle requiring two hosts: an invertebrate mosquito vector belonging to the genus *Culex*, *Aedes*, *Psorophora*, *Mansonia* or *Anopheles*; and a mammalian definitive host (Bowman and Atkins, 2009). The mosquito vector becomes infected when it takes a blood meal from a microfilaremic host (Figure 1). The microfilariae (mf) migrate from the mosquito midgut to the Malpighian tubule within 24 hours of ingestion (McCall et al. 2008, Simón et al. 2012). The mf molt to the L2 larval stage 8 – 10 days post-infection (dpi). Approximately 2 – 3 days later they undergo a second molt from the L2 to L3 larval stage (McCall et al. 2008, Simón et al. 2012). The L3 larvae perforate the distal tubules and migrate via the haemocoel to the mouthparts of the mosquito, where they become infective (Figure 1) (McCall et al. 2008).

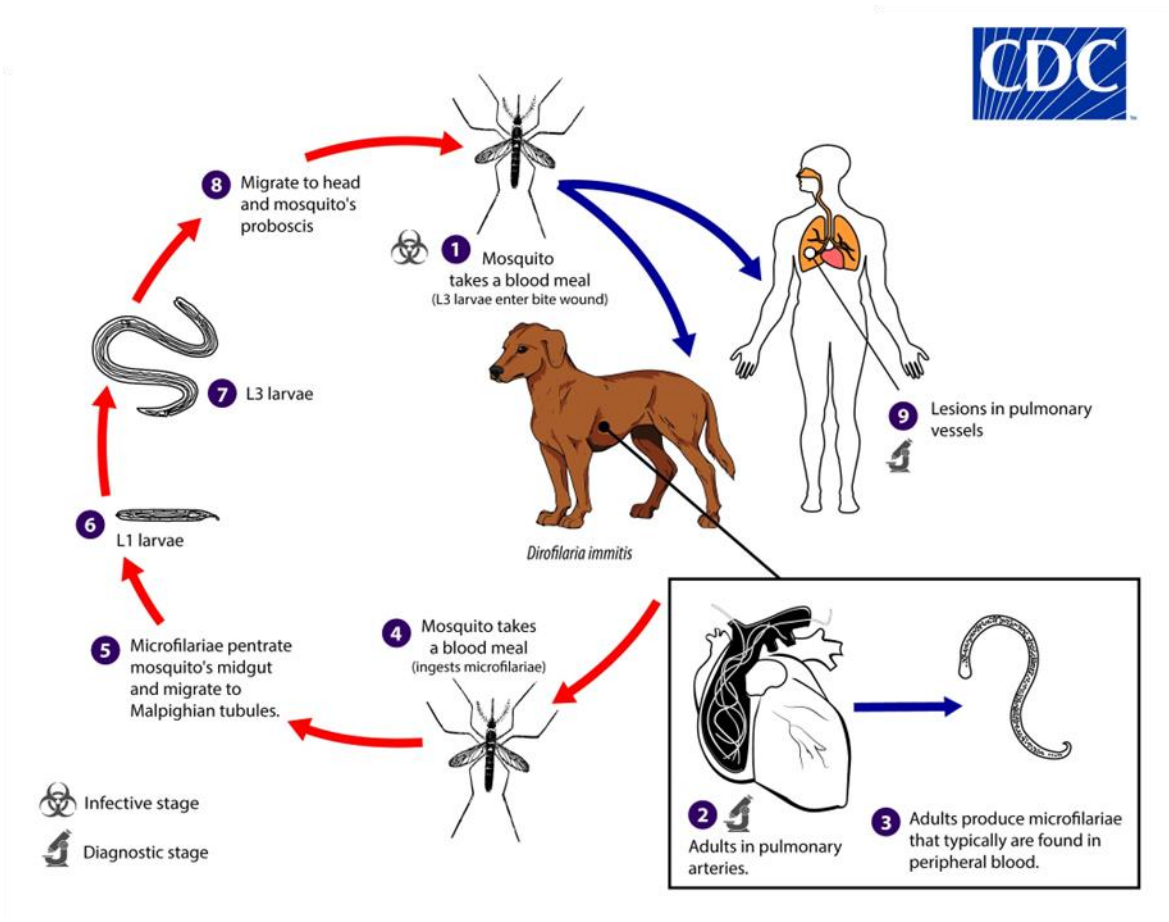

Figure 1 Schematic of *Dirofilaria immitis* lifecycle. Image retrieved from https://www.cdc.gov/parasites/dirofilariasis/biology.html; accessed December 1st, 2022.

The infective L3 larvae are transmitted to the mammalian host via the infected hemolymph deposited in proximity of the bite wound of the mosquito vector's next bloodmeal (Manfredi et al. 2007, Simón et al. 2012). The L3 larvae penetrate the skin through the bite wound and migrate from the subcutaneous tissue to the muscle. The L3 molt to the L4 larval stage within three dpi (McCall et al. 2008). The L4 larvae molt into the pre-adult stage between 50 – 70 dpi. The pre-adults migrate from the muscular tissues and thoracic / abdominal cavities to pulmonary arteries between 70 – 85 dpi (Manfredi et al. 2007). The adults reach sexual maturity within 120 dpi and the adult females will begin producing the bloodborne mf within 6

– 9 months post infection (Simón et al. 2012). The mf travel throughout the circulatory system where they can be picked up by a competent mosquito vector, continuing the lifecycle (Figure 1).

Clinical presentation of dirofilariosis

The clinical presentation of dirofilariosis is chronic and varied based on the burden of infection. Animals with dirofilariosis are often asymptomatic in the pre-patent stages of infection or in instances of low adult worm burden (McCall et al. 2008, Simón et al. 2012). The symptoms of a patent infection are the result of the colonization of the pulmonary artery and right side of the heart by adult *D. immitis* worms. The symptoms include fatigue, shortness of breath, chronic cough, dyspnea, cachexia, and Caval syndrome (AHS 2018). As the disease progresses, additional complications resulting from the pulmonary and cardiac symptoms can develop. These include renal dysfunction, eosinophilic pneumonia, liver failure, congestive splenomegaly, and in rare instances, sudden death (AHS 2018).

Diagnosis of dirofilariosis

Dirofilariosis infections are primarily diagnosed through routine annual screening via tandem antigen and microfilaria tests (Hoch 2006, AHS 2018). The antigen test is composed of enzyme-linked immunosorbent assay (ELISA) and immunochromatographic test systems which detect circulating heartworm antigen produced primarily by the adult females; as a result, these tests cannot detect pre-patent infections (Prichard 2021). The microfilaria test is a simple blood smear used to confirm the presence of the bloodborne mf in instances of patent infections (Hoch 2006, Prichard 2021). In addition to routine annual screening supplemental diagnostic tests can be performed on animals with suspected dirofilariosis infections. The results of the antigen and microfilaria tests can be further corroborated by thoracic radiography and echocardiography.

Dirofilariosis prevention and treatment

The one class of drug approved for the preventative treatment of dirofilariosis infections is the macrocyclic lactones (ML) (Diakou and Prichard 2021, Noack et al. 2021). MLs are typically administered as a monthly chemoprophylactic treatment, or in the case of moxidectin may be depot injected every 6 or 12 months (Prichard 2021). In *D. immitis*, the MLs act against the developing L3 / L4 larvae preventing the establishment of a patent infection.

In cases of ML chemoprophylactic failure and / or owner non-compliance a patent dirofilariosis infection can develop. The ML treatment can be supplemented with doxycycline. Doxycycline targets the Wolbachia endo-symbiotes harboured by all *D. immitis* life-stages. A month-long course of doxycycline can be lethal to L3 / L4 larvae and gradually aid in suppression of the blood circulating mf (Wolstenholme et al. 2015, AHS 2018, Prichard 2021). The only FDA Center for Veterinary Medicine (FDA / CVM) approved adulticidal therapy is melarsomine dihydrochloride. This harsh arsenical treatment is administered via a three-dose protocol of repeated intramuscular injection and requires exercise restrictions to reduce the risk of pulmonary complications caused by the degradation of the adult worms in the heart and lungs (AHS 2018).

Macrocyclic Lactones

The MLs are a large class of amphiphilic compounds with two subclasses: the avermectins and the milbemycins (Lespine, 2013, Wolstenholme et al. 2015). The avermectins consist of abamectin, ivermectin, eprinomectin, doramectin, and selamectin. The milbemycins include moxidectin, milbemycin oxime, and nemadectin (Merola and Eubig 2012).The MLs are broad spectrum parasiticides which are highly potent against endo- and some ectoparasites. They are generally used at low dose rates, e.g., 6 – 12 µg / kg for ivermectin and 3 µg / kg for moxidectin for oral treatment (Bowman et al. 2017, Prichard 2021). In *D. immitis* the MLs target the

developing L3 / L4, at slightly higher dose rates they are also microfilaricidal and can reduce the fecundity of adult parasites (Prichard 2021).

The MLs target the invertebrate specific glutamate gated chloride channels (GluCl). In parasitic filarial nematodes the MLs bind to the GluCl alpha subunits (Wolstenholme and Rogers 2005, Noack et al. 2021). The MLs act as allosteric modulators binding between the membrane spanning domains of adjacent GluCl alpha subunits which push the membrane spanning regions apart opening the channels (Figure 2) (Wolstenholme 2012). This leads to hyperpolarization and paralysis of the neuromuscular system which is vital to controlling alimentation, locomotion, and mediation of sensory input and response (Hibbs and Gouaux 2011, Wolstenholme 2012). However, a direct link between these phenotypes and the ML *in vivo* mode of action in *D. immitis* is hypothetical (Noack et al. 2021).

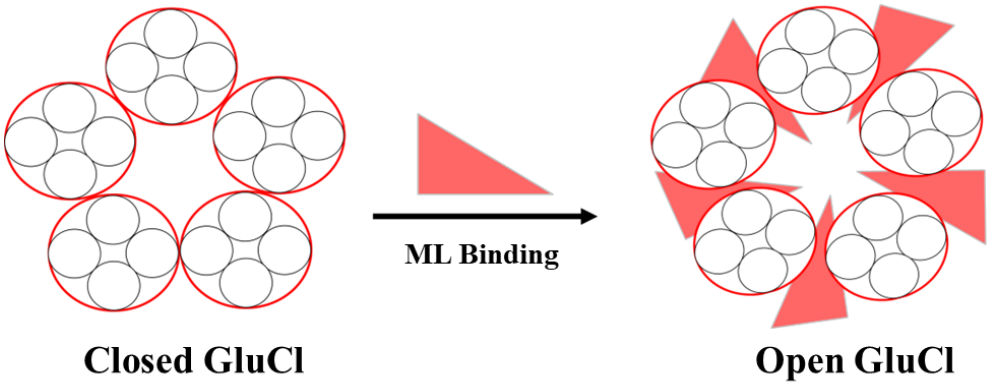

Figure 2 Top view of macrocyclic lactones (red triangles) binding between the membrane-spanning domains of adjacent alpha subunits of a glutamate gated chloride channel which pushes the membrane-spanning regions of the subunit apart to promote the opening of the channel (adapted from Wolstenholme et al. 2012).

Interestingly, the mf of the closely related filarial parasite *B. malayi*, express one GluCl, AVR-14. AVR-14 is localized in the musculature surrounding the excretory-secretory pore

(ESP) (Moreno et al. 2010). In the mf lifestage the ESP likely acts as the main putative target of ML-drug activity. High internal turgor pressure tends to keep the ESP closed and active contraction against this force permits the expulsion of metabolic products in a regulated fashion. The metabolic products secreted by the ESP may produce immunomodulatory effects, allowing the *D. immitis* mf to evade the host's immune system (Hewitson et al. 2014, Vatta et al. 2014, Carithers 2017, Moreno et al. 2021). The analysis of the interaction between the host immune system and secreted ESP products *in vitro* supports this hypothesis (Harischandra et al. 2018, Tritten and Geary 2018, Berrafato et al. 2019). Given the high selectivity of the MLs for the parasite receptors, they are generally safe drugs.

Macrocyclic Lactone Drug Resistance

The first cases of drug loss of efficacy (LOE) in animals on ML-based chemoprophylaxis were brought to the FDA / CVM as early as 1998, eleven years after being placed on the market (Hampshire 2005). The establishment of *Dirofilaria* infections in animals on ML-based chemoprophylaxis can indicate a drug LOE and a potentially ML-resistant population. However, it is difficult to prove unequivocally that ML chemoprophylactics have been administered wholly in compliance with the recommended treatment schedule. A missed treatment or a delay in scheduled treatment can result in a patent infection, unrelated to resistance. In 2011, ML LOE was demonstated both *in vivo* and *in vitro*, confirming the presence of potentially resistant populations circulating in North America (Bourguinat et al. 2011a, 2011c, 2015). The heritability of true ML resistance was subsequently validated by experimentally infecting canines in laboratory settings in 2014 (Pulaski et al. 2014). The confirmartion of true ML resistance led to research to phenotypically and genotypically differentiate these ML-resistant populations from ML-susceptible populations *in vitro*.

Phenotypic assays for macrocyclic lactone resistance

The bloodborne mf are the ideal lifestage for the development an *in vitro* assay to differentiate ML-susceptible and ML-resistant *D. immitis* isolates. The adult worms are usually only available following necropsy. In addition to the limited sample availability, the variation in size, body composition, and sexual maturity makes it difficult to standardize adult *D. immitis* samples. Similarly, the infective L3 larvae can only be obtained by mosquito dissection, which is labour intensive, low yielding, and time consuming. Conversely, the mf are easily accessible and available in large numbers via a minimally invasive blood draw.

The development of an *in vitro* assay requires a measurable phenotype in response to ML exposure. The mf lifestage does not possess a functioning pharynx; moreover, MLs do not appear to effect mf motility. Larval migration and motility assays performed on the mf lifestage *in vitro* could not differentiate ML-susceptible and ML-resistant isolates at a pharmacologically relevant dose rates (Evans et al. 2013, Evans et al. 2017, Maclean et al. 2017). To date, an *in vitro* phenotypic assay which can differentiate *D. immitis* isolates at a pharmacologically relevant ML dose rate is unavailable.

Molecular markers of macrocyclic lactone resistance

The establishment of heritable ML resistance elucidated genetic changes which could differentiate the ML-susceptible and ML-resistant *D. immitis* isolates. Two single nucleotide polymorphism (SNP) molecular markers on an unidentified P-glycoprotein (Pgp) were the first genetic changes associated with ML resistance in *D. immitis* (Bourguinat et al. 2011b, 2011c). Following whole genome analysis, 186 potential SNP molecular markers were identified and associated with the ML-resistant phenotype (Bourguinat et al. 2015).

The top 42 of these potential SNP molecular markers were analyzed via MiSeq sequencing in 10 well-characterized USA laboratory-maintained *D. immitis* isolates (Bourguinat et al. 2017a, 2017b). The top 10 SNP molecular markers which best differentiated the ML-susceptible and ML-resistant phenotypes were clinically validated in 2018 (Ballesteros et al. 2018). Various combinations of the 10 SNP molecular markers were analyzed as potential predictive SNP models. All combinations tested were highly predictive; however, a 2-SNP model (Scaffold nDi.2.2scaf00046; Positions 76278 and 22857) was superior to the other models tested. These SNP markers have since been used to assess clinical samples in Europe and Australia (Lau et al. 2021, Curry et al. 2022a, Power 2022). Four of the top 10 SNP markers: SNPs 1, 2, 3, and 7, have been further validated through the development of ddPCR diagnostic assays (Ballesteros et al. 2018, Kumar et al. forthcoming). The clinical validation of these SNP markers provided the first genetic tests to differentiate between ML-resistant infections and cases of opportunistic infections or owner non-compliance.

***Dirofilaria immitis* P-glycoprotein 11**

Pgps are ATP dependant efflux pumps with broad substrate specificity and are known for their involvement in ML pharmacology. The MLs bind with high affinity to the Pgp hydrophobic binding pocket, the first in a series of events which transport the MLs through the lipid bilayer, out of the cell and the organism (Figure 3) (Schinkel et al. 1994, Xu et al. 1998, Lespine et al. 2007, 2008, 2012, 2013, David et al. 2016, 2018). Genetic changes impacting the sequence and expression of Pgps have been identified as a relevant factor contributing to lower ML efficacy and the development of ML resistance (De Graef et al. 2013, Demeler et al. 2013, Janssen et al. 2013, Ménez et al. 2016, Raza et al. 2016, Prichard and Geary 2019).

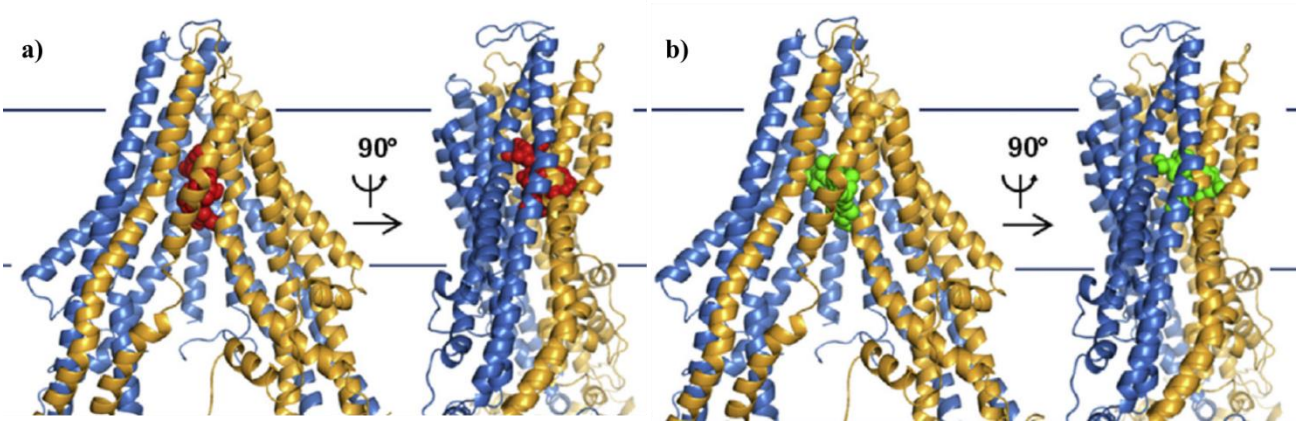

Figure 3 *In silico* model of the structure-affinity relationship of ML-drug a) ivermectin (red spheres) and b) moxidectin (green spheres) binding to the hydrophobic binding pocket of Caenorhabditis *elegans* P-glycoprotein 1 (blue ribbon: N-term, yellow ribbon: C-term) (David et al. 2016).

Whole genome analysis determined that *D. immitis* possesses three full length Pgps: P-glycoprotein 3 (*Dim*Pgp-3), P-glycoprotein 10 (*Dim*Pgp-10), and P-glycoprotein 11 (*Dim*Pgp-11) (Bourguinat et al. 2016). A comparable number of Pgps compared to the closely related *B. malayi* (3 Pgps) and *Onchocerca volvulus* (2 Pgps); however, significantly fewer compared to *Caenorhabditis elegans* (15 Pgps) or *Haemonchus contortus* (10 Pgps) (Issouf et al. 2014, Bourguinat et al. 2016, Doyle et al. 2017, Prichard and Geary 2019, Langeland et al. 2021). The genetic changes first isolated on an unidentified Pgp were located on the *Dim*Pgp-11 gene (Bourguinat et al. 2011c). Notably, P-glycoprotein 11 (Pgp-11) has been linked to the development of ML resistance in the model organism *Caenorhabditis elegans* and parasitic filarial nematodes of veterinary importance.

In *C. elegans*, P-glycoprotein 11 (*Cel*Pgp-11) is strategically located within the intestine and surrounding the ESP (Zhao et al. 2004, Hunt-Newbury et al. 2007, Spencer et al. 2011). ML-resistant *C. elegans* isolates constitutively overexpress several genes involved in xenobiotic

metabolism and transport, including *Cel*Pgp-11 (James and Davey, 2009, Ménez et al. 2016). Adults of the ML-resistant *Con*IVR08 isolate of *Cooperia oncophora*, the parasitic intestinal nematode of cattle, upregulate P-glycoprotein 11 (*Con*Pgp-11) 3 to 5 – fold *in vivo* and 4 – fold *in vitro* compared to the ML-susceptible *Con*IVSus isolate when both are exposed to ivermectin (IVM) (De Graef et al. 2013). In jirds, treatment with the Pgp inhibitor, verapamil, restores IVM sensitivity in ML-resistant *H. contortus* and *C. oncophora* isolates (Molento and Prichard 1999, Molento and Prichard 2001, Demeler et al. 2013). The parasitic intestinal nematode of equines, *Parascaris spp.*, also demonstrates genetic variations on P-glycoprotein 11 (*Peq*Pgp-11). Three SNPs identified via SeqDoc analyses result in missense mutations of the second transmembrane domain of *Peq*Pgp-11 which correlated with reduced ML sensitivity (Janssen et al. 2013). The localization, expression levels, and genetic changes on Pgp-11 in these nematodes indicate it is likely playing a functional role in the ML detoxification mechanism and the development of resistance.

The genetic changes on *Dim*Pgp-11 associated with the ML-resistant phenotype were SNP (A11G) and SNP (A618G) (Bourguinat et al. 2011b). The SNP (A11G) is located in a coding region and confers an amino acid change from lysine to arginine at position 1203 within the second nucleotide binding domain (NBD) (Figure 4). This change introduces a basic polar group prior to the ATP binding domain (Mani et al. 2017). Analogous changes in the second NBD have been shown to modulate ATP turnover and transport activity in the mammalian transporter homolog (Verhalen et al. 2017). The SNP (A618G) is located in a non-coding region.

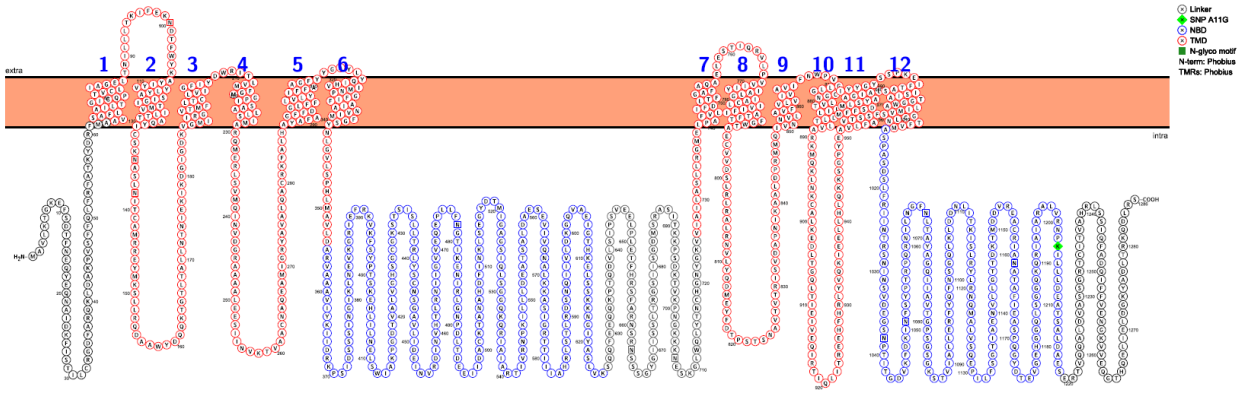

Figure 4 Two-dimensional structure of *Dirofilaria immitis* P-glycoprotein 11. The sequence of the transmembrane domains (TMDs), TMD1 (residues 64 – 354) and TMD2 (residues 726 – 1012) are framed in red. The nucleotide binding domains (NBDs), NBD1 (residues 355 – 625) and NBD2 (residues 1013 – 1218), are framed in blue. The linker region is framed in grey (626 – 725). Putative N-glycosylation motifs (Asn 100, 134, 138, 478, 663, 706, 1051, 1067, 1161) are highlighted in dark green. The SNP (A11G) in the second NBD is highlighted in a light green diamond. Visualization prepared using the Protter interactive protein visualization tool.

The two SNPs were combined for diplotypic analysis and known as the GG – GG genotype. The *Dim*Pgp-11 GG – GG genotype helped validate the heritability of true ML resistance in 2014 and was subsequently patented as a marker of ML resistance in 2015 (Pulaski et al. 2014, Patent WO2011120165A1). The SNP (A11G) was also among the top 10 molecular markers of ML resistance clinically validated in 2018 (Ballesteros et al. 2018).

Dirofilaria immitis Kynureninase

A previously unknown SNP molecular markers was identified in USA clinical samples during the validation of the top 10 SNP molecular markers in 2018 (Ballesteros et al. unpublished). The new SNP molecular marker was located on the *D. immitis* kynureninase (*Dim*KYNU-1) gene.

Kynureninase (KYNU-1) is a PLP-dependant enzyme and a member of the aminotransferase superfamily (Phillips 2014). It is found within the tryptophan catabolism L-

kynurenine (KYN) pathway and catalyzes the synthesis of anthranilic acid (AA) and 3-hydroxyanthranilic acid (3HA) from KYN and 3-hydroxykynurenine (3HKYN) respectively. The KYN pathway produces a number of metabolites and immunomodulators with important biological effects such as quinolinic acid, picolinic acid, cinnabarinic acid and kynurenic acid.

KYNU-1 is also a precursor to the biosynthesis of rhodoquinone (RQ) in eukaryotes. RQ is the electron carrier of an alternative form of anaerobic metabolism unique to helminths, including *D. immits*, molluscs, and annelids (Jaffe and Doremus 1970, Köhler 1991, Van Hellemond et al. 1995, Oliveira and Oliveira, 2002, Müller et al. 2012, Bryant, 2018, Buceta et al. 2019, Salinas et al. 2020). RQ is structurally similar to ubiquinone (UQ); however, it differs due to the presence of an amine group at position 2 on the quinone ring. The KYNU-1 downstream product 3HA provides the amine group to the RQ quinone ring (Buceta et al. 2019, Del Borrello et al. 2019, Salinas et al. 2020). The presence of the amine group gives RQ a lower redox potential (-63 mV) compared to UQ (110 mV). The lower redox potential of RQ creates the correct electro-potential needed to drive the reverse reactions of anaerobic metabolism (Figure 5**)** (Erabi et al. 1976, Unden and Bongaerts 1997).

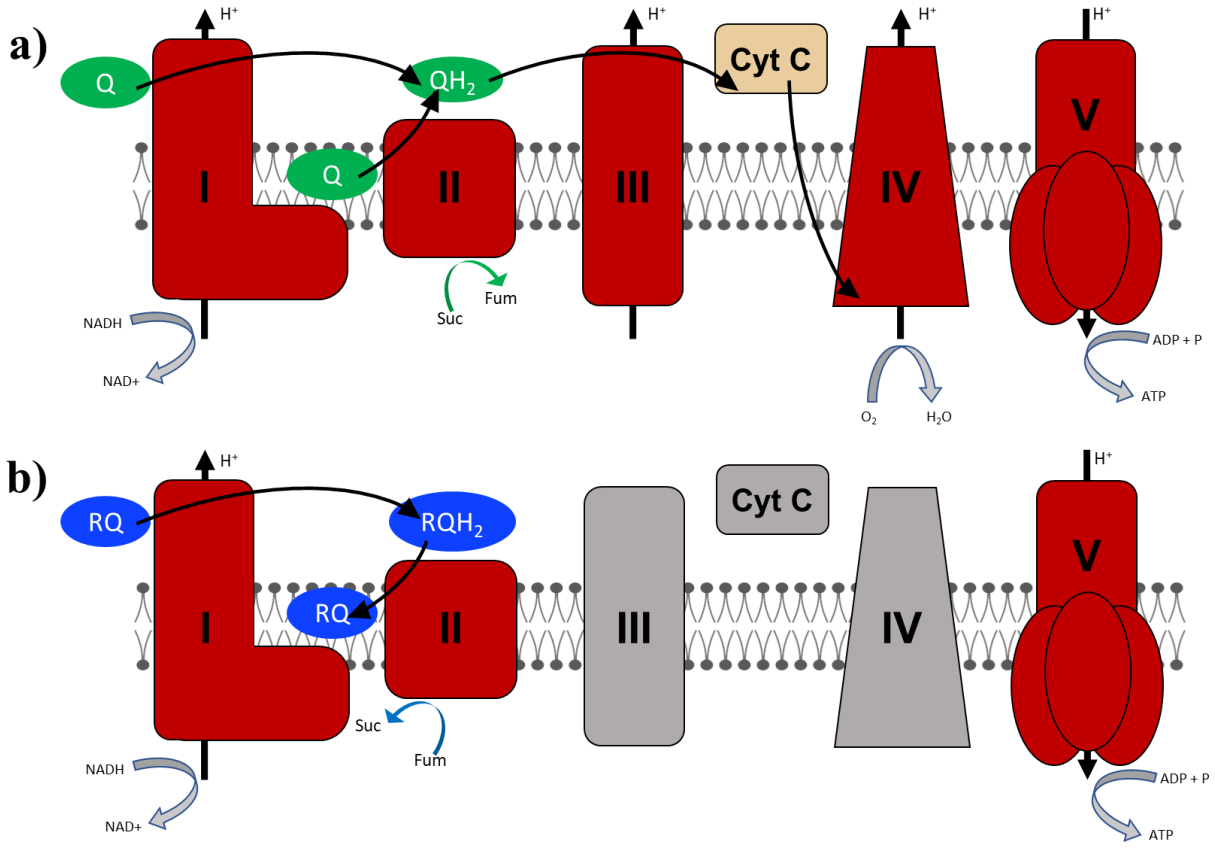

Figure 5 The mitochondrial electron transport chain in a) aerobic conditions and b) anaerobic conditions (Adapted from Buceta et al. 2019)

In RQ-dependant anaerobic metabolism Complex II is reversed from a succinate dehydrogenase and acts as a fumarate reductase (Van Hellemond et al. 1995, Tielens and Van Hellemond 1998, Yamashita et al. 2004, Iwata et al. 2008, Müller et al. 2012). The two electrons required to convert fumarate to succinate are derived from RQ. RQ receives electrons from NADH through Complex I and donate them to fumarate via Complex II as the final electron acceptor (Figure 5).

KYNU-1 has been shown to be essential to RQ biosynthesis. In the model organism *C. elegans* dysreguation of metabolites along the tryptophan catabolism KYN pathway such as tdo-2, kmo-1, coq-5, and coq-6 can leads to reduced RQ production. Knowdown of KYNU-1 result

in abolished RQ production (Buceta et al. 2019, Del Borrello et al. 2019). Genetic changes and differential expression of *Dim*KYNU-1 may have importance as biological marker and upstream target for future development of anti-filarial pharmaceuticals.

Rationale and objectives

Over the last decade research has been undertaken to elucidate genotypic and phenotypic markers which can differentiate *D. immitis* populations with varying ML susceptibility profiles. It has proved difficult to identify an *in vitro* phenotype which can successfully differentiate ML-susceptible and ML-resistant isolates at pharmacologically relevant concentrations. Multiple genes have been identified with genetic changes associated with the ML-resistant phenotype; however, the expression and localization of these genes remain unexamined. Characterizing the phenotypic implications of ML resistance and the effect SNPs have on gene expression is essential to better understand the development and modulation of multigenic ML resistance in *D. immitis*. These considerations led me to the following hypotheses and objectives:

1. **In ML-resistant *D. immitis* an insufficient ML concentration reaches the GluCls surrounding the excretory-secretory pore and they are not adequately activated to inhibit the secretion of immunomodulatory products.**

   The ESP is likely the main putative target of ML-drug activity in the *D. immitis* mf lifestage. I aim to demonstrate a phenotypic variation between ML-susceptible and ML-resistant *D. immitis* mf when both are exposed to IVM concentrations normally effective on susceptible parasites. The change in enzyme activity level acts as an indirect measure of the ML induced inhibition of the ESP. Objective 1 is detailed in Chapter 2.

2. **In ML-resistant *D. immitis* there may be a change in ML transport by *Dim*Pgp-11 reducing the effect of the anthelmintic on the nematode.**

Genetic changes on *Dim*Pgp-11 have been strongly linked to ML-resistant phenotypes; however, its expression and localization in *D. immitis* remain uncharacterized. I aim to (1) measure the level of the *Dim*Pgp-11 SNP genetic polymorphism in USA laboratory-maintained isolates with different ML-susceptibilities, (2) measure the constitutive expression of *Dim*Pgp-11 in USA laboratory-maintained isolates with different ML-susceptibilities, and (3) localize the expression sites of *Dim*Pgp-11 via immunofluorescence assay. Objective 2 is detailed in Chapter 3.

3. **In *D. immitis* a genetic change on nDi.2.2.scaf01096 may be associated with the ML-resistant phenotype and result in the differential expression of kynureninase.**

The genetic changes on the *Dim*KYNU-1 gene could impact gene expression and alter the production of its downstream product 3HA, an integral component of the tryptophan catabolism KYN pathway and the precursor to rhodoquinone biosynthesis. I aim to (1) measure the level of the *Dim*KYNU-1 in USA laboratory-maintained isolates with different ML-susceptibilities; (2) measure the constitutive expression of *Dim*KYNU-1 in the adults of isolates with different ML-susceptibilities; and (3) measure the constitutive expression of the *Dim*KYNU-1 downstream product 3HA in the adults of isolates with different ML-susceptibilities. Objective 3 is detailed in Chapter 4.

Chapter 2.

Development of rapid *in vitro* colorimetric enzymatic activity assay to differentiate macrocyclic lactone susceptible and resistant *Dirofilaria immitis* isolates

Emily Curry[1] and Roger Prichard[1]

[1]Institute of Parasitology, McGill University, Sainte Anne-de-Bellevue, QC, Canada

Published in Veterinary Parasitology (Curry et al. 2022)

Abstract

The filarial parasite *Dirofilaria immitis* causes dirofilariosis, a potentially fatal pulmonary condition in canids and felines. Dirofilariosis can be prevented by treatment with a prophylactic macrocyclic lactone (ML) regimen. Unfortunately, ML-resistant *D. immitis* isolates, genetically distinct from the wildtype population, have been confirmed via molecular markers. DNA-based tests for ML resistance are costly and time-consuming. There lacks a simple and reliable *in vitro* biological test to differentiate *D. immitis* infections resulting from inadequate adherence to recommended prophylaxis regimens from those caused by truly resistant *D. immitis* isolates. The goal of the current study was to develop a minimally invasive rapid diagnostic *in vitro* biological assay to differentiate ML-susceptible from ML-resistant *D. immitis* isolates. The *in vitro* assay was developed based on the concept that MLs act on the microfilariae (mf) by paralyzing the excretory pore muscle, inhibiting the release of molecules, including enzymes, that regulate host immunity. The basis of the *in vitro* diagnostic assay is to assess the effects of ivermectin (IVM) exposure on the secretion of enzymes by the *D. immitis* mf at a concentration that distinguishes the ML-susceptible from ML-resistant isolates. The metabolic enzyme, triosephosphate isomerase (TPI), was chosen due to high abundance in the *D. immitis* secretome. In this study, the *in vitro* TPI enzymatic assay was optimized and tested in eight laboratory-maintained isolates. The ML-susceptible Missouri, Berkeley, and Georgia II isolate; the putative ML-susceptible Georgia III, and Big Head; and the ML-resistant JYD-34, Metairie, and WildCat. We observed mixed results, Missouri and Berkeley had statistically significant decreases in TPI activity following 24 hours *in vitro* IVM exposure. The three resistant isolates, JYD-34, Metairie, and WildCat showed no change in TPI activity following IVM exposure. The susceptible, or putative susceptible Georgia II, Georgia III, and Big Head isolates had a

phenotypic response consistent with ML resistance based on the *in vitro* assay. However, increasing genotypic evidence has presented a mixed genotype for the three isolates, indicating they may be partially selected for ML resistance. The measurement of changes in enzymatic activity and the *in vitro* TPI enzymatic activity assay consequently does not appear to be a reliable detection method for ML resistance but may be useful for identifying fully susceptible isolates.

Keywords: *Dirofilaria immitis*, Macrocyclic Lactones, Resistance, *in vitro* Diagnostic Assay, Triosephosphate Isomerase.

1. Introduction

Dirofilaria immitis is a parasitic filarial nematode. It is the cause of dirofilariosis, a potentially fatal veterinary pulmonary infection which primarily effects canids and felines. The one drug class approved to prevent the development of dirofilariosis is the macrocyclic lactones (ML). MLs were first approved as a monthly prophylactic treatment for dirofilariosis in 1987 and remain the standard of care (Chabala et al. 1980, Campbell 1981, Campbell et al. 1983, Ohishi et al. 1987a, 1987b, Wolstenholme 2015, Diakou and Prichard 2021). ML are usually administered as a monthly chemoprophylactic treatment (McCall et al. 2008). In *D. immitis*, the MLs target and kill the developing L3 / L4 larvae, preventing the establishment of a patent infection. The MLs act against these larval stages at low dose rates and have been used as effective and generally safe drugs for preventing dirofilariosis.

It was brought to public attention in 2005 that complaints of heartworm preventative product ineffectiveness were reported to the United States FDA Center for Veterinary Medicine (FDA / CVM) as early as 1998 (Hampshire 2005). Genetic changes associated with ML resistance were documented both *in vivo* and *in vitro*, and in 2014 heritable ML resistance was

validated by experimentally infecting laboratory canines (Bourguinat et al 2011a, 2011b, 2011c, Pulaski et al. 2014, Bourguinat et al 2015, Wolstenholme et al 2015).

The establishment of true heritable ML drug resistance led to research into the development of diagnostic tests to differentiate dirofilaroisis caused by true ML resistance from those due to opportunistic infections and lack of owner compliance. Whole genome analysis isolated several single nucleotide polymorphisms (SNP) associated with a resistant phenotype defined as a lack of / reduced mf reduction in mf suppression tests (Bourguinat et al. 2015, Bourguinat et al. 2017a, 2017b, Ballesteros et al. 2018). The top 10 SNP markers which best differentiated the ML-susceptible phenotype, and the ML-resistant phenotype were validated in clinical *D. immitis* samples collected within the USA (Ballesteros et al. 2018). The clinical validation of the molecular markers provides a genetic test to differentiate between ML-resistant *D. immitis* isolates and cases of incomplete use of heartworm preventatives. The SNP molecular markers have been subsequently used to analyze clinical samples collected in both Europe and Australia (Lau et al. 2021, Curry et al. 2022a). Genetic testing is relatively expensive and time consuming. Research into *in vitro* tests was also pursued. Larval migration and motility assays were performed on the blood-borne mf; however, these tests could not definitively differentiate between ML-susceptible and ML-resistant isolates (Evans et al. 2013, Evans et al 2017, Maclean et al. 2017). It was determined that motility measurements of the mf in the presence of ivermectin (IVM) were not reliable detection methods for ML resistance. A new *in vitro* assay model was required.

The primary target of ML activity are the invertebrate specific glutamate gated chloride channels (GluCls). The MLs act as allosteric modulators and bind pseudo-irreversibly to open the GluCls leading to hyperpolarization and paralysis of the neuromuscular system

(Wolstenholme 2012, Moreno et al. 2021). The mf of the closely related *Brugia malayi*, express one GluCl: AVR-14, which is localized in the musculature surrounding the excretory-secretory pore (ESP) (Moreno et al. 2010). In the *D. immitis* mf life stage the ESP is the main delivery source of regulated metabolic products into the host and likely the main putative target of ML-drug activity. The metabolic products secreted by the ESP can produce immunomodulatory effects, allowing the *D. immitis* mf to evade the host's immune system (Hewitson et al. 2014, Vatta et al. 2014, Moreno et al. 2021). Consequently, the mf ESP is an ideal target for the development of a minimally invasive *in vitro* assay to differentiate ML-susceptible and ML-resistant *D. immitis* isolates.

The *D. immitis* ESP secretes several enzymes and metabolites which can be measured via commercially available assays. One of these enzymes is triosephosphate isomerase (TPI). TPI is a ubiquitous dimeric enzyme which catalyzes the reversible interconversion of dihydroxyacetone phosphate and D-glyceraldehyde 3-phosphate during glycolysis (Wierenga et al. 2010). It has been shown to have auto-antigenic properties (Hewitson et al. 2014, Mónica and Ruy, 2019). TPI is abundant in the *D. immitis* secretome and is exclusively expressed in the mf ESP of *B. malayi* (Moreno and Geary 2008, Moreno et al. 2010, Geary et al. 2012).

The phenotypic variation in TPI levels caused by ML resistance can act as a basis for the development of an *in vitro* diagnostic assay to differentiate ML-susceptible and ML-resistant *D. immitis* mf when both are exposed to IVM concentrations normally effective on susceptible parasites. The change in levels of TPI *in vitro* is an indirect measure of the ML induced inhibition of the ESP. Currently, a time-efficient and cost effective *in vitro* diagnostic method is lacking. The result of the current study suggests that the measurement of *in vitro* TPI enzymatic activity may have utility for detecting truly susceptible *D. immitis* isolates.

2. Methods

2.1 Dirofilaria immitis isolates and isolation from canine blood

In *D. immitis* parasites ML resistance is defined as the failure of a ML drug, often only tested at one dose rate, to clear 100 % of parasite development; some percentage (not specifically defined, but > 0 %) of the parasites survive exposure to a ML in an *in vivo* chemoprophylactic study. ML-drug resistance occurs at varying degrees due to the heterologous nature of the population, and may be influenced by the ML tested, the dose rate tested and the number of treatments (Prichard 2021). In the current study eight laboratory-maintained *D. immitis* isolates were tested.

Table 1 Laboratory-maintained *Dirofilaria immitis* isolate name, origin, duration of laboratory-maintenance, and known or putative ML resistance status.

D. immitis Isolate	Origin	Laboratory Maintenance	ML resistance Phenotypic Status
Missouri	MO	2005	Susceptible
Berkeley	Berkeley County, SC	2014	Susceptible
Georgia II	Vidalia, GA	2013	Susceptible
Georgia III	Oconee County, GA	2017	Putative susceptible
Big Head	Livonia, LA	2015	Putative susceptible
JYD-34	Keytesville MO*	2010	Resistant
Metairie	Metairie, LA	2017	Resistant
WildCat	West Liberty, KY	2012	Resistant

*Via Pittsfield, IL

The ML-susceptible Missouri isolate was provided by the Filariasis Research Reagent Resource Center (FR3). Missouri, Berkeley, and Georgia II have been shown to be susceptible based on 100 % parasite clearance in *in vivo* chemoprophylaxis studies (Maclean et al, 2017; Elanco GmbH 2021). The other putative ML-susceptible isolates Georgia III, and Big Head do not have published information on their ML heartworm preventive phenotypes but were purported to be susceptible by the provider TRS Labs. JYD-34, Metairie, and WildCat are known ML-resistant isolates based on suboptimal parasite clearance in *in vivo* chemoprophylaxis studies (Maclean et al. 2017, McTier et al, 2017, Elanco GmbH 2021). The Metairie isolate was

provided by Dr. Ray Kaplan of the University of Georgia. Berkeley, Georgia II, Georgia III, Big Head, JYD-34, and WildCat were purchased from TRS Laboratories (Table 1; Figure 1).

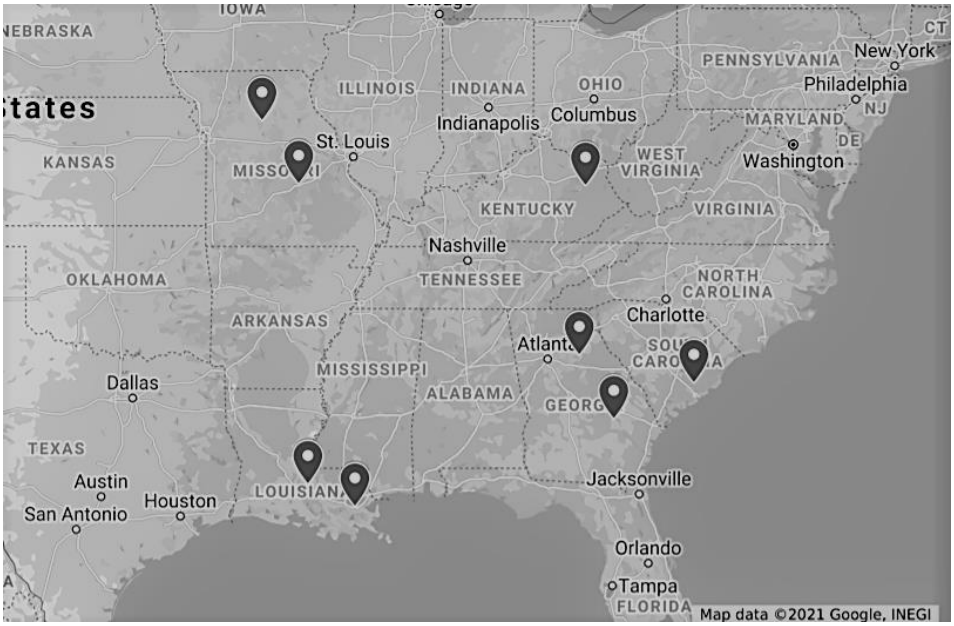

Figure 1 Origins of the US laboratory-maintained *Dirofilaria immitis* isolates obtained from the Filariasis Research Reagent Resource Center (FR3) and TRS Laboratories. Map created using Google Maps, accessed August 26th, 2021. https://www.google.com/maps/d/edit?mid=1i4vn

Canine venous blood samples were shipped overnight to McGill University for immediate processing. All subsequent work was performed in a biological safety cabinet (BSC). The mf were extracted from the blood by filtration. The venous blood was diluted 1 : 1 with $NaHCO_3$ solution and passed through polycarbonate membrane filters (3.0 µm; 25 mm; Sterlitech®) to isolate mf (Bourguinat et al. 2015). The mf were resuspended in 10 mL phosphate buffered saline (PBS). A modified Knott's test was performed using 1 mL blood, with 3 counts. A total 8000 mf were removed and resuspended in 2 mL RPMI 1640 culture media, supplemented with Penicillin-Streptomycin, Amphotericin B, and Gentamicin, in a 15 mL Falcon tube and kept overnight at 37 $^{\circ}$C and 5 % CO_2 to acclimate to the culture conditions.

2.2 Ivermectin drug solutions

IVM stock solutions (10 mM) were prepared by dissolving powdered IVM (Sigma-Aldrich®) in DMSO (Sigma-Aldrich®). Stock solutions were serially diluted to 50 nM IVM in RPMI 1640 and mixed 1 : 1 with untreated RPMI 1640 media for a final working concentration of 25 nM IVM and 0.2 % (v / v) DMSO.

2.3 Triosephosphate Isomerase Colorimetric Enzymatic Activity Assay Optimization

2.3.1 Ivermectin Concentration and Dose Response

The TPI colorimetric enzymatic activity assay was first tested with the known ML-susceptible Missouri isolate and the known ML-resistant JYD-34 isolate (Bourguinat 2017b, Maclean et al. 2017, McTier et al 2017). The following IVM concentrations were tested: an untreated 0 nM control, 25 nM, 50 nM, 75 nM, and 100 nM. The changes in TPI activity were compared between the two isolates. The decrease in TPI activity of the known ML-susceptible Missouri isolate was further analyzed via dose response studies.

2.3.1 24 hours Incubation Conditions

The sensitivity of the TPI colorimetric enzymatic activity assay following 24 hours IVM exposure was assessed to determine the minimum number of mf and minimum volume of media required to obtain reliable results. The following conditions were tested with the known ML-susceptible Missouri isolate: 1000 mf / 150 µL, 1000 mf / 100 µL, 500 mf / 100 µL, 1000 mf / 75 µL, and 500 mf / 75 µL.

2.4 Triosephosphate Isomerase Colorimetric Enzymatic Activity Assay

The next morning the mf were separated into two IVM treatment groups: 0 nM IVM and 25 nM IVM. The untreated, 0 nM IVM, was exposed to 0.2 % (v / v) DMSO to control for any effect of the DMSO. The two treatment groups were pre-incubated for four hours in 2 mL media with the respective IVM treatments in 15 mL Falcon tubes. Following pre-incubation, the two IVM

treatment groups were washed twice. The samples were resuspended in fresh media at 0 nM and 25 nM IVM. The two IVM treatment groups were transferred into a 96-well culture plate in triplicate. Each well contained 1000 mf in 100 µl of media. The 96-well culture plate was incubated for 24 hours at 37 ° C and 5 % CO_2.

After the 24 hours incubation, the culture plate was centrifuged at 15 000 g for 5 minutes at 4 ° C using an Allegra 25R Benchtop Centrifuge and S5700 Rotor (Beckman Coulter®). The mf pelleted to the bottom of the culture plate and the top 50 µl of media was removed for the TPI colorimetric enzyme activity assays. The top 50 µL of media from each sample was re-plated on a new 96 – well assay plate. The standards and controls were prepared following protocols provided by the supplier (Abcam Inc.). The reaction mix was added to the sample, standard, and control wells just prior to the kinetic read. The optical density (OD) was measured on the H4 Synergy microplate reader (BioTek®) using the GEN5™ software at an OD of 450 nm every 2 minutes for one hour at 37 ° C.

2.5 Statistical Analysis

All experiments were performed in triplicate. Results presented are shown as mean data + standard deviation (SD). Data analysis was performed as outlined in the protocol provided by the supplier (Abcam Inc.). The difference in TPI activity (mU/mg) between IVM treatments of each *D. immitis* isolate was calculated by Sidak multiple comparison test with two-tailed p value, and 95 % confidence interval. All analyses were performed using Prism 7.0c (Graph Pad Software, Inc.).

3. Results

3.1 TPI Colorimetric Enzymatic Activity Assay Optimization

3.1.1 Ivermectin Concentration and Dose Response

The changes in TPI activity were tested with the known ML-susceptible Missouri isolate and the known ML-resistant JYD-34 isolate with the following IVM concentrations: an untreated 0 nM control, 25 nM, 50 nM, 75 nM, and 100 nM (Bourguinat 2017b, Maclean et al. 2017, McTier et al 2017). Missouri showed a sharp decrease in TPI activity at an IVM concentration of 25 nM IVM or greater when compared to the untreated control (Figure 2). The ML-resistant JYD-34 maintained a fairly stable TPI activity across the five IVM treatment groups up to 100 nM IVM.

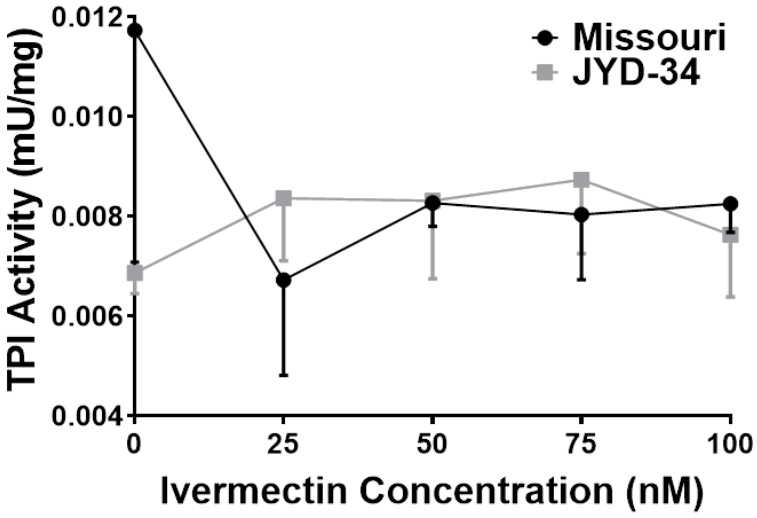

Figure 2 The change in TPI enzyme activity (mU/mg) in two *D. immitis* isolates the ML-susceptible Missouri isolates (black ●), and the ML-resistant isolate JYD-34 (grey ■) at OD 450 nm. The isolates were incubated at 2000 mf / 150 µL for 24 hours at 37 º C, 5 % CO_2 and exposed to one of the following ivermectin conditions: an untreated ivermectin control (0 nM), 25 nM, 50 nM, 75 nM, or 100 nM ivermectin. All experiments were performed in three to four biological replicates.

The decrease in the TPI activity of the Missouri isolate between 0 nM and 25 nM IVM was further analyzed via dose response studies. Missouri was exposed to nine IVM concentrations ranging from 1.25 nM to 30 nM. The change in TPI enzyme activity was varied

and inconsistent at low IVM concentrations (Figure 3). A dose response curve and EC50 could not be determined. The 25 nM IVM treatment was chosen as the marker to delineate between the ML-susceptible and ML-resistant *D. immitis* isolates. A statistically significant decrease in TPI enzyme activity at an IVM concentration of 25 nM when compared to the untreated 0 nM control was taken to indicate a ML-susceptible isolate.

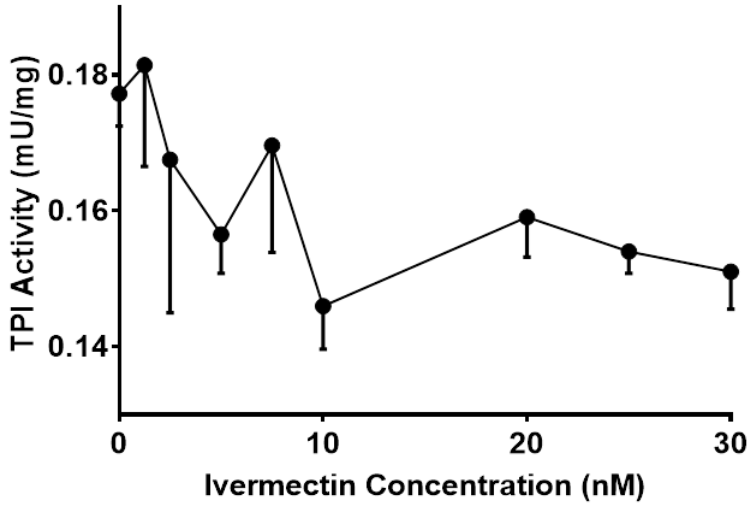

Figure 3 The change in TPI enzyme activity (mU/mg) in the ML-susceptible Missouri isolate at OD 450 nm. The Missouri isolate was incubated with 2000 mf / 150 µL for 24 hours at 37 º C, 5 % CO_2 and then exposed to one of the following ivermectin conditions: an untreated ivermectin control (0 nM), 1.25 nM, 2.5 nM, 5 nM, 7.5 nM, 10 nM, 20 nM, 25 nM, 30 nM. All experiments were performed in three biological replicates (means ± SD).

3.1.2 24 hours Incubation Conditions

The number of mf per well was reduced to accommodate potentially low levels of blood-borne mf found in clinical blood samples. The ML-susceptible Missouri isolate was used to analyze clinical infections with low, as well as high mf counts, the following conditions were tested: 1000 mf / 150 µL, 1000 mf / 100 µL, 500 mf / 100 µL, 1000 mf / 75 µL, and 500 mf / 75 µL to

determine the lowest effective number of mf and volume of media per well to successfully run the TPI enzyme assay (Figure 4).

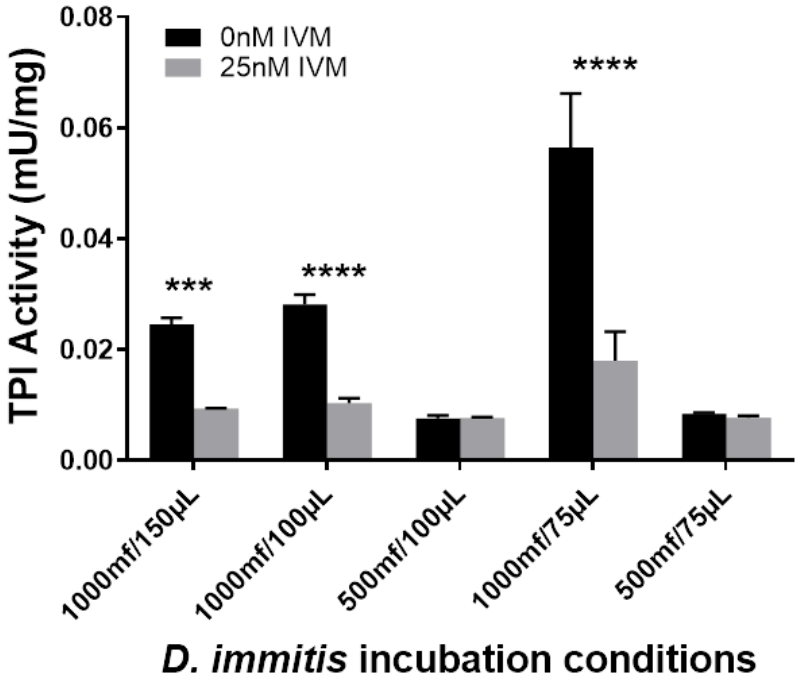

Figure 4 The change in TPI enzyme activity (mU / mg) in the ML-susceptible *D. immitis* Missouri isolate under 5 distinct incubation treatment conditions: 1000 mf/150 µL, 1000 mf/100 µL, 500 mf / 100 µL, 1000 mf / 75 µL, and 500 mf / 75 µL at 0nM ivermectin (black) and 25 nM ivermectin (grey). All experiments were performed with three biological replicates. Results presented are shown as mean data ± standard deviation (SD). The difference in TPI activity (mU/mg) between IVM exposure groups was calculated using the Sidak multiple comparison test with two-tailed p-value, and 95 % confidence interval (*$p < 0.05$, **$p < 0.01$, ***$p < 0.001$, ****$p < 0.001$). All analyses are performed using Prism 7.0c (Graph Pad Software, Inc).

Three of the five incubation conditions tested, 1000 mf / 150 µL, 1000 mf / 100 µL, and 1000 mf / 75 µL, had a statistically significant decrease in TPI enzymatic activity between the 0 nM and the 25 nM IVM treatments following a 24 hours incubation. The 1000 mf / 100 µL and

1000 mf / 75 µL incubation conditions had the most statistically significant change in TPI activity between IVM treatments (Figure 4). The 1000 mf / 75 µL incubation condition was not used in further analyses because the low media volume can result in some mf being transferred from the culture plate to the assay plate. The mf transferred to the assay plate can interfere with the OD reading. The 1000 mf / 100 µL incubation condition showed a similar significant decrease in TPI enzymatic activity and no mf transfer from the culture plate. These incubation conditions were the lowest effective number of mf and volume of media and were used in subsequent analyses.

3.2 Macrocyclic Lactone Response Profiles

The optimized *in vitro* enzymatic activity assay was used to test the TPI enzymatic activity in eight laboratory-maintained *D. immitis* isolates: three confirmed ML-susceptible isolates, by *in vivo* phenotypic response to chemoprophylaxis: Missouri, Berkeley, and Georgia II; two putative ML-susceptible isolates: Georgia III, and Big Head; and three confirmed ML-resistant isolates: JYD-34, Metairie, and WildCat (Maclean et al. 2017, Maclean et al. 2017; McTier et al. 2017; Elanco GmbH 2021) (Table 1; Figure 5). The three isolates confirmed as ML-resistant shared a consensus ML-response profile. The three isolates maintained relatively stable low levels of TPI activity between the two treatments following the 24 hours IVM exposure. Missouri and Berkeley, confirmed ML-susceptible isolates, had a statistically significant decrease in TPI enzymatic activity between 0 nM and 25 nM IVM. The three remaining ML-susceptible or putative ML-susceptible isolates: Georgia II, Georgia III, and Big Head, had a ML-response profile similar to the three ML-resistant isolates (Figure 5).

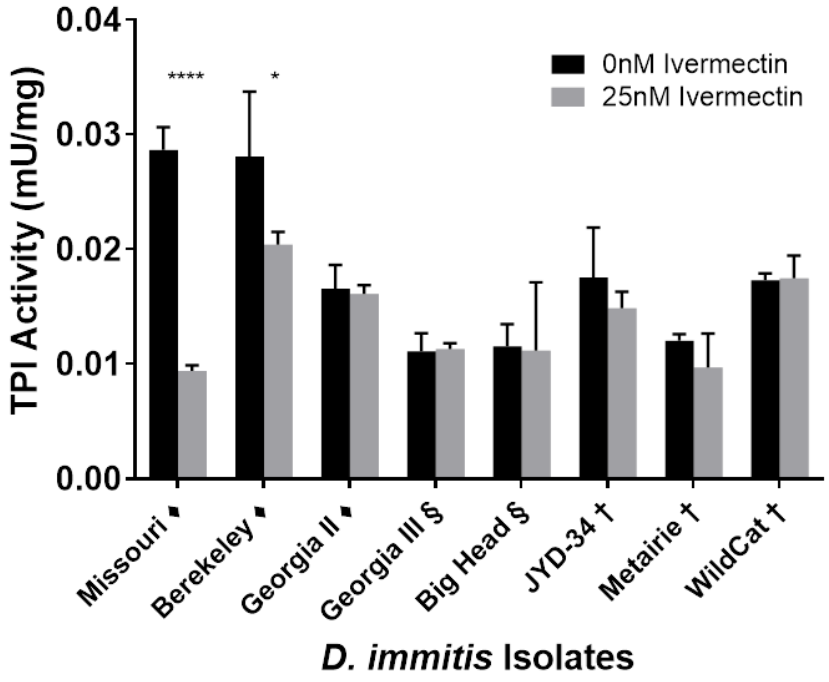

Figure 5 The change in TPI enzyme activity (mU / mg) in eight *D. immitis* isolates which include the three known phenotypic ML-susceptible isolates Missouri, Berkeley, and Georgia II (annotated with a [*]), two putative ML-susceptible/developing resistant isolates: Georgia III, and Big Head (annotated with a [§]), and three known ML-resistant isolates: JYD-34, Metairie, and WildCat (annotated with a [†]). All isolates were incubated with 1000 mf / 100 µL and exposed to an untreated, ivermectin control (black) or 25 nM ivermectin exposure (grey) for a 24 hours incubation at 37 º C. All experiments were performed with three biological replicates. Results presented are shown as mean data + standard deviation (SD). The difference in TPI activity (mU/mg) between IVM exposure groups was calculated by the Sidak multiple comparison test with two-tailed p-value, and 95 % confidence interval (*$p < 0.05$, **$p < 0.01$, ***$p < 0.001$, ****$p < 0.001$). All analyses were performed using Prism 7.0c (Graph Pad Software, Inc.).

4. Discussion

The development of an *in vitro* diagnostic assay for ML resistance requires the determination of a phenotype to differentiate ML-susceptible from ML-resistant *D. immitis* populations. The infective L3 are not readily available in a clinical setting and the adults are only available via surgical excision or necropsy (McCall et al. 2008, AHS 2018). The mf life stage was chosen for our *in vitro* observations because it is readily available via a minimally invasive blood draw, which can be taken in a clinic at the time a dog is examined by a veterinarian. In contrast to the *in vivo* microfilarial suppression test which requires two blood draws, two to four weeks apart, for the *in vitro* assay examined here, only one blood draw is required (Ballesteros et al. 2018).

Physiologically, the mf life stage does not possess a functioning pharynx and MLs do not appear to impact motility (McCall et al. 2008, Bowman et al. 2009, Evans et al. 2013, Evans et al. 2017, Maclean et al. 2017). The sole compartment that appears to be under neuromuscular control and the main putative target of ML activity in the mf life stage is the ESP. The mf ESP and its secreted metabolic products are an ideal target for the development of a minimally invasive *in vitro* diagnostic assay. Colorimetric enzymatic activity assays were chosen due to their commercial availability and robust sensitivity. Enzymatic assays for several enzymes, highly secreted by the *D. immitis* secretome, were tested. The TPI enzymatic assay was selected based on measurable variation in enzyme activity following 24 hours IVM exposure in the known ML-susceptible Missouri isolate.

The initial experimental design of the *in vitro* diagnostic assay included nine IVM treatment groups to elucidate a dose-response curve (Figure 3). An EC50 for IVM exposure could not be determined but there was a marked decrease in TPI activity secreted by the Missouri mf incubated in greater than 10 nM IVM. The mf showed a high degree of variability in enzyme

activity at lower IVM concentrations. The levels of TPI enzyme activity in the Missouri isolate stabilized and demonstrated little deviation at IVM concentrations greater than 25 nM (Figure 3). A statistically significant decrease in TPI enzyme activity between 0 nM and 25nM IVM was chosen to identify a ML-susceptible isolate and differentiation between ML-susceptible and ML-resistant *D. immitis* populations.

The incubation conditions were designed based on the ready availability of laboratory-maintained *D. immitis* isolates. Access to clinical blood samples from dogs with a patent *Dirofilaria* infection with high mf burden are limited. Low numbers of blood circulating mf in patent infections are the result of low levels of infection, sexually immature adult worms, or the time of day the blood sample is drawn. Upon consultation with veterinary clinicians and review of the literature the protocol was adapted to accommodate the variability of infection intensity seen in veterinary clinics (Figure 4). The 1000 mf / 100 µL incubation conditions were chosen as the most feasible, to facilitate obtaining a result when the mf count is low. The optimized protocol requires 8000 mf and allows for low mf count, naturally occurring infections to be tested.

The *in vitro* enzyme assay was tested in eight laboratory-maintained isolates. The results proved mixed but are surprisingly consistent with genetic analysis for resistance. The three known ML-resistant isolates, JYD-34, Metairie, and WildCat had similar ML response profiles, which differentiated them from the known ML-susceptible isolate, Missouri. These three resistant isolates had a consistent low level of TPI enzymatic activity that did not vary between 0 nM and 25 nM IVM. The known susceptible isolates Missouri and Berkeley had statistically significant decreases in TPI enzymatic activity between 0 nM and 25 nM IVM, following 24 hours exposure.

The three remaining ML-susceptible or putative ML-susceptible isolates, Georgia II, Georgia III, and Big Head showed low levels of TPI enzymatic activity at 0 nM and 25 nM IVM; a phenotypic response similar to the ML resistance isolates in the *in vitro* assay. New findings call into question the ML-susceptible or putative ML-susceptible status of Georgia II, Georgia III, and Big Head. The three isolates do not have a genotype consistent with their claimed ML-susceptible profiles. MiSeq analysis of Georgia II using the highly predictive 2-SNP pairwise F_{ST} model show a F_{ST} value of 0.07; compared to known susceptible isolates, Missouri, and Berkeley, which had F_{ST} values of 0.00 in MiSeq analysis **(**Ballesteros et al. 2018; Curry et al. 2022a**)**. Digital drop PCR (ddPCR) duplex analysis of the same two highly predictive SNP sites demonstrated a similar alternate allele frequency; Georgia II has an average alternate allele frequency of 13.5 % at the two SNP locations (Kumar et al. forthcoming) It is not clear whether Georgia II, used in the current study is related to the three isolates, designated GA2.At.a2 t, GA2.At.b2 t and GA2.At.c2 t.3 in Sanchez et al. (2020). However, the three isolates cluster with various known resistant isolates in the neighbor-tree presented in the population genetics microsatellite analysis and are far from the other known ML-susceptible isolates (Sanchez et al. 2020). Taken together these studies suggest the possibility that Georgia II has genotypic characteristics more aligned with a developing resistant isolate.

Georgia III displayed variable SNP frequencies for the four SNP markers analyzed via duplex ddPCR which were variable and intermediate between known resistant and susceptible isolates (Kumar et al. forthcoming). It is of note that the SNP frequencies for Georgia III were variable between samples from different canine hosts (Kumar et al. forthcoming). It has been documented that distinct passages of a *D. immitis* isolate can display a degree of genetic drift,

which may account for the degree of alternate allele variability between different canine hosts for the same isolate (Sanchez et al. 2020).

In addition, Big Head, when analysed via ddPCR duplex had an average alternate allele frequency of up to 29 %, consistent with the resistant isolates analysed in the same study (Kumar et al. forthcoming). Big Head's ML-response profile in the *in vitro* enzyme assay and its documented genetic variability at two highly predictive SNP markers via ddPCR duplex analysis indicate the isolate may be developing ML resistance. Taken together, the MiSeq, ddPCR duplex, and microsatellite genotyping results, indicate that the isolates, Georgia II, Georgia III and Big Head are genetically mixed and may be developing resistance. This would be consistent with the results from the *in vitro* TPI assay.

The known ML-susceptible Missouri and Berkeley isolates and known ML-resistant isolates JYD-34, Metairie, and WildCat had distinct TPI enzyme activity profiles when comparing the untreated 0 nM IVM control (Figure 2). JYD-34, Metairie, and WildCat have lower levels of TPI enzymatic activity compared to the known susceptible Missouri and Berkeley isolates. The difference in TPI enzymatic activity when untreated suggests the physiological effects of the genetic changes associated with ML resistance may have an impact on the mf homeostatic processes independent of the ML drug activity. The genetic changes could be shared between the known ML-resistant isolates JYD-34, Metairie, and WildCat; as well as the potentially mixed or developing resistant isolates Georgia II, Georgia III, and Big Head.

If this is the case, the phenotypic *in vitro* TPI enzymatic activity assay would be unable to differentiate genetically mixed or developing resistance populations and fully resistant isolates, but would be valuable for identifying fully susceptible populations, compared with isolates developing resistance and fully resistant isolates.

Prichard (2021) has summarized evidence that the expression of ML resistance will depend on the dose rate used, the number of doses used, and the inherent potency of the different MLs used as heartworm preventives. Evidence for developing resistance may only become apparent, *in vivo*, if dose response profiles are obtained. In addition, a lack of history of prophylactic use in a particular dog does not mean that the ancestors of the challenge worms were not exposed to ML treatment prior to the challenge worms being placed under laboratory conditions. There may be *D. immitis* populations which appear susceptible at a given ML dose rate but may show a shift in susceptibility if a dose response curve is investigate and may be on the way to developing resistance. These "developing resistance" populations may show changes in genetic profile, similar to the genotype of established resistant populations and in some phenotypic assays, *in vivo* or *in vitro*, and may behave somewhat similar to resistant populations, depending on the assay.

The results of the TPI enzymatic assay suggests it is not the optimal basis for a robust *in vitro* assay to differentiate isolates developing phenotypic ML resistance from isolates that are clearly resistant. Currently, the most accurate test to differentiate ML-susceptible and ML-resistant isolates remains to obtain an estimate of the degree of genetic shift towards resistance via the SNP molecular markers. However, the phenotypic data collected from the eight laboratory-maintained *D. immitis* isolates further corroborates published SNP molecular marker MiSeq and ddPCR duplex analysis, as well as microsatellite genotyping data on Georgia II, Georgia III, and Big Head. These three isolates do not have a genotypic or phenotypic profile consistent with their ML susceptible or putative ML-susceptible label.

5. Conclusion

Currently, US laboratory-maintained isolates are characterized as ML-susceptible based on their ability to be cleared at the proposed commercial dose rate of treatment. Based on the AHS recommendation of year-round chemoprophylaxis and the widespread use of MLs in the US, it is becoming increasingly rare to find a *D. immitis* isolate whose ancestors are truly naïve to ML prophylaxis in North America. The measurement of changes in enzymatic activity and the *in vitro* TPI colorimetric enzymatic activity assay may have utility for detecting isolates that remain truly susceptible. Further research is required to develop a rapid and cost effective *in vitro* diagnostic assay to accurately differentiate dirofilariosis caused by ML-susceptible, genetically mixed *D. immitis* isolates which may be developing resistance, and infections with clearly resistant parasites.

Declarations

Ethics approval and consent to participate

All experimental procedures were approved by McGill University in accordance with relevant guidelines and regulations.

Availability of data and materials

The data supporting the conclusions of this article are included within the article.

Competing interests

The authors declare that they have no competing interests.

Funding

This research was supported by grants to RKP from the National Center for Veterinary Parasitology, USA, and the Natural Sciences and Engineering Research Council of Canada.

Authors' contributions

Experiments were conceived and designed by EC and RKP. Experiments and data analysis were performed by EC. The manuscript was written by EC and RKP. The authors read and approved the final manuscript.

Acknowledgements

We thank Kathy Keller and Cristina Ballesteros for their invaluable patience, guidance, and advice in development of the protocol and sample preparation. We also thank Timothy Geary of McGill University and Yovany Moreno of Boehringer Ingelheim for helpful advice. We are indebted to the FR3 for providing the Missouri *D. immitis* isolate. We thank Ray Kaplan of the University of Georgia for providing the Metairie *D. immitis* isolate. We thank TRS Lab Inc. for providing the Berkeley, Georgia II, Georgia III, Big Head, JYD-34, and WildCat *D. immitis* isolates.

Connecting Statement I

In Chapter 2, the *in vitro* triosephosphate isomerase (TPI) colorimetric enzymatic activity assay could detect *Dirofilaria immitis* isolates which remained truly susceptible to macrocyclic lactones (ML). The ML-susceptible isolates, Missouri and Berkeley, had statistically significant decreases in TPI enzymatic activity in response to 24 hours ivermectin (IVM) exposure, which was not seen in the ML-resistant isolates. The phenotypic results of the *in vitro* TPI colorimetric enzymatic activity assay also identified three isolates: Georgia II, Georgia III, and Big Head, which did not have phenotypic ML response profiles consistent with their *in vivo* ML susceptible or putative ML-susceptible label. These results corroborate MiSeq sequencing, ddPCR duplex analysis, and microsatellite genotyping data, indicating the three isolates are genetically mixed and may be partially selected for ML resistance.

The results of the *in vitro* TPI colorimetric enzymatic activity assay further substantiate the mf excretory-secretory pore (ESP) as a likely putative target of ML activity. Genetic changes, possibly shared by the genetically mixed and ML-resistant populations, may affect drug efflux in proximity to the ESP, which could impact the efficacy of MLs in the mf life stage.

Importantly, one of the first genes with genetic changes associated with ML resistance in *D. immitis* was P-glycoprotein 11 (*Dim*Pgp-11). The Pgps are efflux pumps known for their involvement in ML pharmacology. It is hypothesized, due to its homology with *Caenorhabditis elegans* P-glycoprotein (*Cel*Pgp-11), that *Dim*Pgp-11 may be strategically located in the musculature surrounding the ESP where it may help regulate the response to MLs, including the secretion of immunomodulatory molecules. Chapter 3 aims to characterize *Dim*Pgp-11 by providing an extensive study on its genetic polymorphism, constitutive expression, and tissue localization in the *D. immitis* microfilaria (mf) lifestage.

Chapter 3.

Genetic polymorphism, constitutive expression, and tissue localization of *Dirofilaria immitis* P-glycoprotein 11: a putative marker of macrocyclic lactone resistance

Emily Curry[1], Roger Prichard[1], and Anne Lespine[2*]

[1] Institute of Parasitology, McGill University, Sainte Anne-de-Bellevue, QC, Canada

[2] INTHERES, Université de Toulouse, INRAE, ENVT, 31027 Toulouse Cedex 3, France

EC: emily.curry@mail.mcgill.ca

RP: roger.prichard@mcgill.ca

AL: anne.lespine@inrae.fr

Published in Parasites and Vectors (Curry et al. 2022)

Abstract

Background: *Dirofilaria immitis* causes dirofilariosis, a potentially fatal condition in canids. *Dirofilaria* infections can be prevented with a macrocyclic lactone (ML) prophylactic regimen. However, some *D. immitis* isolates have become resistant to MLs. Genetic changes on the P-glycoprotein 11 gene, encoding an ABCB transporter, have been linked to the ML-resistant phenotypes and have been proposed as markers of drug resistance. However, nothing is known about the expression and the localization of this transporter in *D. immitis*, despite being strongly linked to ML-resistant phenotypes.

Methods: We examined the clinically validated *Dim*Pgp-11 single nucleotide polymorphism (SNP) via MiSeq analysis in the ML-susceptible Missouri, MP3, and Yazoo; and the ML-resistant JYD-34 and Metairie isolates and correlated the data with previously published MiSeq results of USA laboratory-maintained *D. immitis* isolates. The level of the expression of the *Dim*Pgp-11 mRNA transcript was analyzed by droplet digital PCR (ddPCR) and compared in the USA laboratory-maintained isolates: the ML-susceptible Missouri and Berkeley, the putative ML-susceptible isolates Georgia III and Big Head; and the ML-resistant isolate JYD-34. The immunolocalization of *Dim*Pgp-11 was visualized in the microfilaria (mf) lifestage of the Missouri isolate using confocal microscopy.

Results: We confirmed that the SNP found on *Dim*Pgp-11 is differentially expressed in the USA laboratory-maintained isolates. The ML-susceptible isolates had an alternate allele frequency between 0 – 15 %, while it ranged between 17 – 56 % in the ML-resistant isolates. The constitutive expression of *Dim*Pgp-11 was similar in the Berkeley, Georgia III, and Big Head isolates; while it was significantly decreased in the ML-resistant JYD-34 ($p < 0.05$), when compared to the Missouri isolate. The *Dim*Pgp-11 protein was distinctly localized within the

excretory-secretory (ES) duct, pore cells and the excretory cell, and more faintly along the mf body wall.

Conclusion: Our data confirm that genetic polymorphism of *Dim*Pgp-11 is associated with ML resistance in USA laboratory-maintained *D. imminits* isolates. A link between *Dim*Pgp-11 and ML resistance in *D. immitis* is further supported by the lower protein expression in the ML-resistant JYD-34 isolate when compared with the susceptible Missouri isolate. Interestingly, *Dim*Pgp-11 is strategically located surrounding the ES pore where it could play an active role in ML efflux.

Keywords: *Dirofilaria immitis*, Dirofilariosis, macrocyclic lactones, resistance, P-glycoprotein 11, MiSeq sequencing, constitutive expression, immunofluorescence assay.

Introduction

The parasitic nematode *Dirofilaria immitis* is the causative agent of dirofilariosis, a pulmonary infection which primarily affects canids and felines. The macrocyclic lactones (MLs) remain the only class of drug approved for prophylactic treatment to prevent the development of dirofilariosis infection (Chabala et al. 1980, Campbell et al. 1981, 1983, Diakou and Prichard 2021). In *D. immitis*, the MLs act against larval stages killing the developing L3/L4 larvae and preventing the establishment of adult infection, which causes the pathology. They are used at low dose rates, e.g., 6 – 12 µg / kg for ivermectin (Prichard 2021). At slightly higher dose rates the MLs are also microfilaricidal and reduce the fecundity of adult parasites (Prichard 2021). MLs are generally safe drugs for preventing *Dirofilaria* infections and have been used for dirofilariosis prevention since 1987.

Heartworm chemoprophylactives are required to be 100 % effective at preventing the establishment of *D. immitis* infections in registration trials (Prichard 2021). Thus, in theory, any

decrease in efficacy below 100 % could be considered as resistance. The establishment of *D. immitis* infections in animals on ML-based heartworm preventatives indicates a loss of efficacy of the drug and a potentially ML-resistant population. However, the establishment of an infection does not itself prove ML resistance in *D. immitis*. A missed treatment or a delay in the scheduled treatment may be the cause of the establishment of infection, unrelated to resistance. It is difficult to prove unequivocally that heartworm prevention has been wholly in compliance with the recommended treatment. Furthermore, a resistance phenotype may depend on the dose rate, the number of treatments administered, the formulation, and the MLs administered (Prichard 2021). As true drug resistance is genetic, it is heritable (Pulaski et al. 2014). Since resistance to ML in nematodes is a complex mechanism that may involve multiple genes, the conditions for unequivocally determining ML resistance can be quite challenging.

The P-glycoprotein (Pgp) efflux transporters have been identified as one of the relevant factors affecting ML efficacy and contributing to ML resistance in nematodes. Pgps belong to a class of protein known for their involvement in ML pharmacology as efflux pumps (Schinkel et al. 1994, Xu et al. 1998, Lespine et al. 2007, 2008, 2013, David et al. 2016, 2018). MLs bind with high affinity on the Pgps in the hydrophobic binding pocket, the first of a series of events, including ATP hydrolysis, that furnish the energy needed for drug translocation out of the cells and the organisms (Lespine et al. 2013). Changes on Pgps, genetic or induced, may impact the pump activity subsequently leading to lower drug efficiency.

Genetic changes associated with the ML loss of efficacy (LOE) phenotype were documented in a subset of genes in 2011, including the gene for a yet unidentified Pgp (Bourguinat et al. 2011a, 2011b). Two single nucleotide polymorphisms (SNP) in the Pgp gene were highly associated with the LOE phenotype: Position 11 and Position 618. The SNP (A11G)

is located in a coding region and confers an amino acid change from lysine to arginine at position 1203 within the second nucleotide binding domain (NBD) adjacent to the Walker B site (Mani et al. 2016, 2017). This change introduces a basic polar group prior to the ATP binding domain, and similar changes at this position have been shown to modulate ATP turnover and the transport activity of the mammalian transporter homolog (Verhalen et al. 2017). The SNP (A618G) is located in a non-coding region. These two SNPs on the *D. immitis* Pgp were combined for diplotypic analysis and known as the GG – GG genotype. Whole genome-wide association determined that *D. immitis* possesses three functional full length Pgps: P-glycoprotein 3 (*Dim*Pgp-3), P-glycoprotein 10 (*Dim*Pgp-10), and P-glycoprotein 11 (*Dim*Pgp-11) (Mani et al. 2016). The diplotypic GG – GG genotype was isolated on *Dim*Pgp-11 (Bourguinat et al. 2016). The *Dim*Pgp-11 diplotypic GG – GG genotype was used as one of four criteria to help validated the heritability of true ML resistance in *D. immitis* (Pulaski et al. 2014).

The SNP (A11G) is the focus of the current research and is hereafter referred to as the *Dim*Pgp-11 SNP. The Pgp-11 gene has been associated with the development of ML resistance in the model organism *Caenorhabditis elegans* and several nematode species of veterinary importance, making *Dim*Pgp-11 a gene of interest for characterization in the context of ML resistance. In *C. elegans*, P-glycoprotein 11 (*Cel*Pgp-11) is strategically located within the intestine and the excretory cell (Zhao et al. 2004, Hunt-Newbury et al. 2007, Spencer et al, 2011). ML-resistant *C. elegans* isolates constitutively overexpressed several genes involved in xenobiotic metabolism and transport, including *Cel*Pgp-11 (James et al. 2009, Ménez et al. 2016). The parasitic intestinal nematode of cattle, *Cooperia oncophora*, shows a 3 to 5 – fold upregulation of P-glycoprotein 11 (*Con*Pgp-11) in the ivermectin (IVM) resistant CoIVR08 isolate compared to the IVM susceptible CoIVSus isolate *in vivo* and *in vitro* (De Graef et al.

2013). Treatments, with the Pgp inhibitor verapamil in jirds, have demonstrated restoration of IVM sensitivity in ML-resistant *Haemonchus contortus* and *C. oncophora* isolates (Molento and Prichard 1999, 2001, Demeler et al. 2013). Similarly, *Parascaris spp.*, a severely pathogenic intestinal nematode of equines, demonstrates genetic variations on P-glycoprotein 11 (*Peq*Pgp-11) transcripts that are correlated with reduced ML sensitivity (Janssen et al. 2013). Transgenic expression of *Peq*Pgp-11 has been shown to modulate IVM sensitivity in *Cel*Pgp-11 knockout *C. elegans* strains (Janssen et al. 2015). The localization, expression levels, and genetic changes on Pgp-11 in *C. elegans*, *H. contortus, C. oncophora*, and *P. equorum* indicate Pgp-11 is likely playing a functional role in the modulation of ML susceptibility and the development of resistance in these nematodes.

The characterization of *Dim*Pgp-11 is of particular interest in order to better understand the development of ML resistance in *D. immitis*. We provide an extensive study on the expression of *Dim*Pgp-11 and its localization in *D. immitis* mf.

Methods

Dirofilaria immitis isolates

Eight USA laboratory-maintained *D. immitis* isolates, collected from canine blood samples, were used to complete the various experiments (Table 1). The *D. immitis* samples were obtained while host dogs were not under drug pressure. The ML-susceptible Missouri, MP3, and Yazoo isolates, as well as the ML-resistant Metairie isolate were provided by the Filariasis Research Reagent Resource Center (FR3) (Maclean et al. 2017). The ML-susceptible Berkeley; putative ML-susceptible isolates Georgia III and Big Head; and the ML-resistant isolate JYD-34 were provided by TRS Laboratories (Maclean et al 2017, McTier et al. 2017, Curry et al. 2022a).

Table 1 Laboratory-maintained *Dirofilaria immitis* isolates used or cited in the various experiments: MiSeq analysis, ddPCR constitutive expression analysis and immunofluorescence assay. *D. immitis* isolate name, origin in the USA, duration of laboratory-maintenance, and known or putative ML resistance status.

D. immitis Isolate	Origin in the USA	Laboratory Maintenance	ML resistance Phenotypic Status
Missouri [abc]	Puxico, MO	2005	Susceptible
MP3 [a]	Athens, GA	2011	Susceptible
Yazoo [a]	Yazoo, MS	2017	Susceptible
Berkeley [b]	Berkeley County, SC	2014	Susceptible
Georgia II [a]	Vidalia, GA	2013	Susceptible
GCFL [a]	Fort Myers, FL	2014	Susceptible
ZoeAL [a]	Westover, AL	2015	Susceptible
Georgia III [b]	Oconee County, GA	2017	Putative susceptible
Big Head [b]	Livonia, LA	2015	Putative susceptible
JYD-34 [ab]	Keytesville MO	2010	Resistant
Metairie [a]	Metairie, LA	2017	Resistant
WildCat [a]	West Liberty, KY	2012	Resistant
ZoeAMAL [a]	Westover, AL	2014	Resistant

[a] MiSeq analysis
[b] ddPCR constitutive expression analysis
[c] Immunofluorescence assay

The sample providers, the FR3 and TRS labs, have the appropriate ethical permissions to house the nematode's lifecycle, including the mosquito colonies and canine definitive hosts. McGill University, where the experiments were conducted, does not house the *D. immitis* lifecycle, and maintains the required biohazard importation permits from the Canadian Food Inspection Agency (Permit: A-2022-00829-1) (CFIA) to receive and work with the canine blood samples containing *D. immitis* mf.

***Dirofilaria immitis* microfilariae isolation**

The canine venous blood samples were shipped overnight to McGill University for immediate processing. The mf were extracted from the blood by filtration as described by Bourguinat et al. in 2015 (Bourguinat et al. 2015). The venous blood was diluted 1 : 1 with $NaHCO_3$ solution, and

polycarbonate membrane filters (3.0 µm; 25 mm; Sterlitech® Corporation) were used to isolate mf. A modified Knott's test was performed using 1 mL blood.

Measurement of *Dim*Pgp-11 genetic polymorphism

DimPgp-11 SNP marker

The *Dim*Pgp-11 SNP marker, found on *Dim*Pgp-11, scaffold nDi.2.2.scaf00004 at position 79766, was one of 10 SNP markers validated in USA clinical samples (Ballesteros et al. 2018). We analyzed the following isolates: the ML-susceptible Missouri, MP3, and Yazoo; and the ML-resistant, JYD-34 and Metairie at this position and compared the alternate allele frequency with results previously described in the following USA laboratory-maintained isolates: the ML-susceptible Berkeley, Georgia II, GCFL, and ZoeAL; and the ML-resistant WildCat and ZoeAMAL to confirm the continued assosciation of the *Dim*Pgp-11 SNP with phenotypic ML resistance (Table 2) (Bourguinat et al. 2017, Curry et al. 2022a).

Sample processing and DNA extraction

The genomic DNA (gDNA) from the total pooled mf of each isolate sample, ranging from 25 000 – 150 000 mf, was extracted using the QIAamp® DNA Micro kit (Qiagen Inc.). DNA concentrations were determined with the Quant-iT™ PicoGreen DNA Assay Kit (Invitrogen®, Life Technologies Inc.). The samples were stored at - 80 º C prior to being sent to Génome Québec for quality control and MiSeq Illumina sequencing.

MiSeq Illumina sequencing

The gDNA samples were sent to Génome Québec and the regions encompassing the *Dim*Pgp-11 SNP were sequenced on an Illumina MiSeq Platform, at a coverage of 2000X. The Fluidigm Access Array system performed target enrichment using array-based PCR amplification of the genomic target region. The samples underwent parallel amplification using custom primers with

added CS1 and CS2 tails, as described in Ballesteros et al. (2018). The samples were barcoded during target enrichment which allowed for multiplexed sequencing, and adapter sequences were added during the PCR amplification reaction.

MiSeq Illumina sequencing data analysis

Trimmomatic was used to trim for minimal trailing quality (30 PHRED score) and to filter for minimum read length by removing the Illumina sequencing adapters from read and adapter clippings (Bolger et al. 2014). The resulting read pairs were aligned to the *D. immitis* reference genome nDi.2.2 (http://www.nematodes.org/genomes/dirofilaria_immitis) using BWA-mem (http://bio-bwa.sourceforge.net/) resulting in binary alignment map (BAM) files (Li and Durbin 2009). The alignments were processed with Picard (https://broadinstitute.github.io/picard) for the realignment of indels, mate fixing, and marking of duplicate reads. BVATools (https://bitbucket.org/mugqic/bvatools/src) was used to extract base frequencies for the *Dim*Pgp-11 SNP and the read frequencies were assimilated to the allele frequencies. The alternate allele variance of all samples were compared to the *D. immitis* Reference Genome nDi.2.2. The BAM files for the Missouri, MP3, Yazoo, JYD-34, and Metairie *Dirofilaria immitis* isolates are openly available on the NCBI Sequence Read Archive under BioProject PRJNA847600.

Quantification of *Dim*Pgp-11 constitutive expression

Dirofilaria immitis microfilariae RNA extraction

The RNA extraction, primer optimization, and constitutive expression quantification protocol were optimized with the ML-susceptible Missouri isolate. The optimized protocol was further validated using the Missouri isolate and the ML-susceptible Berkeley isolate, the putative ML-susceptible Georgia III and Big Head isolates, and the ML-resistant JYD-34 isolate (Bourguinat et al. 2017, Curry et al. 2022a).

The RNA extraction protocol is a modified TRIZol protocol used to accommodate the fracture-resistant cuticle of the *D. immitis* mf. Frozen samples of 100 000 mf were thawed and centrifuged for five minutes at high speed. The phosphate buffer saline (PBS) supernatant was removed, and the mf were washed with 0.1 x TE buffer twice. All subsequent work was performed in a fume hood. Samples were resuspended in a 1 : 4 ratio of 0.1 x TE buffer and TRIzol™ LS reagent (Thermo Fisher Scientific). The samples were flash frozen in liquid N_2 and broken down with a plastic pestle thrice. Two hundred µL of acid washed glass beads (425 to 600 µm; Sigma-Aldrich®) were added to each sample. Samples were vortexed for one minute and flash frozen in liquid N_2 five times. One hundred µL of chloroform was added and the samples were vortexed for 15 seconds. Samples were incubated at room temperature for five minutes and centrifuged at 12 000 g for five minutes at 4 ° C. The supernatant was recovered in a Phasemaker™ tube (Invitrogen®, Life Technologies Inc.) and centrifuged again at 12 000 g at 4 ° C for 15 minutes. The aqueous phase was transferred to a sterile Eppendorf tube. Two hundred and fifty µL ice-cold isopropanol was added and the samples were centrifuged 12 200 g at 4 ° C for 30 minutes. The samples were placed at - 20 ° C overnight for RNA precipitation.

Samples were removed from - 20 ° C and centrifuged at 12 200 g for 30 minutes at 4 ° C. The supernatant was removed. The RNA pellet was washed with 1 mL of 75 % ethanol and centrifuged at 12 200 g for 10 minutes twice at 4 ° C. The ethanol supernatant was removed, and the samples dried in a fume hood for several hours until all remaining ethanol evaporated. The RNA pellet was resuspended in 0.1 x TE buffer and incubated at 55 ° C to resolubilize. The RNA samples were treated with the Invitrogen DNA-free kit (Invitrogen®, Life Technologies Inc.) following the manufacturer's instructions. The RNA concentration was assessed via NanoDrop™ One^C spectrophotometer (Thermo Fisher Scientific), and the RNA quality was

determined on native agarose gel. Complementary DNA (cDNA) was obtained by reverse transcription using the SuperScript™ VILO™ mix (Thermo Fisher Scientific). Prepared cDNA was serially diluted for ddPCR analysis and frozen at - 80 ° C.

Droplet digital PCR primer design

The PCR primers for *Dim*Pgp-11 and the three reference genes were prepared using NCBI Primer-BLAST (Table S1). The nucleotide sequences and primers were blasted against the entire *D. immitis* genome. The primer design parameters included the following: PCR size between 70 – 150 base pair (BP), forward and reverse primer melting temperature (T_M) difference $\leq$ 3 ° C, "GC" content $\geq$ 40 %, T_M between 50 – 65 ° C, and no BP $\geq$ 3. Three sets of primers were prepared and tested for each gene. Primer validation was performed by quantitative PCR (qPCR) melt curve and droplet digital PCR (ddPCR) thermogradient.

Droplet digital PCR quantification of DimPgp-11 constituitive expression

*Dim*Pgp-11 constitutive expression quantification was determined using ddPCR. The samples were prepared in three biological replicates and plated in two technical replicates per isolate. The ddPCR master mixes, prepared for *Dim*Pgp-11 and the three reference genes, *Dim*GAPDH, *Dim*Actin, *Dim*pmp-3, comprise QX200™ ddPCR™ EvaGreen Supermix (Bio-Rad, Ltd), the forward and reverse primers, cDNA sample, and nuclease-free water. The PCR master mix of each sample was mixed with droplet generation oil (Bio-Rad, Ltd) and partitioned into 20 000 nanoliter-sized droplets by a QX200™ Droplet Generator (Bio-Rad, Ltd). The new sample emulsions were plated on a 96 – well plate using a multichannel pipette and heat sealed with a foil heat seal to undergo standard PCR amplification (Table S2). Following the PCR amplification each sample was read with the QX200™ Droplet Reader (Bio-Rad, Ltd) to determine the target concentration using Poisson's statistics.

Statistical analysis of DimPgp-11 constitutive expression

The ddPCR results of *Dim*Pgp-11 constitutive expression were analysed by normalizing copy numbers against the geometric mean of the copy numbers of the three reference genes: *Dim*GAPDH, *Dim*Actin, and *Dim*pmp-3. All experiments were performed in three biological replicates. All data is reported as mean fold change, with error bars corresponding to the standard deviation of three biological replicates. The replicates for the five isolates were prepared at a concentration of 100 000 mf. The known ML-susceptible Missouri isolate was used as the 1 – fold expression standard. The significance of the fold changes in constitutive expression were compared to the Missouri isolate and were analyzed by parametric unpaired t-test with Welch correction, two-tailed p value, and 95 % confidence interval using Prism 9.3.0c (Graph Pad Software, Inc.).

***Dim*Pgp-11 immunofluorescence assay**

Antibody design and validation

The amino acid sequences of the three *D. immitis* Pgps: *Dim*Pgp-3, *Dim*Pgp-10, and *Dim*Pgp-11 were collected from WormBase ParaSite (Godel et al. 2012, Howe et al. 2016, 2017). Multiple sequence alignment of the *D. immitis* Pgps was performed using ExPASy – BoxShade (Figure 1a) (Gasteiger et al. 2003). The topology of the full length *Dim*Pgp-11 protein sequence across the membrane bilayer was visually represented using Protter (Omasits et al 2013). The transmembrane helices and 9 N-glycosylation motifs were represented as predicted by the program.

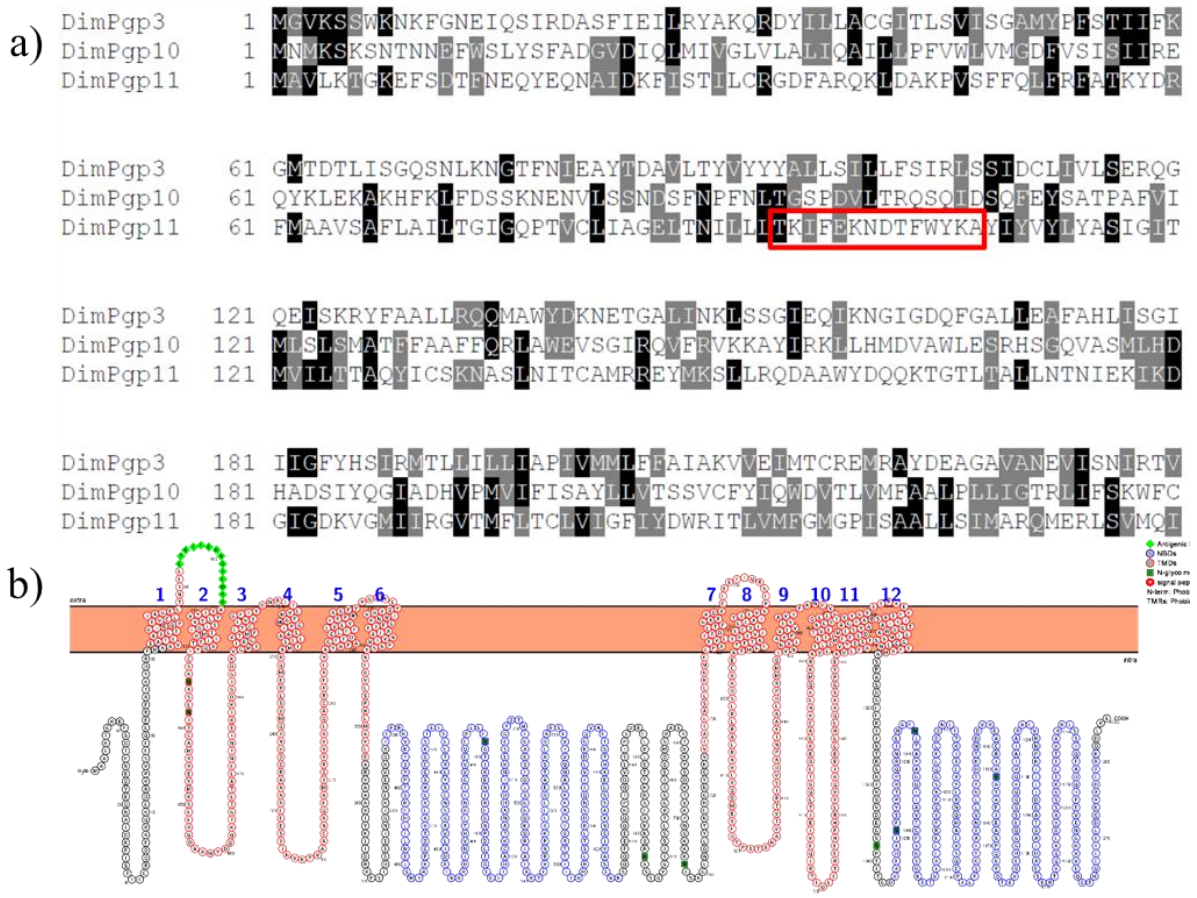

Figure 1 a) Multiple Sequence alignment of *Dirofilaria immitis* P-glycoprotein 3, P-glycoprotein 10, and P-glycoprotein 11 amino acid sequences. The protein regions chosen as the antigenic determinant is highlighted in red. Visualization prepared using the ExPASy BoxShade (embnet.vital-it.ch/software/BOX_form.html). b) 2D visualization of *Dirofilaria immitis* P-glycoprotein 11. The sequence of the transmembrane domains (TMDs), TMD1 (residues 64 – 354) and TMD2 (residues 726 – 1012) are framed in red. The nucleotide binding domains (NBDs), NBD1 (residues 389 – 625) and NBD2 (residues 1045 – 1218), are framed in blue. Putative N-glycosylation motifs (Asn 100, 134, 138, 478, 663, 706, 1051, 1067, 1161) are highlighted in dark green. The peptide region chosen as the antigenic determinant, the first extracellular loop of the first transmembrane domain, is highlighted in light green diamonds. Visualization prepared using the Protter interactive protein visualization tool.

The peptide target of the *Dim*Pgp-11 antigen affinity antibody, LTKIFEKNDTFWYK, located in the first extracellular loop of the first transmembrane domain (TMD) between helices 1 and 2, was isolated (Figure 1b). The chosen sequence was blasted against the entire *D. immitis* genome to confirm the sequence specificity to *Dim*Pgp-11. All information, including the *Dim*Pgp-11 molecular weight, at ~140 kDA, was reported to GenScript®. GenScript® analyzed the suitability and specificity of the antigen, and subsequently prepared an antibody which indicated high specificity to the target peptide. The antigen affinity antibody was further validated via Western blot and Competitive binding assay in *D. immitis* membrane protein lysate and a HEK cell membrane protein lysate control (Figure S1).

Immunofluorescence assay

D. immitis mf were fixed and permeabilized following an adaption of the WormBook Immunohistochemistry tube fixation protocol for *C. elegans*, as described by Moreno et al. in 2010. The mf were centrifuged for five minutes at 1000 g. Freeze-cracking was performed in fixing solution (3.7 % wt / vol paraformaldehyde in PBS) by placing the samples in liquid N_2 for 2 minutes and thawing in a 37 ° C water bath, three times. The samples were incubated in the paraformaldehyde fixative on a shaker for 4 hours at 4 ° C. The samples were centrifuged and washed three times with PBST (0.1 % Triton X - 100 in PBS). To permeabilize the mf cuticle, the samples were resuspended in fresh β - mercaptoethanol and incubated overnight at 37 ° C. The samples were then washed extensively in PBST. Worms were incubated for three hours in collagenase solution (1000 U / mL collagenase type XI (Sigma-Aldrich®)), 1 mM $CaCl_2$, 0.1 % Triton X - 100, 100 mM Tris, pH 7.4) at 37 ° C. The mf were washed with PBST and then incubated overnight with antibody diluent solution (AbD) (0.1 % BSA, 0.1 % sodium azide in PBST).

The incubation with the *Dim*Pgp-11 1 ° affinity-purified antibody in AbD (1 : 100; GenScript®) was performed for three days at 4 ° C. The unbound 1 ° antibody was removed by several washes in AbD and incubated overnight at 4 ° C. The incubation with 2 ° AlexaFluro 488 antibody diluted in AbD (1 : 1000; Invitrogen®, Life Technologies Inc.) was performed for 12 hours at 4 ° C. The unbound 2 ° antibody was removed by several washes in AbD and incubated overnight at 4 ° C. Rhodamine-phalloidin (200 ng / mL; Cytoskeleton Inc.) and Dapi (50 ng / mL; Sigma-Aldrich®) were used to counterstain the muscle tissue and cell nuclei, respectively, by overnight incubation. The samples were washed in AbD and incubated overnight. The fully stained mf samples were fixed in Mounting Media (Sigma-Aldrich®) on slides. The slides were observed on a Nikon A1R MP confocal microscope (Figure S2, Figure S3). The control observation of mf with omission of 1 ° antibody was also tested (Figure S4).

Results

*Dim*Pgp-11 genetic polymorphism in ivermectin resistant *Dirofilaria immitis*

The SNP marker on *DimPgp-11* was analyzed in the following *D. immitis* isolates: the ML-susceptible Missouri, MP3, and Yazoo; and the ML-resistant JYD-34 and Metairie. The three susceptible isolates had an alternate allele frequency ranging between 0 – 12 %, while it was ranging from 36 – 40 % in the two resistant isolates (Table 2). The previously described USA laboratory-maintained ML-susceptible isolates Berkeley, Georgia II, GCFL, and ZoeAL shown an alternate allele frequency ranging between 0 – 15 %; and the ML-resistant WildCat and ZoeAMAL isolates had alternate allele frequencies ranging between 17 – 56 % (Table 2) (Bourguinat et al. 2017, Curry et al. 2022a). The MiSeq results of the ML-susceptible Missouri, MP3, and Yazoo; and the ML-resistant JYD-34 and Metairie fall within the the range of these previously described isolates.

Table 2 The alternate allele frequency of the *Dirofilaria immitis* P-glycoprotein 11 SNP marker, scaffold nDi.2.2.scaf00004 at position 79766, in the ML-susceptible isolates Missouri, MP3, Yazoo, Berkeley, Georgia II, GCFL, and ZoeAL; and the ML-resistant isolates JYD-34, Metairie, WildCat, and ZoeAMAL compared to the *Dirofilaria immitis* reference genome nDi.2.2.

D. immitis Isolate	ML-Susceptibility Phenotype	Alternate Allele Frequency (%)
Missouri	Susceptible	12
MP3	Susceptible	0
Yazoo	Susceptible	0
Berkeley[a]	Susceptible	15
Georgia 2[a]	Susceptible	6
GCFL[b]	Susceptible	4
ZoeAL[b]	Susceptible	3
JYD-34	Resistant	40
Metairie	Resistant	36
WildCat[a]	Resistant	56
ZoeAMAL[b]	Resistant	17

[a] MiSeq analysis performed in 2021 (Curry et al. 2022a)
[b] MiSeq analysis performed in 2017 (Bourguinat et al. 2017)

Droplet digital PCR primer design and validation

The primers for *Dim*Pgp-11 and the three reference genes were tested and validated using the known ML-susceptible Missouri isolate (Maclean et al. 2017). Three sets of primers were designed for each gene. Each set of primers was first tested via qPCR. cDNA dilutions were prepared at 1 : 1, 1 : 5, 1 : 25, 1 : 125. Those with a single melting curve, indicating amplification of a single discrete product were subsequently validated with ddPCR. The cDNA dilutions utilized in the ddPCR analysis were chosen based on the qPCR cycle. The ddPCR thermogradient cycle ranged from 51 – 63 ° C and was utilized to determine ideal annealing temperature. The *Dim*Pgp-11 primers were designed to not include the SNP found in the second

transmembrane domain. The ideal annealing temperature for the *Dim*Pgp-11 primer set was 55.7 ° C (Table S2, Figure S5).

The three housekeeping genes utilized in ddPCR analysis were *Dim*Actin, *Dim*GAPDH, and *Dim*pmp-3. *D. immitis* currently does not have a set of known high quality reference genes. Six genes were analyzed to choose the optimal reference genes: Actin, GAPDH, pmp-3, Histone H3, cdc-42, and Y45F10D.4. These genes were chosen because they have been previously multi-software validated as high-quality reference genes for *C. elegans* and *Brugia malayi* via geNorm, NormFinder, BestKeeper, and Comparative ΔCt (Li et al. 2004, Hoogewijs et al. 2008, Zhang et al. 2012). Three sets of primers were prepared for each of the six genes. All six genes underwent qPCR melt curve analysis. Of the six genes tested, 4 genes had clean melt curves in the *D. immitis* samples: *Dim*Actin, *Dim*GAPDH, *Dim*pmp-3, and *Dim*Histone H3. The four potential reference genes then underwent ddPCR thermogradient analysis. The four reference genes demonstrated clean droplet separation indicating there was no non-specific amplification. The *Dim*Actin, *Dim*GAPDH, and *Dim*pmp-3 were selected at an annealing temperature at 58.4 ° C. *Dim*Histone H3 had an ideal annealing temperature at 51 ° C and was not used in subsequent analysis (Figure S5).

Quantification of *Dim*Pgp-11 constitutive expression

Constitutive expression of *Dim*Pgp-11 was measured in mf from five *D. immitis* isolates: the susceptible Missouri and Berkeley isolates, the putative susceptible Georgia III and Big Head isolates, and the ML-resistant isolate JYD-34 (Maclean et al 2017, McTier et al. 2017, Curry et al. 2022a). The known ML-susceptible Missouri isolate was set as the 1 – fold standard, as it is a well characterized ML-susceptible isolate (Maclean et al. 2017). The fold expression reported is the mean fold change of three biological replicates (Figure 2).

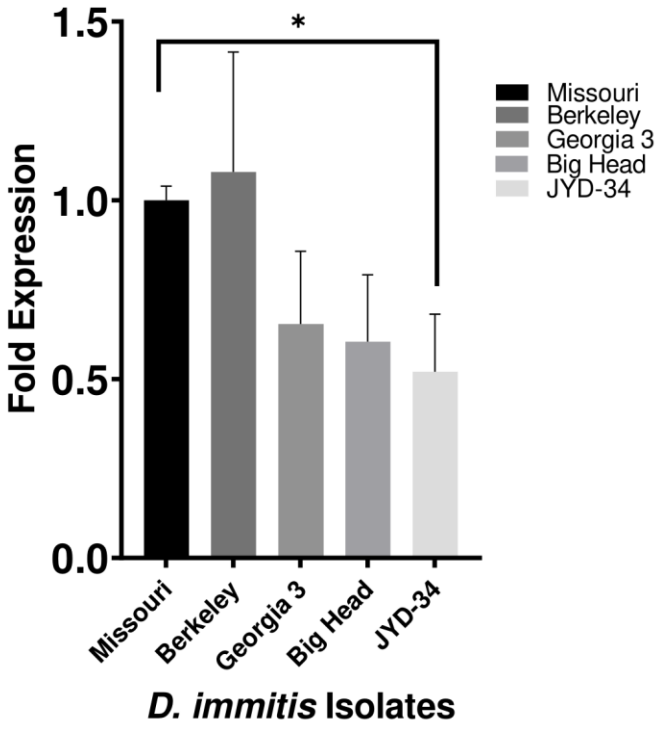

Figure 2 Constitutive expression of *Dirofilaria immitis* P-glycoprotein 11 in the mf lifestage of the Missouri, Berkeley, Georgia III, Big Head, and JYD-34 isolates determined using droplet digital PCR. The changes in constitutive expression were calculated relative to the ML-susceptible Missouri isolate, set as the 1 – fold control. The copy numbers of DimPgp-11 were normalized to the copy numbers of the three reference genes: DimGAPDH, DimActin, and Dimpmp-3. All data are reported as mean fold change, with error bars corresponding to the standard deviation of three individual replicates. The three biological replicates of each of the five USA laboratory-maintained isolates were prepared at a concentration of 100 000 mf. The significance of the constitutive expression fold changes relative to the Missouri isolate was analyzed by parametric unpaired t-test with Welch correction, two-tailed p value, and 95 % confidence interval using Prism 9.3.0c (Graph Pad Software, Inc.).

When compared to the Missouri isolate reference, the ML-susceptible Berkeley isolate, and the two putative-susceptible isolates did not show statistically significant differences in

*Dim*Pgp-11 constitutive expression (Figure 2). Interestingly, the ML-resistant JYD-34 isolate demonstrated a statistically significant decrease in *Dim*Pgp-11 constitutive expression when compared to the Missouri isolate ($P = 0.03$; Figure 2).

_Dim_Pgp-11 immunofluorescence assay

The validated polyclonal antibody was used in an immunofluorescence assay (IFA) to localize *Dim*Pgp-11 in the mf lifestage of the ML-susceptible Missouri isolate. The mf were counterstained with Rhodamine-phalloidin and Dapi which distinguished major anatomical figures such as the mouth, excretory pore, excretory cell, inner body, anus, and tail (Figure 3, Figure S2, Figure S3). *Dim*Pgp-11 was strongly expressed in the pore and duct cells which surround the excretory-secretory pore (ESP), the excretory cell, and more faintly along the mf body wall.

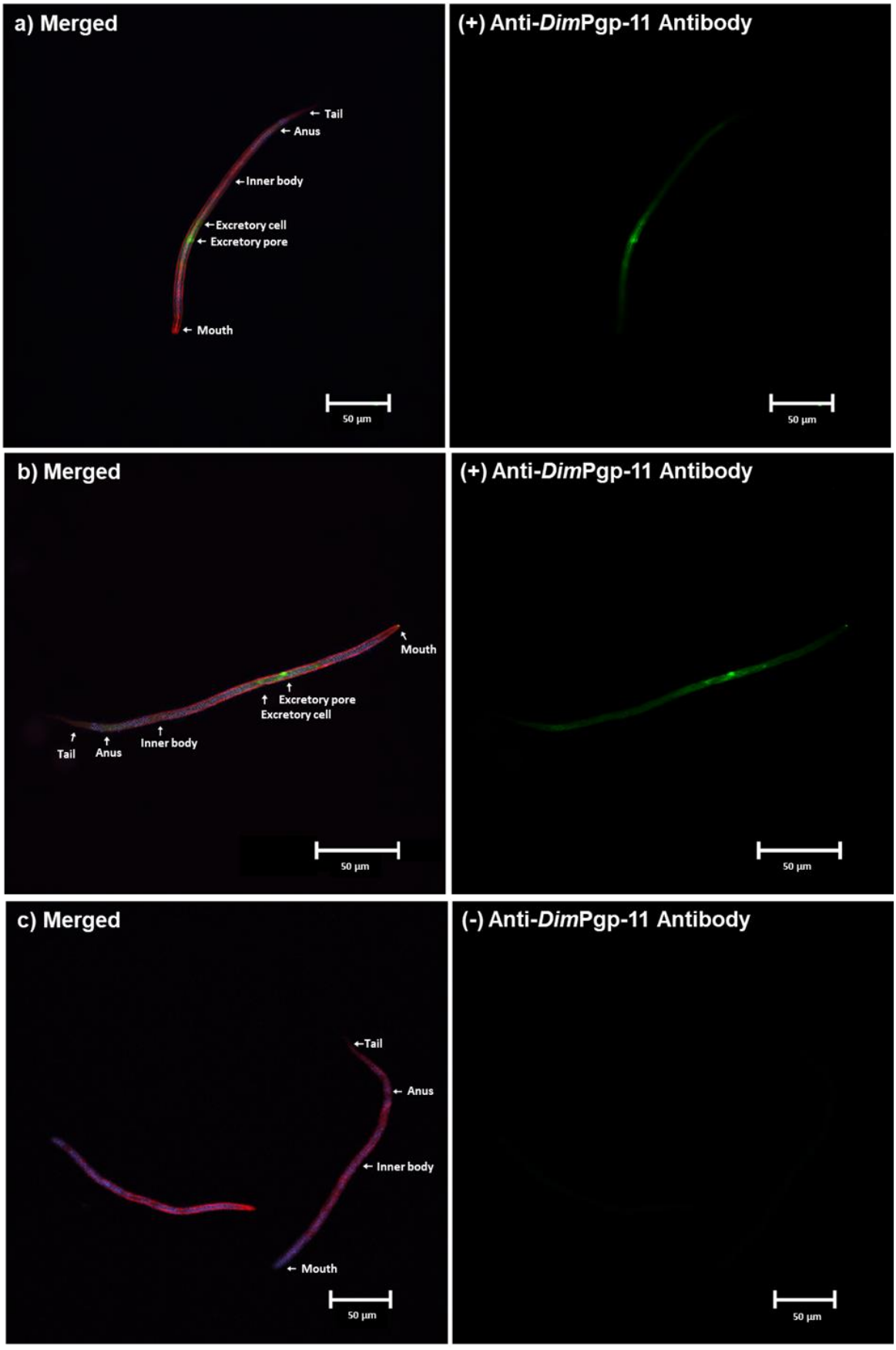
a) Merged
← Tail
← Anus
← Inner body
← Excretory cell
← Excretory pore
← Mouth
50 µm
(+) Anti-*Dim*Pgp-11 Antibody
50 µm
b) Merged
Mouth
Excretory pore
Excretory cell
Tail
Anus
Inner body
50 µm
(+) Anti-*Dim*Pgp-11 Antibody
50 µm
c) Merged
←Tail
← Anus
← Inner body
← Mouth
50 µm
(-) Anti-*Dim*Pgp-11 Antibody
50 µm

Figure 3 Immunofluorescence assay of *Dim*Pgp-11 in *Dirofilaria immitis* mf by confocal laser microscopy. *Dim*Pgp-11 specific signals detected in proximity to the ESP, excretory cell and faintly within the body wall with 1 ° *Dim*Pgp-11 antigen affinity antibody and the 2 ° AlexaFluro488 antibody (green). Counterstaining of Actin with Rhodamine-Phalloidin (red), and cell nuclei with Dapi (blue) distinguished major anatomical features such as the mouth, excretory pore, excretory cell, inner body, anus, and tail in merged immunofluorescence images. a) *Dim*Pgp-11 localization in Worm 1 and b) *Dim*Pgp-11 localization in Worm 2. c) Non-primary antibody control. The non-primary antibody control was incubated in antibody diluent rather than the 1 ° *Dim*Ppg-11 antigen affinity antibody and then incubated with 2 ° AlexaFluro488 antibody. The absence of immunostaining confirms the specificity of the *Dim*Pgp-11 signal observed in Worm 1 (a) and 2 (b).

Discussion

The SNP changes on *Dim*Pgp-11 between the ML-susceptible and ML-resistant *D. immitis* populations were one of the first genetic markers of ML resistance (Bourguinat et al. 2011b). The *Dim*Pgp-11 was among the top 10 SNP markers validated in US clinical samples and was similarly one of the 42 nodes used to assess the genetic profiles of ten *D. immitis* isolates with known ML-susceptible or ML-resistant phenotypes to dirofilariosis preventives (Bourguinat et al. 2017, Ballesteros et al. 2018). In the current study we have confirmed differences in the frequency of the alternative nucleotide on scaffold nDi.2.2.scaf00004 at position 79766, *Dim*Pgp-11 SNP, between USA laboratory-maintained ML-susceptible and ML-resistant isolates. The ML-resistant isolates showed higher alternate allele frequencies in comparision to the reference genome and the ML-susceptible isolates (Bourguinat et al, 2017, Curry et al. 2022a).

Our results demonstrate that there are genotypic differences in the *Dim*Pgp-11 gene between ML-susceptible and ML-resistant USA laboratory maintained *D. immitis* isolates. However, the gene sequence and the presense of the *Dim*Pgp-11 SNP marker do not predict the level of expression that can possibly also alter protein activity. We assessed the constitutive expression of *Dim*Pgp-11 in ML-suscpetible and ML-resistant USA laboratory-maintained *D. immitis* isolates via ddPCR analysis. The lower level of *Dim*Pgp-11 constitutive expression in the ML-resistant JYD-34 isolate, when compared to the ML-susceptible Missouri isolate, suggests a possible change in the activity of *Dim*Pgp-11. It is an indication that Pgps are an important factor in ML resistance, as previously reported in other nematodes of veterinary importance nematodes, even if changes in Pgp expression associated with ML resistance are generally an overexpression of the Pgps (James et al. 2009, De Graef et al. 2013, Ménez et al. 2016). Gene transcription, however, is not always a one-to-one indication of expression levels or protein activity. The documented genetic changes on *Dim*Pgp-11, such as the *Dim*Pgp-11 SNP may impact the configuration of the ATP binding sites, and drug efflux activity, possibly changing transporter activity. Conversely, analysis of additional ML-resistant isolates as they become available to academic labs may provide increased clarity on whether this reduction in constitutive expression is associated with an ML-resistant genotype or whether it is specific to the JYD-34 isolate, but not specifically associated with resistance.

The *Dim*Pgp-11 protein was localized in the ML-susceptible Missouri isolate within the excretory-secretory pore / duct cells and excretory cell, and more faintly within the mf body wall. The strategic location of *Dim*Pgp-11 making up the ES system suggests the Pgp may play an active role in regulating ML in the mf ESP.

Since ML resistance in *D. immitis* may depend on several factors, we do not yet fully understand the genetics of ML resistance in *D. immitis,* and a number of genes may make variable contributions to a resistance phenotype. Within a single host producing mf, there will be a number of individual heartworms, each with its own genotype. Thus, *D. immitis* populations are genetically diverse, unlike populations of drug resistant clonal organisms, such as bacteria. Phenotypic susceptibility, using a single ML preventive at a single dose rate, may not be a clear indication of the ML-susceptibility status of each individual worm in a population. Evidence for developing resistance may only become apparent, *in vivo*, if dose response studies are performed. There may be *D. immitis* populations which appear susceptible at a given ML dose rate but may show a shift in susceptibility if a dose response curve is investigated. Recent enzymatic, MiSeq, ddPCR duplex, and microsatellite results have demonstrated that the current definitions used to define "ML-susceptible", and "ML-resistant" isolates lack nuance (Sanchez et al. 2020, Curry et al. 2022b). Apparent phenotypic ML-susceptibility, at a given preventive dose regime may not correlate perfectly with genotypic ML-susceptibility due to the heterologous nature of the population. *Dim*Pgp-11 is possibly one of several genes linked with the development of ML resistance in *D. immitis.* By considering the heterologous *D. immitis* populations and the nature of multigenic drug resistance, *Dim*Pgp-11 may be the first of multiple genes used to assess the genotypic variability and distinguish ML-susceptible, genetically mixed, and ML-resistant isolates.

Conclusion

The first genetic changes found to differentiate ML-susceptible and ML-resistant isolates were SNPs on *Dim*Pgp-11 and this gene remains of interest in understanding ML resistance in *D. immitis*. Constitutive expression of *Dim*Pgp-11 in the ML-resistant JYD-34 isolate was

significantly lower when compared to a well characterized ML-susceptible isolate. The transcription level does not always provide a one-to-one indication of protein activity and drug efflux. However, the site of expression of *Dim*Pgp-11 and the differences in constitutive expression between resistant and susceptible isolates suggest that *Dim*Pgp-11 may help regulate the ESP response to MLs, including the secretion of immunomodulatory molecules. Further analysis is required to review the multiple genetic changes found in the *Dim*Pgp-11 genetic sequence and how these changes may impact protein folding, the configuration of the ATP binding sites, and drug efflux activity.

Declarations

Ethics approval

All experimental procedures were approved by McGill University in accordance with relevant guidelines and regulations.

Availability of data and material

The data presented in this study is included within the article. Bioinformatic files for the Missouri, MP3, Yazoo, JYD-34, and Metairie *Dirofilaria immitis* isolates: SAMN28946274, SAMN28946275, SAMN28946276, SAMN28946277, and SAMN28946278 are openly available on the NCBI Sequence Read Archive as BAM files under BioProject PRJNA847600.

Competing interests

The authors declare that they have no competing interests.

Funding

This research was supported by grant to RP from the Natural Sciences and Engineering Research Council of Canada, Grant ID: RGPIN/2777-2017.

Author Contributions

Emily Curry: Conceptualization, Methodology, Formal analysis, Investigation, Writing – original draft. **Roger Prichard**: Conceptualization, Writing – review & editing, Supervision, Funding acquisition. **Anne Lespine**: Conceptualization, Writing – review & editing, Supervision, Funding acquisition.

Acknowledgements

We thank Kathy Keller and Cristina Ballesteros for their guidance in the development of the protocols and sample preparation. We thank Norma Bautista-Lopez and Ashish Jain for training in confocal microscopy. We thank the FR3 for providing the Missouri, MP3, and Yazoo *D. immitis* isolates. We thank Ray Kaplan of the University of Georgia for providing the Metairie *D. immitis* isolate. We thank TRS Lab Inc. for providing the Berkeley, Georgia II, Georgia III, Big Head, JYD-34, and WildCat *D. immitis* isolates.

Supplementary Information

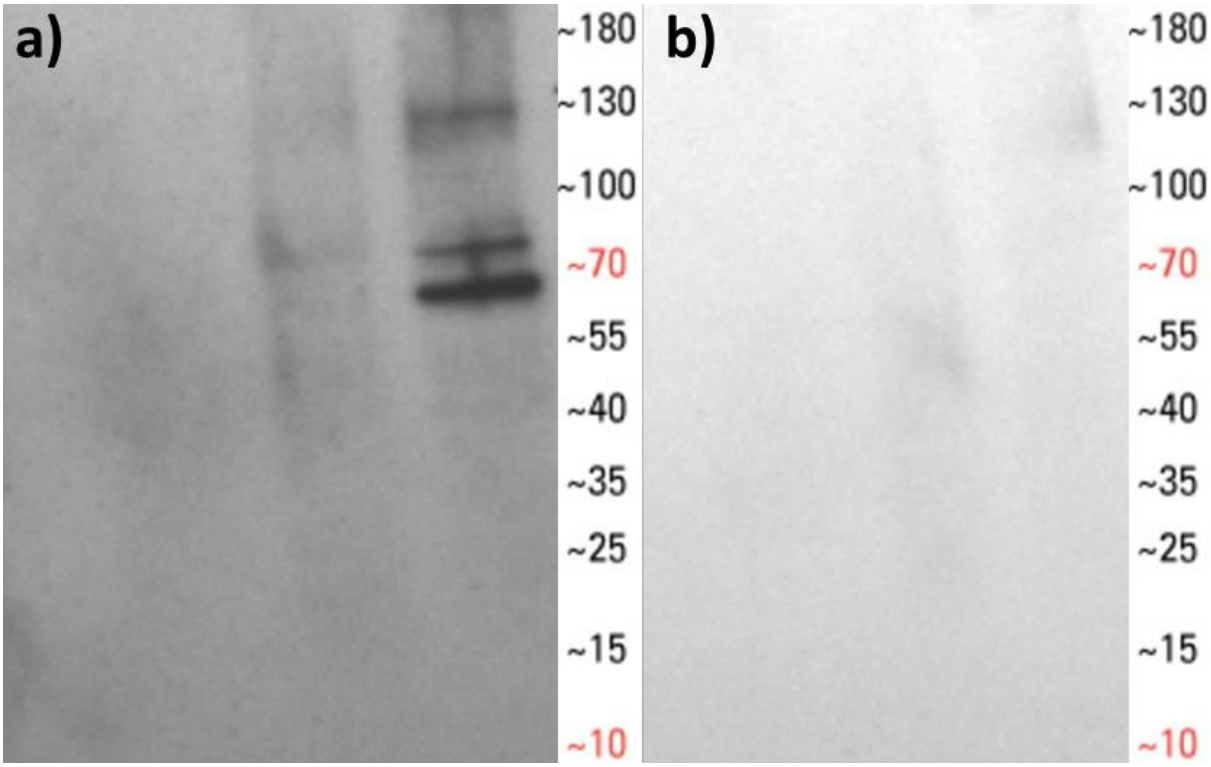

[D] *Dirofilaria immitis* whole membrane protein lysate
[H] HEK Cell whole membrane protein lysate

Figure S1 a) Western Blot analysis of *Dirofilaria immitis* P-glycoprotein 11 (D) from whole membrane protein lysate using anti-*Dim*Pgp-11 1 ° polyclonal antigen affinity antibody (1 : 1000 dilution) and an α-rabbit HRP 2 ° antibody (1 : 5000 dilution) with a HEK cell whole membrane protein lysate (H) negative control. Bands located at *Dim*Pgp-11 molecular weight of ~140 kDa and two bands at ~70 kDA, the molecular half weight of the full-length transporter, and likely proteolytic fragments of the full-length *Dim*Pgp-11; b) Competitive ligand binding assay analysis of anti-*Dim*Pgp-11 1° polyclonal antigen affinity antibody tested with 5X incubation with immunizing peptide (LTKIFEKNDTFWYK), which shows the disappearance of the ~140 kDA full length *Dim*Pgp-11 band and the half-size bands (likely proteolytic fragments).

Table S1 Droplet digital PCR forward and reverse primer sequences for *Dirofilaria immitis* P-glycoprotein 11, and reference genes Actin, GAPDH, and pmp-3.

Gene		**Primer Sequence**
P-glycoprotein 11	Forward	TACGTGAAGCTTGCAGAATA
	Reverse	TTCTGTGTCATATCCCTGTG
Actin	Forward	GTTCACAACCACGGCAGAAC
	Reverse	AAAGCTTCTGGGCATCGGAA
GAPDH	Forward	CGGCCACTCAGAAGACTGTT
	Reverse	GTTGGCACACGAAAGCCAT
pmp-3	Forward	TACTGTCCCATCCTCAGTAG
	Reverse	TAAGTGACCTTGTTTGCCAT

Table S2 Droplet digital PCR amplification cycle for constitutive expression quantification of *Dim*Pgp-11.

Steps	**1**	**2**	**3**	**4**	**5**	**6**	**7**	**8**
Temp	95 ° C	95 ° C	55.7 ° C[a]	72 ° C	Go To Step 2	4 ° C	90 ° C	12 ° C
Time (min)	5:00	0:30	1:00	0:30	49 X	5:00	5:00	∞

[a] 55.7 ° C for *Dim*Pgp-11 samples; 58.4 °C for *Dim*Actin, *Dim*GAPDH, and *Dim*pmp-3

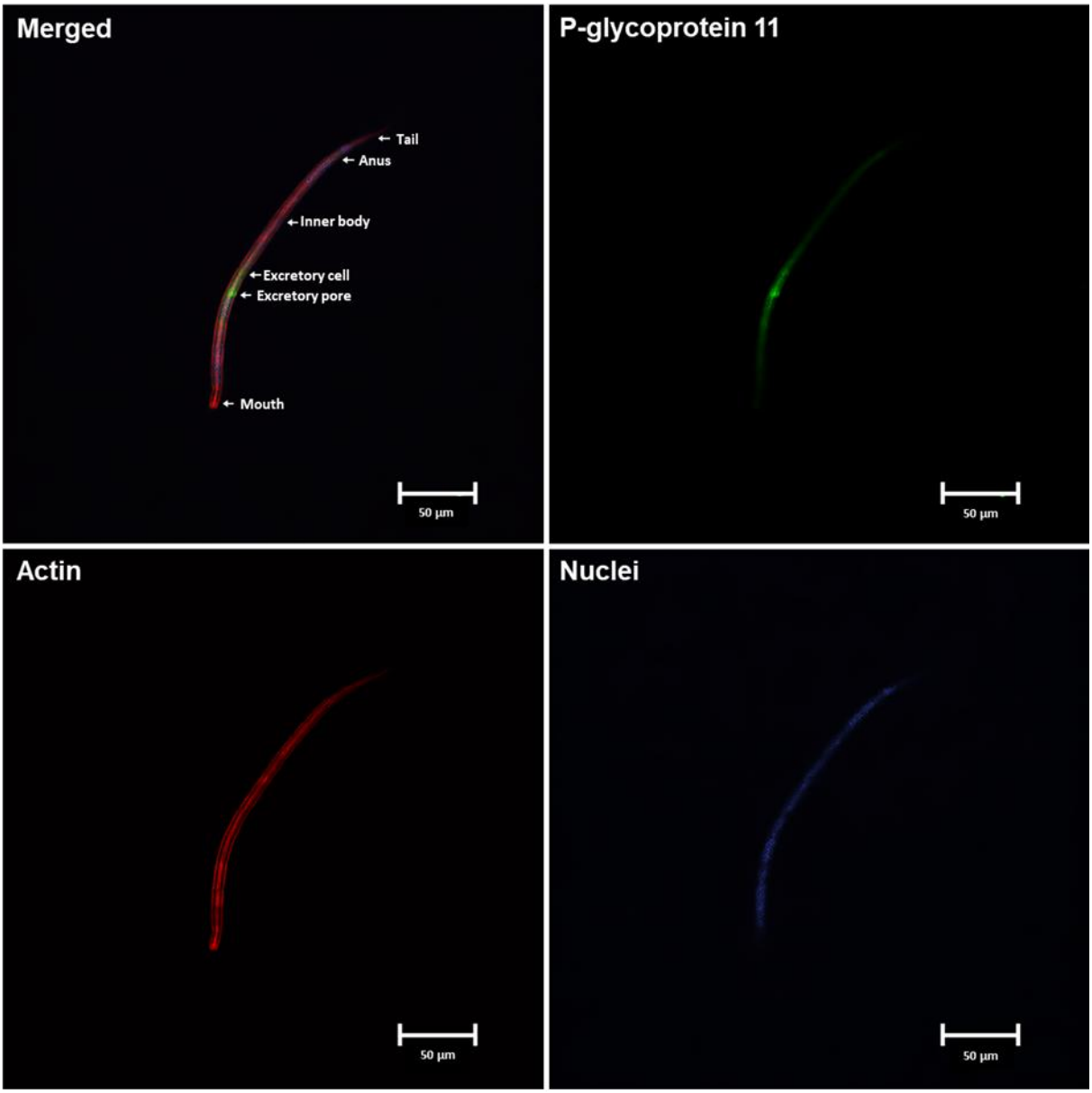

Figure S2 Immunofluorescence assay of *Dim*Pgp-11 in *Dirofilaria immitis* mf by confocal laser microscopy. *Dim*Pgp-11 specific signals was detected in proximity to the ESP, excretory cell and faintly within the body wall using the 1 ° *Dim*Pgp-11 antigen affinity antibody and the 2 ° AlexaFluror 488 antibody (green). Actin was counterstained with Rhodamine-Phalloidin (red), and nuclei were counterstained with Dapi (blue). The counterstain controls distinguish major anatomical features such as the mouth, excretory pore, excretory cell, inner body, anus, and tail.

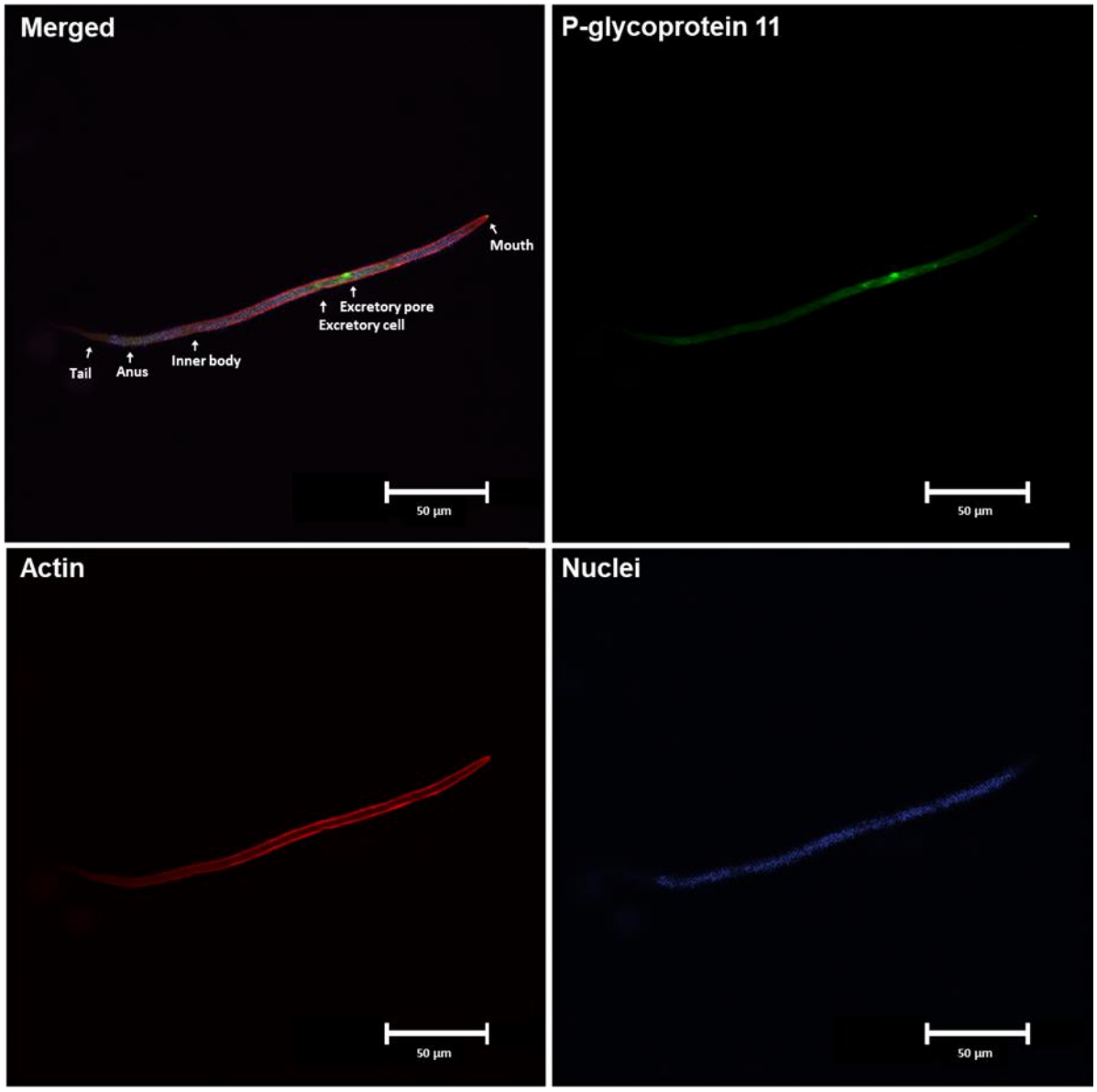

Figure S3 Immunofluorescence assay of *Dim*Pgp-11 in *Dirofilaria immitis* mf by confocal laser microscopy. *Dim*Pgp-11 specific signals was detected in proximity to the ESP, excretory cell and faintly within the body wall using the 1 ° *Dim*Pgp-11 antigen affinity antibody and the 2 ° AlexaFluror 488 antibody (green). Actin was counterstained with Rhodamine-Phalloidin (red), and nuclei were counterstained with Dapi (blue). The counterstain controls distinguish major anatomical features such as the mouth, excretory pore, excretory cell, inner body, anus, and tail.

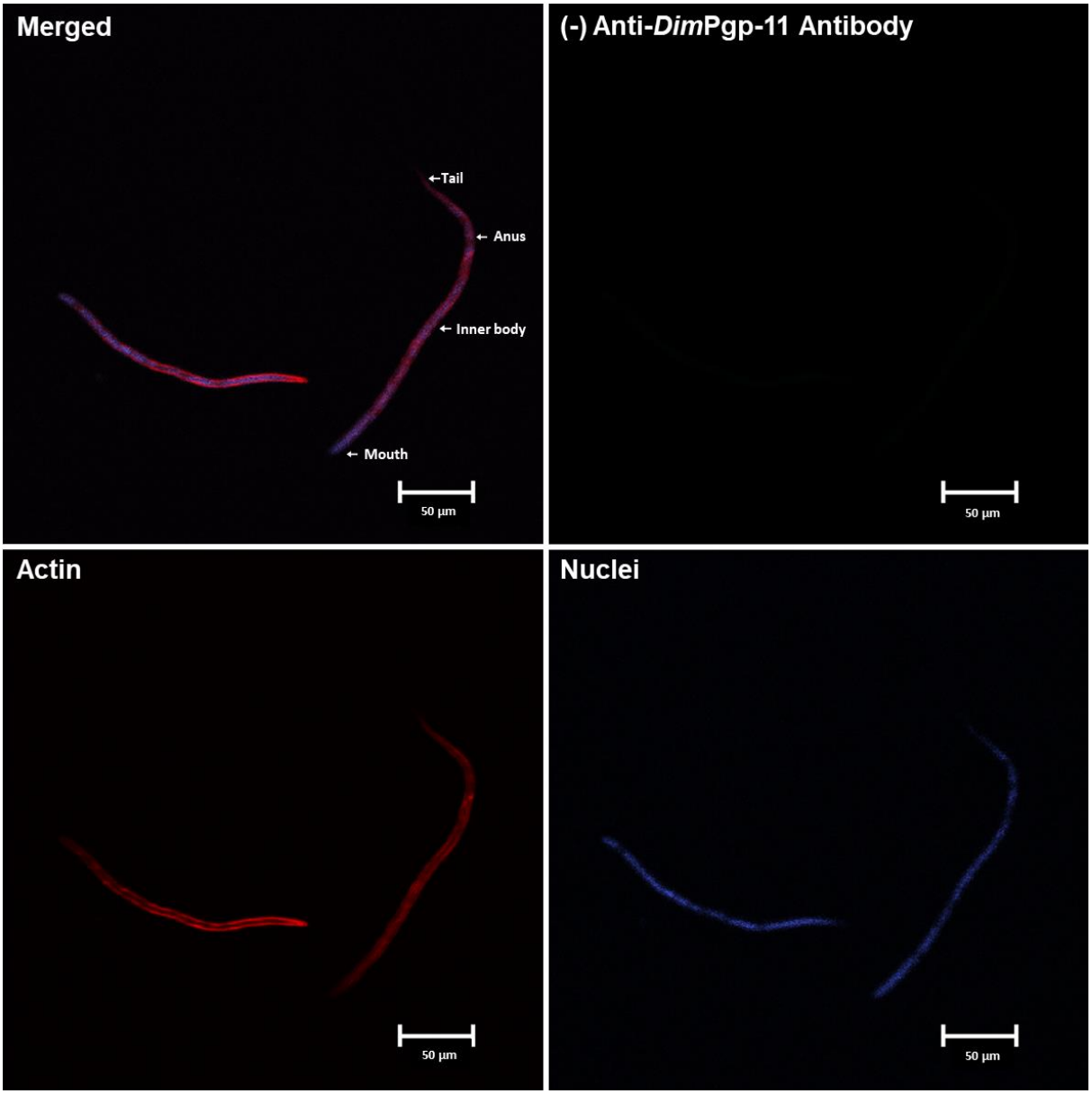

Figure S4 Non-primary antibody control of immunofluorescence assay of *Dim*Pgp-11 in *Dirofilaria immitis* mf by confocal laser miroscopy. Samples were incubated in antibody diluent rather than 1 ° *Dim*Ppg-11 antigen affinity antibody and the 2 ° AlexaFluro488 antibody. The absence of immunostaining confirms the specificity of the signal. Actin was counterstained with Rhodamine-Phalloidin (red), and nuclei were counterstained with Dapi (blue). The counterstain controls distinguish major anatomical features such as the mouth, excretory pore, excretory cell, inner body, anus, and tail.

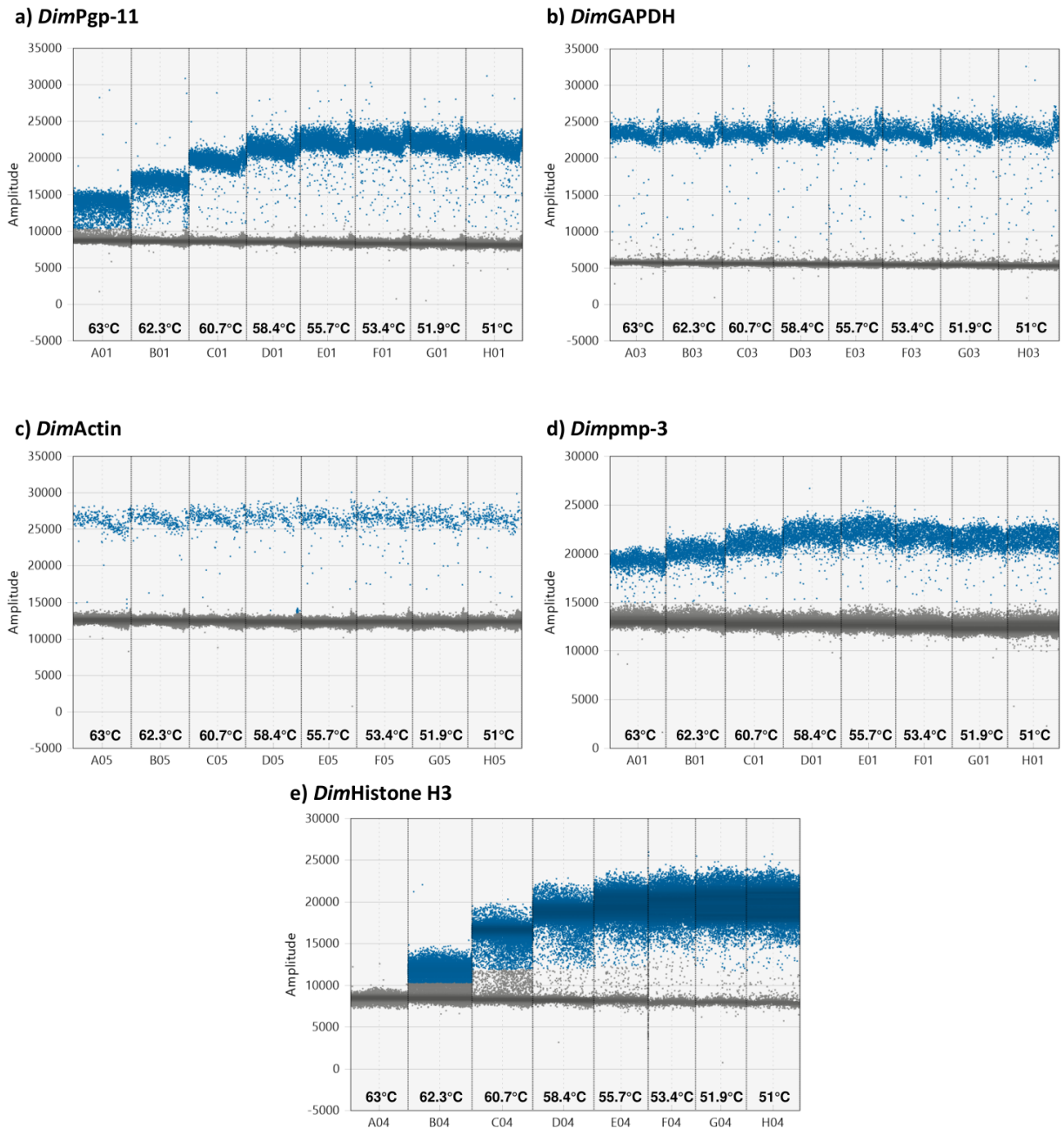

Figure S5 Raw thermogradient (51 ° C – 63 ° C) constitutive expression data of a) *Dirofilaria immitis* Pgp-11 and b) *D. immtis* GAPDH c) *D. immitis* Actin d) *D. immitis* pmp-3 e) *D. immitis* Histone H3 in the Missouri isolate determined using droplet digital PCR.

Connecting Statement II

Chapter 3 provided an extensive characterization of *Dirofilaria immitis* P-glycoprotein 11 (*Dim*Pgp-11). The MiSeq sequencing results indicated the *Dim*Pgp-11 single nucleotide polymorphism (SNP) molecular marker is still associated with ML resistance in USA laboratory-maintained *D. imminits* isolates. The link between *Dim*Pgp-11 and ML resistance was further supported by the lower constitutive expression of *Dim*Pgp-11 in the ML-resistant JYD-34 isolate compared to the ML-suscpetible isolates. The expression sites of *Dim*Pgp-11 were strategically located, for the first time, in the musculature surrounding the mf ESP where it could potentially play a role in ML efflux.

D. immitis is a non-model organism. The molecular biology techniques, reference genes, primers, and antibodies used in Chapter 3 were optimized and designed *de novo* to assess the impact of genetic polymorphisms on constitutive gene expression. These protocols are not exclusive to *Dim*Pgp-11. Chapter 4 expands upon the methodologies optimized in Chapter 3 to characterize a newly identified SNP molecular marker located on the *D. immitis* kynureninase (*Dim*KYNU-1) gene which is differentially expressed in ML-resistant isolates. *Dim*KYNU-1 is an enzyme found along the tryptophan catabolism L-kynurenine (KYN) pathway. It is a precursor molecule to the biosynthesis of rhodoquinone (RQ), the election carrier of an alternative anaerobic metabolism utilized by helminths. Chapter 4 provides an extensive study on the genetic polymorphism of *Dim*KYNU-1, and the differential constitutive expression of *Dim*KYNU-1 and its downstream product 3-hydroxyanthranilic acid (3HA) in *D. immitis* USA laboratory-maintained isolates with different ML-susceptibility profiles.

Chapter 4.

Genetic polymorphism and differential expression of the integral tryptophan catabolism component kynureninase in *Dirofilaria immitis*.

Emily Curry[1], Cristina Ballesteros[1,2] Anne Lespine[3], and Roger Prichard[1*]

[1] Institute of Parasitology, McGill University, Sainte Anne-de-Bellevue, QC, Canada

[2] Charles River Laboratories Montreal ULC, Laval, QC, Canada

[3] INTHERES, Université de Toulouse, INRAE, ENVT, 31027 Toulouse Cedex 3, France

EC: emily.curry@mail.mcgill.ca

CB: cristina.ballesteros@crl.com

AL: anne.lespine@inrae.fr

RP: roger.prichard@mcgill.ca

In preparation

Abstract

Background: Dirofilariosis is a potentially fatal pulmonary infection of canids caused by the parasitc helminth *Dirofilaria immitis*. The adult lifestage lives in the pulmonary artery and right side of the heart, where it can survive for up to seven years. This lifestage of the nematode utilizes an alternative anaerobic metabolism which requires the election carrier rhodoquinone (RQ). The biosynthesis of RQ is derived from the tryptophan catabolism L-kynurenine (KYN) pathway. KYNU-1, encoding the kynureninase gene, catalyzes the synthesis of 3-hydroxyanthranilic acid (3HA) which provides the critical amine group to the RQ quinone ring. KYNU-1 is essential for RQ production. In this work we provide an extensive study on a newly identfied genetic polymorphism and the differential constitutive expression of *Dim*KYNU-1 in *D. immitis* USA laboratory-maintained isolates.

Methods: We examined a single nucleotide polymorphism (SNP) on *Dim*KYNU-1 via MiSeq analysis, in the ML-susceptible Missouri, MP3, Berkeley, Yazoo, GCFL, and Georgia II; and the ML-resistant JYD-34, Metairie and WildCat isolates. The constitutive expression of *Dim*KYNU-1 was measured in the adult females and adult males of the ML-susceptible Kentucky isolate and the ML-resistant JYD-34 isolate via droplet digital PCR (ddPCR) and RNASeq comparative transcriptomic analysis. The constitutive expression of the *Dim*KYNU-1 downstream product, 3HA, was measured in the adult females and adult males of the same two isolates via indirect enzyme-linked immunosorbent assay (ELISA).

Results: We established that the *Dim*KYNU-1 SNP was differentially expressed in the USA laboratory-maintained isolates. The ML-susceptible isolates had an alternate allele frequency between 0 – 16 %, while it ranged between 9 – 62 % in the ML-resistant isolates.

The Kentucky isolate showed a sex-specific differential constitutive expression of *Dim*KYNU-1. The Kentucky adult males expressed *Dim*KYNU-1 approximately 4 – fold greater compared with the adult females ($p < 0.05$). The JYD-34 isolate showed similar expression of *Dim*KYNU-1 for the adults of both sexes. These results were corroborated with comparative transcriptomic analyses. The expression of 3HA was significantly greater in the JYD-34 adult males compared to the JYD-34 adult females ($p < 0.04$) and Kentucky adult females ($p < 0.05$).

Conclusion: Our data demonstrated that the frequency of the *Dim*KYNU-1 SNP alternative allele tended to be higher in ML-resistant isolates compared to the ML-susceptible isolates examined in the current study. A link between the *Dim*KYNU-1 SNP and differential expression of kynureninase was further corroborated by the differential constitutive expression of *Dim*KYNU-1 and 3HA in the adult females and adult males.

Keywords: *Dirofilaria immitis*, dirofilariosis, macrocyclic lactones, resistance, tryptophan catabolism, kynureninase, 3-hydroxyanthranilic acid, RNASeq sequencing, constitutive expression

Background

Dirofilaria immitis is a parasitic filarial nematode and the causative agent of dirofilariosis, a potentially fatal pulmonary infection of canids and felines. Dirofilariosis infections are typically treated preventatively with the administration of a monthly macrocyclic lactone (ML)-based chemoprophylactives (Prichard 2021).The MLs are broad spectrum parasiticides at low dose rates and the sole class of drug approved for the chemoprophylactic treatment of dirofilariosis (Prichard 2021). In *D. immitis* infections the MLs target the developing L3 / L4 larvae, preventing the development of patent infections.

The establishment of dirofilariosis in animals on ML-based chemoprophylaxis can indicate a loss of efficacy (LOE) of the drug and a potentially ML-resistant population. In registration trials the MLs must demonstrate 100 % efficacy in preventing the establishment of a patent infections; thus, in principle, any decrease in efficacy below 100 % could be considered possible resistance. Breakthrough *Dirofilaria* infections were first brought to the USA FDA Center for Veterinary Medicine (FDA / CVM) in 1998; however, it is difficult to prove unequivocally that ML-based chemoprophylactics have been administered wholly in compliance with the recommended treatment schedule (Hampshire 2005). Between 2011 – 2014 ML LOE was demonstated both *in vivo* and *in vitro*, and the heritability of true ML resistance was confirmed in laboratory settings (Bourguinat et al. 2011a, 2011b, Pulaski et al. 2014).

As other species of parasitic nematodes, *D. immitis* has developed resistance to ML-based chemotherapy; however, it is somewhat unique. Unlike other nematodes of importance to veterinary and human health they are found within the blood and circulatory system rather than the gut / intestinal tract or lymphatic system (McCall et al., 2008; Prichard, 2021). The adults reside within the pulmonary artery and right side of the heart (McCall et al., 2008; Prichard, 2021). Once sexually mature the adult worms begin to produce the bloodborne microfilariae (mf) which travel throughout the circulatory system. These two lifestages exist within the host for extended periods of time; the adults can inhabit the definitive mammalian host for upwards of 7 years and the mf for more than 2 years (Manfredi et al., 2007; McCall et al., 2008; Bowman and Atkins, 2009).

Adaptation is crucial for the long-term survival of *D. immitis* within the mammalian host. One of these adaptations is the alternation between an aerobic and anaerobic energy metabolism based on lifestage and environment (Jaffe and Doremus 1970, Köhler 1991, Oliveira and

Oliveira, 2002, Yin et al. 2006, Simón et al. 2012). The bloodborne mf predominantly utilize aerobic metabolism; however, they have been show to be be content in both aerobic and anaerobic conditions *in vitro* (Jaffe and Doremus 1970, Köhler 1991, Simón et al. 2012) The adult worms predominantly utilized anaerobic metabolism (Jaffe and Doremus 1970, Köhler 1991, Oliveira and Oliveira, 2002, Bryant, 2018).

In anaerobic metabolism, the mitochondrial electron transport chain Complex II reverses succinate dehydrogenase activity and acts as a fumarate reductase (Prichard and Schofield, 1968; Prichard, 1970; Van Hellemond et al., 1995; Tielens and Van Hellemond, 1998; Yamashita et al., 2004; Iwata et al., 2008; Müller et al., 2012). This process requires the electron carrier rhodoquinone (RQ), as an alternative to ubiquinone (UQ) utilized in aerobic metabolism. RQ is structurally to UQ; however, it differs due to the presence of an amine group at position 2 on the quinone ring. The presence of the amine group gives RQ a lower redox potential (-63 mV) compared to UQ (110 mV) (Erabi et al., 1976; Unden and Bongaerts, 1997). The lower redox potential of RQ creates the correct electro-potential needed to drive the reverse reactions of anaerobic metabolism. In RQ-dependant anaerobic metabolism RQ receives electrons from NADH through Complex I and donate them to fumarate via Complex II as the final electron acceptor.

The production of RQ in eukaryotes is unique to helminths, molluscs, and annelids (Van Hellemond et al. 1995, Müller et al. 2012, Salinas et al. 2020). In bacteria RQ is derived from UQ (Brajcich et al. 2010, Campbell et al. 2019). It has recently been elucidated that this is not the case in eukaryotes. The biosynthsis of RQ in these organisms is derived from the tryptophan catabolism, L-kynurenine (KYN) pathway (Figure 1) (Buceta et al. 2019, Del Borrello et al. 2019).

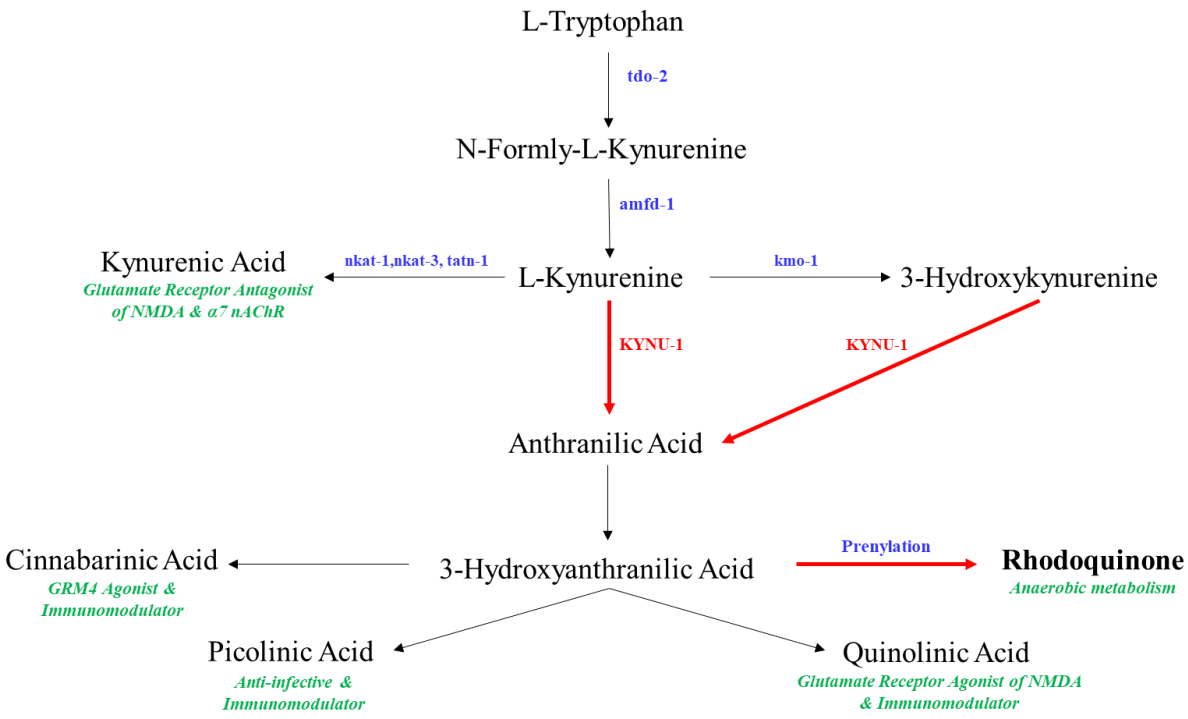

Figure 1 Schematic of the Tryptophan Catabolism pathway

KYNU-1, encoding the kynureninase gene, catalyzes the synthesis of anthranilic acid (AA) and 3-hydroxyanthranilic acid (3HA) from KYN and 3-hydroxykynurenine (3HKYN), respectively (Figure 1). The KYNU-1 downstream product 3HA provides the critical amine group to the RQ quinone ring (Buceta et al., 2019; Del Borrello et al., 2019; Salinas et al., 2020). The KYN pathway also produces metabolites and immunomodulators with important biological effects such as quinolinic acid, picolinic acid, cinnabarinic acid and kynurenic acid (Figure 1).

In the model organism, *Caenorhabditis elegans* dysregulation of the KYN pathway leads to drastically reduced RQ production. Similarly, a deleterious mutation of KYNU-1 results in the abolition of RQ production, indicating that KYNU-1 is essential for RQ biosynthesis (Buceta et al., 2019; Del Borrello et al., 2019). In this work, we analyzed *D. immitis* KYNU-1 (*Dim*KYNU-1) in USA laboratory-maintained isolates with different ML-susceptibility profiles. We identified a new single nucleotide polymorphism (SNP) molecular marker on the *Dim*KYNU-1 gene and

provide information on the constitutive expression of *Dim*KYNU-1 and its downstream product 3HA.

Methods

Dirofilaria immitis isolates

The *D. immitis* mf samples were obtained while host dogs not under drug pressure. The ML-susceptible Missouri, MP3, and Yazoo isolates, as well as the ML-resistant Metairie isolate were provided by the Filariasis Research Reagent Resource Center (FR3) (Maclean et al., 2017). The phenotypically ML-susceptible Berkeley, Georgia II and GCFL; and the ML-resistant isolates WildCat and JYD-34 (mf and adults) were provided by TRS Laboratories (Maclean et al., 2017; McTier et al., 2017; Curry et al., 2022b). The frozen adult Kentucky isolate samples were generously gifted by Zoetis Animal Health. The sample providers, the FR3 and TRS Laboratories, both have the appropriate ethical permissions to house the nematode's lifecycle, including the mosquito colonies and canine definitive hosts. McGill University, where the experiments were conducted, does not house the *D. immitis* lifecycle, but does maintain the required biohazard importation permits from the Canadian Food Inspection Agency (Permit: A-2022-00829-1) to receive and work with the canine blood samples containing *D. immitis* mf.

Dirofilaria immitis microfilariae samples

Canine venous blood samples were shipped to McGill University for processing. The mf were extracted from the blood by filtration as described by Bourguinat et al. (2015). The venous blood was diluted 1 : 1 with NaHCO3 solution, and polycarbonate membrane filters (3.0 µm; 25 mm; Sterlitech® Corporation) were used to isolate mf. A modified Knott's test was performed in duplicate for each sample.

Dirofilaria immitis adult sample

The adult females and adult males of the ML-susceptible Kentucky and ML-resistant JYD-34 isolates were obtained at necropsy and flash frozen in liquid N2 and shipped to McGill University on dry ice. The adult worm samples were stored at - 80 º C.

***DimKYNU-1* genetic polymorphism**

Dirofilaria immitis genomic DNA extraction

Genomic DNA (gDNA) was extracted from pooled mf samples ranging from 25 000 – 150,000 mf. gDNA was extracted using the QIAamp® DNA Micro kit (Qiagen Inc.). The gDNA concentrations were determined with the Quant-iT™ PicoGreen DNA Assay Kit (Invitrogen®, Life Technologies Inc.). The samples were sent to Génome Québec for quality control and MiSeq Illumina sequencing.

DimKYNU-1 SNP marker

A set of primers were designed for the SNP identified on the *Dim*KYNU-1 gene (Forward primer: scaf01096-4740-CS1F TGCTATCTACATGTGTGGTAATTCG; Reverse primer: scaf01096-4740-CS2R TTTTACAGAGAAATCACACTTTTCA).The SNP was located on the intron between exons 9 and 10 at position 4740. The following isolates were analyzed to assess a possible link between the *Dim*KYNU-1 SNP with phenotypic ML susceptibility or resistance in USA laboratory-maintained isolates: the ML-susceptible Missouri, MP3, Berkeley, GCFL, Georgia II and Yazoo; and the ML-resistant, JYD-34, Metairie, and WildCat (Bourguinat et al., 2017; Curry et al., 2022b).

MiSeq Illumina sequencing of DimKYNU-1

The regions encompassing the *Dim*KYNU-1 SNP were sequenced on an Illumina MiSeq Platform, at a coverage of 2000X. The Fluidigm Access Array system was used to perform target enrichment using array-based PCR amplification of the genomic target region. The *D. immitis*

gDNA samples underwent parallel amplification using *Dim*KYNU-1 custom primers. The samples were barcoded during target enrichment, which allowed for multiplexed sequencing, and adapter sequences were added during the PCR amplification reaction.

Trimmomatic software trimmed for trailing quality (30 PHRED score) and filtered for minimum read length by removing the Illumina sequencing adapters from read and adapter clippings (Bolger et al., 2014). The resulting read pairs were aligned to the *D. immitis* reference genome nDi.2.2 (https://parasite.wormbase.org/Dirofilaria_immitis_prjeb1797/) using BWA-mem (http://bio-bwa.sourceforge.net/) to create binary alignment files (BAM) (Li and Durbin, 2009). Picard was used to process the alignments (https://broadinstitute.github.io/picard) for the realignment of indels, mate fixing, and marking of duplicate reads. The base frequencies of the *Dim*KYNU-1 SNP were extracted using BVATools (https://bitbucket.org/mugqic/bvatools/src) and the read frequencies were assimilated to the allele frequencies. The alternate allele variance for the samples were compared to the *D. immitis* reference genome nDi.2.2.

***Dim*KYNU-1 constitutive expression**

Dirofilaria immitis adult RNA extraction

The RNA extraction used a modified TRIZol® protocol. Individual adult worms were placed in petri dishes, cut into 1 cm long pieces using a sterile razor blade, and placed in 15 mL Falcon tubes. The samples were resuspended in a 1 : 4 ratio of 0.1 x TE buffer and TRIzol™ LS reagent (Thermo Fisher Scientific). The adult worms were flash frozen in liquid N2 and disrupted with a homogenizer. This process was repeated five time. RNA was extracted from the samples as previously described (Curry et al., 2022a).

The RNA samples were treated with the Invitrogen DNA-free kit (Invitrogen®, Life Technologies Inc.) following the manufacturer's instructions. The RNA concentration was

assessed via NanoDrop™ OneC spectrophotometer (Thermo Fisher Scientific), and the RNA quality was assessed on native agarose gel. The cDNA was obtained by reverse transcription using the SuperScript™ VILO™ mix (Thermo Fisher Scientific). Prepared cDNA was serial diluted and frozen at - 80 ° C.

Droplet digital PCR quantification of DimKYNU-1 constitutive expression

The constitutive expression of *Dim*KYNU-1, in the adult females and adult males of the ML-susceptible Kentucky isolate and the ML-resistant JYD-34 isolate, was determined via droplet digital PCR (ddPCR) (Forward primer: GAAATGGGCCAACATGGGTG; Reverse primer: GTTCGCTGAGCTCCTACCAA). The samples were prepared in biological triplicate and plated in technical duplicates. Three references genes were used to standardize the expression of *Dim*KYNU-1: *Dim*Actin, *Dim*GAPDH, and *Dim*pmp-3 (Curry et al., 2022a). The ddPCR master mixes for *Dim*KYNU-1 and the reference genes were mixed with droplet generation oil (Bio-Rad, Ltd) and partitioned into 20 000 nanoliter-sized droplets per well by a QX200™ Droplet Generator (Bio-Rad, Ltd). The new sample emulsions were plated on a 96 – well plate using a multichannel pipette and the plate was heat sealed with a pierceable foil. Following standard PCR amplification each sample was analyzed with the QX200™ Droplet Reader (Bio-Rad, Ltd) to determine the target concentration using Poisson's statistics.

Statistical analysis of DimKYNU-1 expression

The *Dim*KYNU-1 constitutive expression for each sample was determined by normalizing the *Dim*KYNU-1 copy number against the geometric mean of the copy numbers of the three reference genes. All data was reported as mean fold change, with error bars corresponding to the standard deviation of three biological replicates. The fold change of *Dim*KYNU-1 constitutive expression in the Kentucky males, JYD-34 females, and JYD-34 males was calculated relative to

the normalized value of the Kentucky females, set as the 1 – fold control. The significance of the difference in constitutive expression compared to the Kentucky female 1 – fold control was determined by parametric unpaired t-test with Welch correction, two-tailed p value, and 95 % confidence interval using Prism 9.3.0c (Graph Pad Software, Inc.).

Comparative Transcriptomics and Tryptophan Catabolism gene expression

D. immitis RNA extraction, library preparation, and NovaSeq sequencing

Four groups were analysed by RNA sequencing: Kentucky adult females, Kentucky adult males, JYD-34 adult females, and JYD-34 adult males. The four groups were analyzed in duplicate, with eight samples total. Total RNA was extracted utilizing the modified TRIZol® protocol described above (Curry et al. 2022a). The RNA concentration of the eight samples was assessed via NanoDrop™ OneC spectrophotometer (Thermo Fisher Scientific). The RNA samples were sent to Génome Québec for quality control and sequencing. Génome Québec conducted bioanalysis of the samples to determine RNA integrity. The RNA samples with an RNA integrity number (RIN) of approximately > 6 were used for messenger RNA (mRNA) stranded library construction. The eight RNA samples underwent NEB mRNA stranded library preparation and Illumina library quality control. Following quantification, the samples underwent Illumina NovaSeq 6000 PE100 sequencing. The samples were barcoded which allowed for multiplexed sequencing, and adapter sequences were added during the PCR amplification reaction. The R1 and R2 fastq files for JYD-34 F1, JYD-34 F2, JYD-34 M1, JYD-34 M2, Kentucky F1, Kentucky F2, Kentucky M1, and Kentucky M2 are openly available on the NCBI Sequence Read Archive under BioProject PRJNA847600.

RNASeq sequencing quality control and read mapping

The Fastq files resulting from the Illumina NovaSeq 6000 PE100 sequencing were assessed using Trimmomatic software to trim for trailing quality (30 PHRED score) and filtered for minimum read length by removing the Illumina sequencing adapters from read and adapter clippings (Bolger et al., 2014). The read pairs were aligned to the *D. immitis* reference genome nDi.2.2 (https://parasite.wormbase.org/Dirofilaria_immitis_prjeb1797/) using BWA-mem (http://bio-bwa.sourceforge.net/) and SAMtools (https://samtools.sourceforge.net/) to create the eight binary alignment files (BAM) (Li and Durbin, 2009). The mapped read counts were summarized using featureCounts (Liao et al., 2014).

The transcript abundance and differential expression analysis was conducted using the R v.4.1.2 edgeR package. The adult females were compared to the adult males of the respective isolates: Kentucky female vs. Kentucky male and JYD-34 female vs. JYD-34 male. The statistically significant differentially expressed transcripts were extracted according to the following criteria: false discover rate (FDR) < 0.05 and a logFC > 1 or < -1.

The top 25 upregulated and top 25 downregulated transcripts identified in the analyses were described using Gene ontology (GO), Panther ID, and Pfam annotation accessed through the WormBase ParaSite Biomart (https://parasite.wormbase.org/biomart/) (Table S1 – 9) (Howe et al., 2016; Howe et al., 2017). WormBase ParaSite was also used to determine the transcript ID of the genes associated with tryptophan catabolism: tryptophan hydrolase (*Dim*tph-1; nDi.2.2.2.t03190), arylformamidase (*Dim*amfd; nDi.2.2.2.t05175), nematode kynurenine aminotransferase (*Dim*nkat; nDi.2.2.2.t08048), tyrosine aminotransferase (*Dim*tatn; nDi.2.2.2.t04992), and *Dim*KYNU-1 (nDi.2.2.2.t09873) (Figure 1).

Validation of transcriptomic sequencing results

The comparative transcriptomic analyses were validated via quantitative PCR (qPCR). The relative differential expression of six randomly selected transcripts were compared. These genes were selected from the JYD-34 female vs. Kentucky female and the JYD-34 male vs. Kentucky male analyses and included genes related to steroid biosynthesis, RNA binding, structural constituents of the cuticle, and a nuclear hormone receptor. The primers for the six genes were designed using NCBI Primer-BLAST using the following criteria: product size between 70 – 150 bp, melting temperature (T_M) 50 – 65 ° C, GC content > 40 %, forward and reverse primer T_M difference < 3 ° C, and no bp repeat > 3 (Table S9). The cDNA was synthesized from the eight original RNA samples sent for Illumina NovaSeq 6000 PE100 sequencing. The transcription level of the selected genes was assessed in biological and technical duplicates using the SYBR® Select Master Mix (Thermo Fisher Scientific). *Dim*Actin, *Dim*GAPDH, and *Dim*pmp-3 were used as the endogenous reference genes (Curry et al. 2022c). The relative fold change of each gene in the ML-resistant JYD-34 isolate was calculated against the ML-susceptible Kentucky isolate using $2^{-\Delta\Delta CT}$ calculations.

3-hydroxyanthranilinic acid expression

Dirofilaria immitis lysate extraction

The expression of 3HA, the downstream product of *Dim*KYNU-1, was measured in the adult females and adult males of the ML-susceptible Kentucky and the ML-resistant JYD-34 isolates (Bourguinat et al., 2017; Maclean et al., 2017; McTier et al., 2017). Individual worms were placed in petri dishes and cut into 1 cm long pieces using a sterile razor blade and then placed in 15 mL Falcon tubes. The worms were suspended in 900 µL PBS and 100 µL 10 x Protease Inhibitor. The samples were flash frozen in liquid N2 and homogenized with a homogenizer five times. The soluble lysate was extracted into the PBS on a shaker overnight at 4 ° C.

The next day the samples were transferred to ultracentrifuge safe tubes, weighed, and balanced with PBS to two significant figures. The samples were spun at 20 000 rpm for 60 minutes at 4 ° C using the Tabletop Ultracentrifuge, Beckman # OPTIMAX with the TLA 1000 rotor. The supernatant, soluble lysate, was transferred to new Eppendorf tubes. The concentration of each sample was determined using the Pierce™ BCA Protein Assay (Thermo Fisher Scientific) following the microplate procedure. All standards and samples were prepared according to the manufacturer's instructions.

3-hydroxyanthranilinic acid indirect ELISA

The *D. immitis* samples were diluted to a final concentration of 5 µg / mL from the final volume of total protein extracted from each biological replicate. Fifty µL of the *D. immitis* sample was used to coat the wells of the PVC microtiter plate. The plate was covered in adhesive plastic and incubated overnight at 4 ° C. The coating solution was removed by washing wells with 200 µL PBS twice.

The remaining protein-binding sites were blocked by coating the wells with 100 µL of 1 % BSA solution and incubated overnight at 4 ° C. The blocking solution was removed by washing the sample wells with 200 µL PBS twice. The blocked sample wells were then incubated in 100 µL of the 3HA 1 ° antibody (1 : 1000; ImmuSmol) in 1 % BSA solution. The plate was covered in adhesive plastic and incubated overnight at 4 ° C. The 1 ° antibody was removed by washing the sample wells with 200 µL PBS four times. The samples were subsequently incubated in 100 µL of the conjugated 2 ° antibody solution of α-rabbit 2° antibody (1 : 5000; Thermo Fisher Scientific). The plate was coved in adhesive plastic and incubated for four hours at 4 ° C. The conjugated 2 ° antibody was removed by washing wells with 200 µL PBS four times.

The relative 3HA expression in the sample wells was detected using the substrate 3,3',5,5'-Tetramethylbenzidine (TMB). One hundred μL of TMB was added to each well using a multichannel pipette and the solution was allowed to develop. After sufficient colour development 100 μL of a 0.16 M sulfuric acid stop solution was added. The absorbance of the sample wells was read on a Synergy H4 plate reader at an absorbance of 450 nm.

Statistical analysis of 3-hydroxyanthranilinic acid ELISA

The adult *D. immitis* samples were prepared from whole worms. The average relative 3HA expression was compared between the Kentucky females, Kentucky males, JYD-34 females, and JYD-34 males. All data is reported as mean relative expression (OD 450 nm), with error bars corresponding to the standard deviation of three biological replicates. The significance of the change in relative 3HA expression was calculated via Brown-Forsythe and Welch ANOVA tests two-tailed p value, and 95 % confidence interval using Prism 9.3.0c (Graph Pad Software, Inc.).

Results

*Dim*KYNU-1 genetic polymorphism

The intronic region between exons 9 and 10 of the *Dim*KYNU-1 gene is not fully sequenced in the *D. immitis* reference genome nDi.2.2. The nucleotides along this region of the genome are called as “N”. Nevertheless, the *Dim*KYNU-1 SNP, at position 4740, was reliably identified as “T” in well characterized ML-susceptible USA laboratory-maintained isolates (Maclean et al., 2017; McTier et al., 2017; Curry et al., 2022b). As a result, “T” was set as the wildtype reference nucleotide.

There was a differential pattern in the frequency of the *Dim*KYNU-1 SNP alternative allele in the USA laboratory-maintained isolates. The ML-susceptible isolates: Missouri, MP3, Yazoo, Berkeley, GCFL, and Georgia II had an alternate allele frequency ranging from 1 – 16 %

(Table 1). The ML-resistant isolates: JYD-34, Metairie, and WildCat had a much broader range in the frequency of the alternate allele, from 9 – 62 % (Table 1).

Table 1 The alternate nucleotide frequency of the KYNU-1 SNP located at position 4740 on the nDi.2.2.scaf01096 scaffold in the ML-susceptible isolates Missouri, MP3, Yazoo, Berkeley, GCFL, Georgia II; and the ML-resistant isolates JYD-34, Metairie, and WildCat compared to the *Dirofilaria immitis* reference genome nDi.2.2.

D. immitis Isolate	ML-Susceptibility	Alternate Allele Frequency (%)
Missouri	Susceptible	1
MP3	Susceptible	4
Yazoo	Susceptible	2
Berkeley	Susceptible	1
GCFL	Susceptible	5
Georgia II	Susceptible	16
JYD-34	Resistant	62
Metairie	Resistant	28
WildCat	Resistant	9

Quantification of *Dim*KYNU-1 constitutive expression

The constitutive expression of *Dim*KYNU-1 was measured in the adult females and adult males of the ML-susceptible Kentucky and ML-resistant JYD-34 isolates, with the Kentucky females set as the 1 – fold standard gene expression (Bourguinat et al., 2017; Maclean et al., 2017; McTier et al., 2017). Interestingly, the Kentucky males had an approximately 4 – fold greater expression of *Dim*KYNU-1 compared to the Kentucky females ($P < 0.04$; Figure 2).

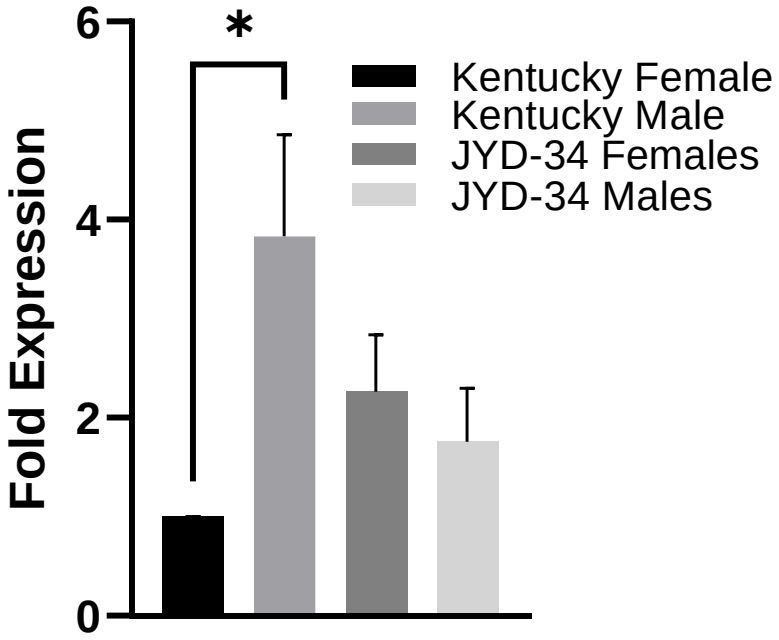

Figure 2 Constitutive expression of *Dirofilaria immitis* KYNU-1 in the female and male of the adult lifestage of the ML-susceptible Kentucky and ML-resistant JYD-34 isolate determined using droplet digital PCR. Expression level fold changes calculated relative to the ML-susceptible Kentucky females. Constitutive expression was normalized to three reference genes: *Dim*GAPDH, *Dim*Actin, and *Dim*pmp-3. All data are reported as mean fold change, with error bars corresponding to the SD of three biological replicates. The significance of the transcript level fold changes to the Kentucky female control was analyzed by Parametric unpaired t-test with Welch Correction with two-tailed p value, and 95 % confidence interval using Prism 9.3.0c (Graph Pad Software, Inc.).

The JYD-34 adult females and JYD-34 adult males showed no statistically significant difference in constitutive expression when compared to the Kentucky female 1 – fold standard (Figure 2). Moreover, the JYD-34 females and JYD-34 males showed similar expression levels between the two sexes. These results indicate a sex-specific variation in the expression of

*Dim*KYNU-1 in the adults of the susceptible Kentucky isolate which was not observed in the resistant JYD-34 isolate.

Comparative transcriptomic analysis and Tryptophan catabolism genes

RNASeq read statistics and data assembly

The comparative transcriptomic analysis of the adult *D. immitis* worms yielded an average of approximately 85,000,000 reads per sample (Table S10). The Q40 average quality of the reads ranged from 35.5 – 36.1. A range of 91.9 – 95.2 % of the clean reads were aligned to the D. immitis reference genome nDi.2.2 (Table S10). A total of 12,926 transcripts were identified and annotated, of which 12,872 represent coding genes. Principal component analysis (PCA) of the nDi.2.2 aligned RNASeq reads demonstrated a high level of consistency between the biological replicates of the same population: Kentucky females, Kentucky males, JYD-34 females, and JYD-34 males (Figure S1).

Differentially expressed gene analysis

Sex specific comparison

In the Kentucky female vs. Kentucky male analysis, a total of 5516 transcripts were significantly differentially expressed (FDR < 0.05 and a logFC > 1 or < - 1) with logFC ranging from - 17.9 – 17.2 (Figure 3a). Among the significantly differentiated transcripts 2734 were downregulated and 2782 were upregulated in the Kentucky females (Figure 3b). A heatmap illustrates the top 50 differentially expressed transcripts (Figure 3d). The top 25 upregulated transcripts in the Kentucky females included collagen helices, homobox proteins, Knirps-related proteins, along with 15 unidentified transcripts (Table S1). Among the top 25 downregulated transcripts were major sperm proteins, hydrolase 4 domain-containing protein, and peroxisomal membrane protein, as well as 19 transcripts were unidentified (Table S2).

The JYD-34 female vs. JYD-34 male analysis yielded 5941 significantly differentially expressed transcripts (FDR < 0.05 and a logFC > 1 or < - 1) with logFC ranging from - 18.6 – 14.2 (Figure 3a). The significantly differentiated transcripts included 2843 downregulated and 3098 upregulated transcripts in the JYD-34 females (Figure 3c). The top 50 differentially expressed transcripts between the JYD-34 adult females and males are shown by heatmap (Figure 3e). The top 25 upregulated transcripts in the JYD-34 females included: MLT-10, collagen helices, Knirps-related protein, and 10 unidentified transcripts (Table S3). Among the top 25 downregulated transcripts there were major sperm proteins, small heatshock proteins, and 14 transcripts which were unidentified (Table S4). A total of 4265 differentially expressed transcripts which were shared between the Kentucky female vs. Kentucky male and JYD-34 female vs. JYD-34 male analyses. Seven of the top 25 upregulated genes and 13 of the top 25 downregulated genes were shared between the Kentucky females and JYD-34 females.

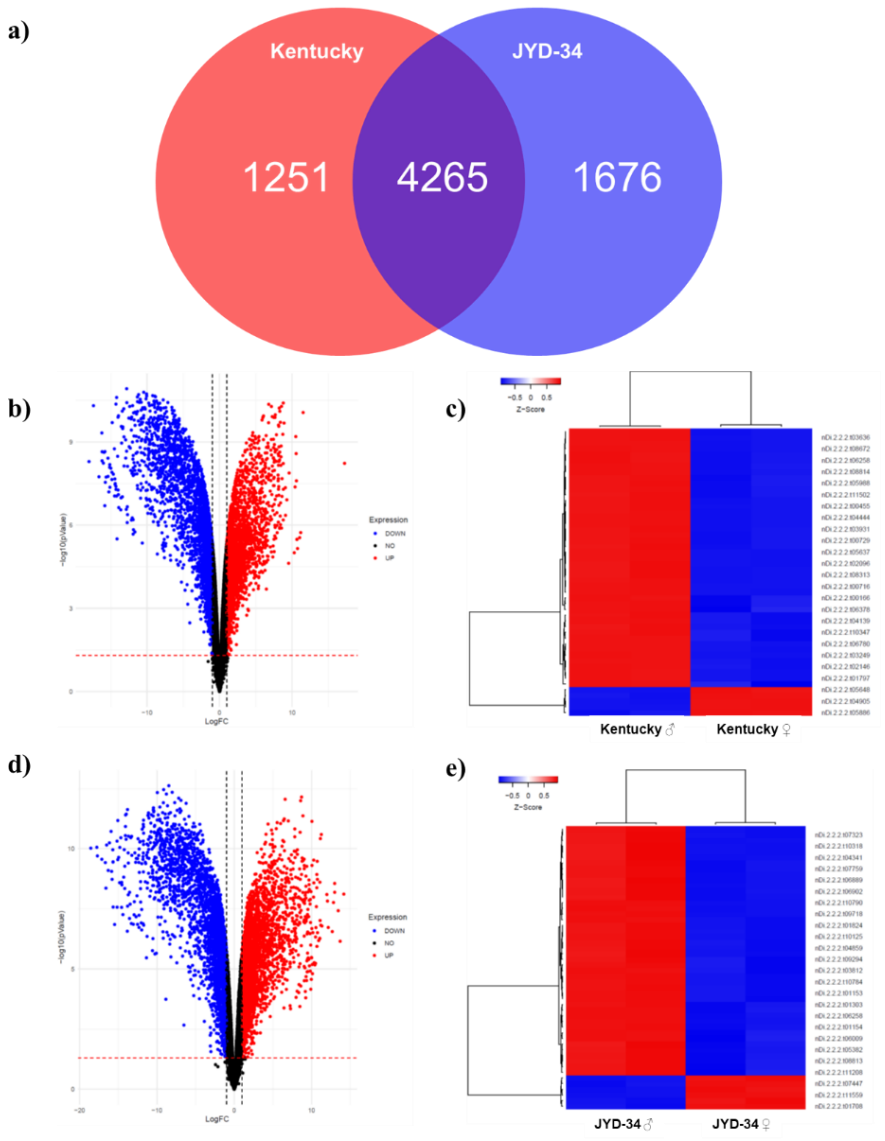

Figure 3 a) Comparison of the common differentially expressed genes between the females and males of the ML-susceptible Kentucky isolate and ML-resistant JYD-34 isolate. Volcano plot of the differentially expressed genes in the b) Kentucky female vs. male analysis and c) JYD-34 female vs. male analysis . Blue, red, and black dots respectively represent downregulated genes, upregulated genes, and genes without statistical significance. Heatmap of 50 most significantly differentially expressed genes by counts per million (cpm) in the d) Kentucky female vs. male analysis and e) JYD-34 female vs. male analysis. Differentially expressed genes with higher expression (red) and lower expression (blue).

Isolate comparison

We subsequently compared the JYD-34 female vs Kentucky female and the JYD-34 males vs. Kentucky males. The female comparison yielded 525 differentially expressed transcripts (FDR $\leq$ 0.05 and a logFC $\geq$ 1 or $\leq$ -1) with logFC ranging from - 6.4 – 5.5 (Figure 4a). Among the significantly differentiated transcripts 371 were downregulated and 154 were upregulated in the JYD-34 females (Figure 4b). A heatmap highlights the top 50 differentially expressed transcripts (Figure 4d). The top 25 upregulated transcripts in the JYD-34 females included four small heatshock proteins, proteins containing kinase domains, and 15 unidentified transcripts (Table S5). The top 25 downregulated transcripts included cell adhesion molecules, integral membrane components, as well as 13 unidentified transcripts (Table S6).

The comparison of the JYD-34 male vs. Kentucky male generated 1251 significantly differentially expressed transcripts (FDR $\leq$ 0.05 and a logFC $\geq$ 1 or $\leq$ - 1), more than double that of the female comparison, with logFC ranging from - 8.3 – 4.9 (Figure 4a) . The significantly differentiated transcripts included 1047 downregulated and 204 upregulated transcripts in the JYD-34 males (Figure 4c). The top 50 differentially expressed transcripts are shown in a heatmap (Figure 4e). The top 25 upregulated transcripts in the JYD-34 males included zinc finger proteins, collagen helices, and Rig-3. There were 10 unidentified transcripts (Table S7). Among the top 25 downregulated transcripts were collagen helices, membrane proteins, structural constituents of the cuticle, and 10 unidentified transcripts (Table S8). Two hundred and forty-four differentially expressed transcripts which were shared between the JYD-34 female vs. Kentucky female analysis and the JYD-34 male vs. Kentucky male analysis.

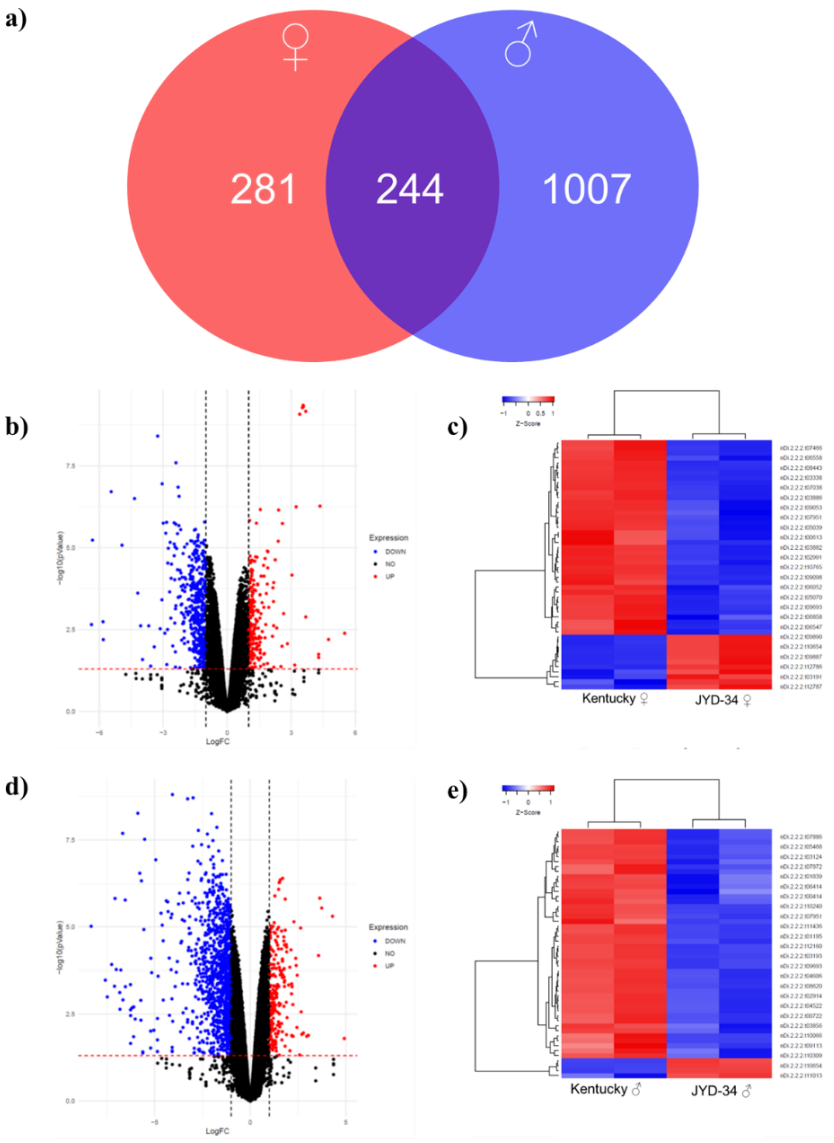

Figure 4 a) Comparison of the common differentially expressed genes between the analysis of the JYD-34 females vs Kentucky females and the JYD-34 males vs Kentucky males. Volcano plot of the differentially expressed genes in the b) JYD-34 females vs. Kentucky females and c) JYD-34 males vs. Kentucky males. Blue, red, and black dots respectively represent downregulated genes, upregulated genes, and genes without statistical significance. Heatmap of 50 most significantly differentially expressed genes between the d) JYD-34 females vs. Kentucky females and e) JYD-34 males vs. Kentucky males. Differentially expressed genes with higher expression (red) and lower expression (blue).

Tryptophan catabolism gene analysis

We compared the constitutive expression of genes which precede *Dim*KYNU-1 in tryptophan catabolism in the Kentucky female vs. Kentucky male and the JYD-34 female vs. JYD-34 male analyses. *Dim*tph was comparably downregulated in the Kentucky adult females (-1.4 logFC; FDR 3.33E-04) and adult JYD-34 females (-2.3 logFC; FDR 1.07E-05) (Table 2). *Dim*amfd, *Dim*nkat, and *Dim*tatn were all upregulated in the Kentucky females and JYD-34 females when compared to their respective male counterparts (Table 2).

Table 2 Comparison of the logFC of downregulated and upregulated genes preceding Kynureninase along the tryptophan catabolism pathway between the females and males of the ML-susceptible Kentucky isolate and ML-resistant JYD-34 isolate.

Tryptophan Catabolism Genes	Kentucky ♀ vs. ♂	JYD-34 ♀ vs. ♂
♀ Downregulated		
Tryptophan Hydrolase	- 1.4 logFC	- 2.3 logFC
♀ Upregulated		
Arylformamidase	1.1 logFC	1.2 logFC
Nematode Kynurenine Aminotransferase	1.5 logFC	2.0 logFC
Tyrosine Aminotransferase	2.2 logFC	1.2 logFC

*Dim*KYNU-1 did not show the same pattern of constitutive expression seen in the preceding tryptophan catabolism genes. The constitutive expression of *Dim*KYNU-1 was significantly upregulated in the Kentucky adult males (1.1 logFC; FDR 3.93E-06) compared to the Kentucky adult females. On the other hand, *Dim*KYNU-1 was stably expressed between the JYD-34 adult females and males, with no statistically significant difference in constitutive expression. These results corroborated data collected via ddPCR analysis. *Dim*KYNU-1 is the one gene among the tryptophan catabolism genes analyzed which showed a sex-specific differential expression in the ML-susceptible Kentucky isolate and not in the ML-resistant JYD-34 isolate.

qPCR validation

Six significantly differentially expressed genes, two in the females: rpl-19 and C32D5.12; two in the males: sul-2 and nid-1; and two shared in the females and males: nhr-48 and Let-2 were randomly selected to validate the RNASeq analysis via qPCR (Figure 5) The expression of these genes was assessed with cDNA prepared from the eight RNA samples sent for sequencing.

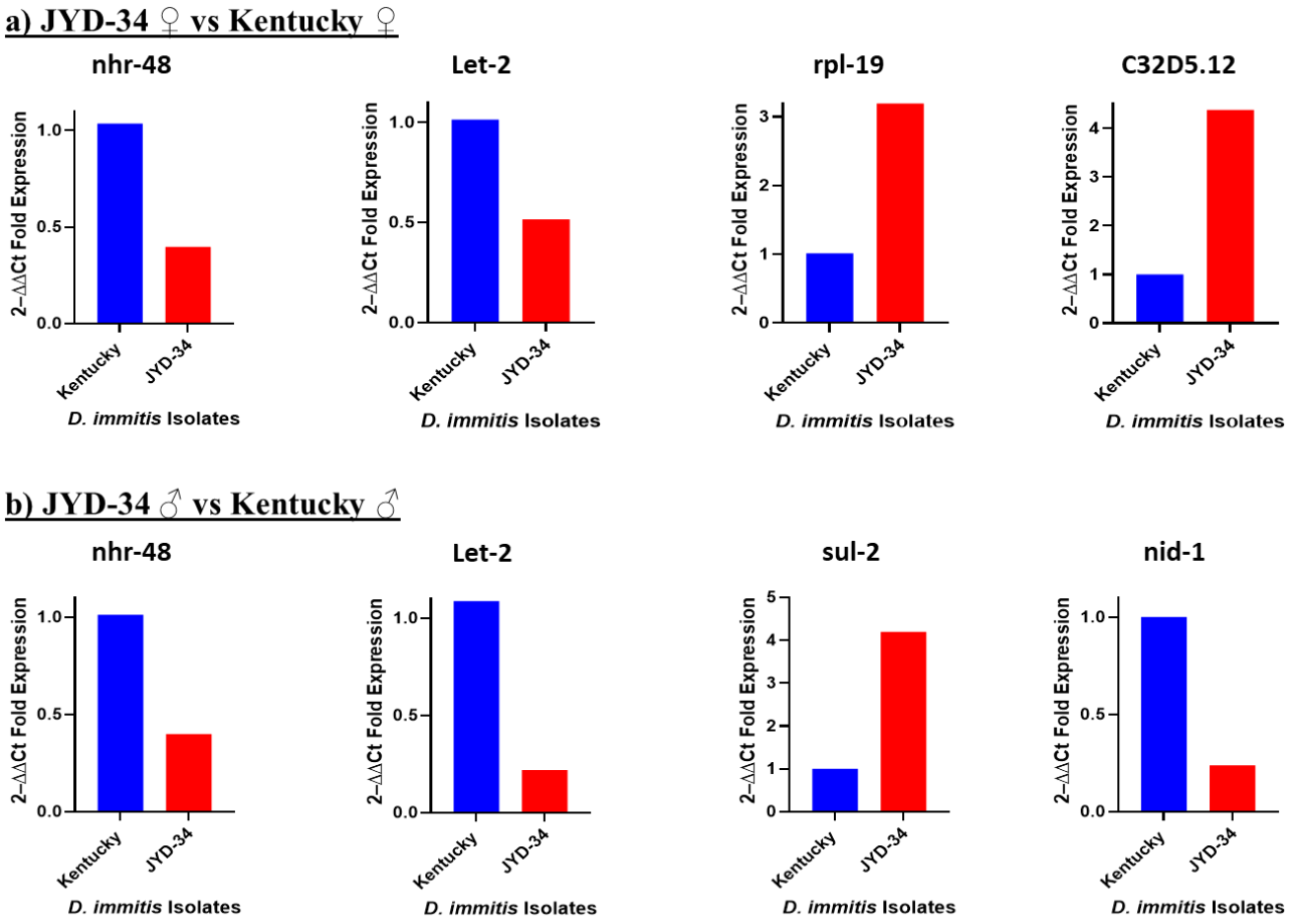

Figure 5 $2^{-\Delta\Delta CT}$ fold expression level of randomly selected differentially expressed genes in the a) JYD-34 females compared to the Kentucky females and b) JYD-34 males and the Kentucky males. The Kentucky isolate is indicated in blue and set as the 1 – fold control, the JYD-34 isolate is indicated in red. Experiments were performed in duplicate using the same RNA samples which were sent for RNASeq sequencing.

The transcriptomic analysis of the JYD-34 female vs. Kentucky female demonstrated an upregulation of rpl-19 (1.95 logFC; FDR 1.39E-02) and C32D4.12 (1.28 logFC; FDR 2.91E-02); and a downregulation of nhr-48 (- 3.00 logFC; FDR 9.38E-04) and Let-2 (- 2.07 logFC; FDR 2.65E-03). The qPCR analysis supported these results, rpl-19 and C32D4.12 were upregulated, and nhr-48 and Let-2 downregulated in the JYD-34 females (Figure 5a).

The RNASeq transcriptomic analysis of the JYD-34 male vs. Kentucky male analysis showed a downregulation of nid-1 (- 3 logFC; FDR 8.20E-06), nhr-48 (- 2.18 logFC; FDR 5.20E-04) and Let-2 (- 2.7 logFC; FDR 2.44E-04) as well as an upregulation of sul-2 (1.38 logFC; FDR 6.63E-03). The qPCR analysis support these results, nid-1, nhr-48, and Let-2 were shown to be downregulated and sul-2 upregulated (Figure 5b). Statistical validation was not conducted as samples were run in biological duplicates. The qPCR results highly correlated with the RNASeq results.

Quantification of 3-hydroxyanthranilic acid

The relative expression of the *Dim*KYNU-1 downstream product 3HA was measured in the adult females and males of the ML-susceptible Kentucky isolate and ML-resistant JYD-34 isolate (Bourguinat et al., 2017; Maclean et al., 2017; McTier et al., 2017). The relative expression of 3HA in the Kentucky adult females and Kentucky adult males showed no statistically significant differences in optical density (OD) at a wavelength of 450 nm (Figure 4). The JYD-34 adult males have a significantly greater level of relative expression of 3HA compared to the JYD-34 adult females ($P < 0.04$; Figure 4) and Kentucky adult females ($P < 0.05$; Figure 4).

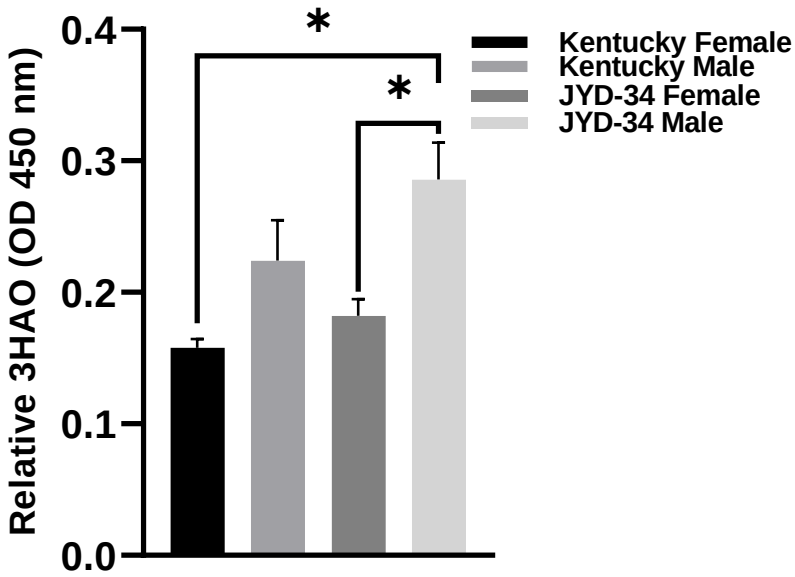

Figure 6 The relative level of 3-hydroxyanthranilic acid (3HA) constitutive expression in the female and male in the adult lifestage of the ML-susceptible Kentucky and ML-resistant JYD-34 *Dirofilaria immitis* isolates determined using indirect ELISA. All data are reported as the mean OD 450 mn reading, with error bars corresponding to the SD of three biological replicates. The significance in the changes of the OD readings were analyzed by Brown-Forsythe and Welch ANOVA test with two-tailed p value, and 95 % confidence interval using Prism 9.3.0c (Graph Pad Software, Inc.).

Discussion

D. immitis is well adapted for long-term survival within the mammalian definitive host. Among these adaptations is the alternation between aerobic and anaerobic metabolism based on lifestage and environment. The adults, located in the pulmonary artery, predominantly utilize an alternate anaerobic metabolism which requires the electron carrier RQ (Manfredi et al., 2007; McCall et al., 2008; Bowman and Atkins, 2009). The expression of *Dim*KYNU-1 is an important biological marker of RQ biosynthesis and anaerobic metabolism.

A highly differentially expressed indel in the intron between exons 9 and 10 of the *Dim*KYNU-1 gene was flagged as a region of interest in 2018 when comparing the genomes of ML resistant and ML-susceptible isolates (Ballesteros and Prichard, unpublished). When comparing pooled ML-resistant populations to pooled ML-susceptible populations the indel region on *Dim*KYNU-1 demonstrated a fixation indexes (F_{ST}) of > 0.80. MiSeq primers were designed to assess this region. Within this indel, we found a SNP at position 4740 of most interest. Here we analyzed this new SNP molecular marker on the *Dim*KYNU-1 gene and the differential constitutive expression of *Dim*KYNU-1 and 3HA in USA laboratory-maintained *D. immitis* isolates with different ML-susceptibility profiles.

The alternate allele frequency of the *Dim*KYNU-1 SNP was measured in six isolates: Missouri, MP3, Yazoo, Berkeley, GCFL, and Georgia II that have been reported as phenotypically susceptible; and three ML-resistant isolates: JYD-34, Metairie, and WildCat via MiSeq sequencing (Maclean et al., 2017; McTier et al., 2017; Curry et al., 2022b). The *Dim*KYNU-1 SNP alternate allele was more abundant in the ML-resistant isolates. The three ML-resistant isolates demonstrated a broad range in the frequency of the alternate allele, from 9 – 62 % (Table 1). The six ML-susceptible isolates had an alternate allele frequency ranging from 1 – 16 % (Table 1). Among the ML-susceptible isolates, Georgia II expressed the highest frequency of the *Dim*KYNU-1 SNP alternate allele at 16 %. Georgia II is of interest as recent MiSeq, ddPCR duplex, and population genetics microsatellite analyses suggest it may have genotypic characteristics more aligned with a mixed or developing resistant isolate (Ballesteros et al., 2018; Sanchez et al., 2020; Curry et al., 2022b, Kumar et al., forthcoming). When reviewing the other five isolates which are clearly characterized phenotypically and genotypically as ML-susceptible, in the absence of Georgia II, the frequency of the alternate

allele drops to < 5 % (Table 1). These results suggest distinct genotypic differences on the *Dim*KYNU-1 gene between the ML-susceptible and ML-resistant isolates analyzed in the current study. Future analysis, in additional *D. immitis* isolates, will help to determine the predictive ability of the *Dim*KYNU-1 SNP as a marker of ML resistance.

We assessed the constitutive expression of *Dim*KYNU-1 in the adult females and adult males of the ML-susceptible Kentucky isolate and the ML-resistant JYD-34 isolate via ddPCR analysis and comparative transcriptomic analysis. The Kentucky isolate demonstrated a sex-specific differential constitutive expression. The Kentucky adult males expressed *Dim*KYNU-1 4 – fold greater in ddPCR analysis and 1.1 logFC greater in RNASeq analysis compared to the Kentucky adult females. The ML-resistant JYD-34 adult females and adult males showed a similar pattern of expression in ddPCR analysis between the sexes. There was no statistically significant change in the constitutive expression of *Dim*KYNU-1 in female and male JYD-34 individuals when compared to the Kentucky female 1 – fold control. This was further corroborated by RNASeq comparative transcriptomic analysis where the differential expression of *Dim*KYNU-1 did not meet the statistical cut-off criteria of the analyses performed, indicating it was stably expressed between the JYD-34 adult females and adult males.

We compared constitutive expression in a selection of genes preceding *Dim*KYNU-1 in tryptophan catabolism to determine whether the differences in the pattern of expression between the Kentucky isolate and JYD-34 isolate may be unique to *Dim*KYNU-1. *Dim*tph, the rate limiting enzyme in the synthesis of the neurotransmitter serotonin, was downregulated in the Kentucky adult females and JYD-34 adult females (Table 2). These results indicate serotonin production may be higher in adult *D. immitis* adult males, regardless of isolate. This is not unexpected as serotonin has been shown to be an essential molecule regulating male-specific

mating behaviour in the model organism *C. elegans* (Loer and Kenyon, 1993; Lints and Emmons, 2002; McCulloch and Gems, 2003; Lipton, 2004). *Dim*amfd, *Dim*nkat, and *Dim*tatn were all upregulated in the Kentucky adult females and JYD-34 adult females which suggests the production of kynurenic acid (KA), a non-competitive antagonist of α7 nicotinic acetylcholine, may be increased in *D. immitis* females (Hilmas et al., 2001) (Table 2). *Dim*amfd catalyzes the hydrolysis of N-formyl-L-kynurenine to KYN, the second step in the kynurenine pathway of tryptophan catabolism (Figure 1). *Dim*nkat and *Dim*tatn converts KYN to the KA in subsequent steps. These results indicate that differences in the pattern of *Dim*KYNU-1 constitutive expression between the Kentucky isolate and JYD-34 isolate was unique among the genes analyzed. However, it is important to note, constitutive expression does not always correlate one-to-one with protein synthesis. The validity of the RNASeq results were corroborated via qPCR analysis of 6 randomly selected significantly differentially expressed genes from the JYD-34 female vs. Kentucky female and JYD-34 male vs. Kentucky male analyses (Figure 5).

We subsequently measured the relative expression of 3HA to assess whether the differences in *Dim*KYNU-1 constitutive expression could result in downstream effects within tryptophan catabolism and / or RQ biosynthesis. Despite the 4 – fold difference in the constitutive expression of *Dim*KYNU-1 in the Kentucky adult males there was no statistically significant change in the relative expression of 3HA compared to the Kentucky adult females (Figure 4). On the other hand, The JYD-34 adult males demonstrated a statistically significant greater relative expression of 3HA compared to their female counterpart, as well as the Kentucky adult females (Figure 4).

The results of the current study demonstrate a correlation between the frequency of the *Dim*KYNU-1 SNP and the differential expression of *Dim*KYNU-1 and 3HA between the two

isolates analyzed, most notably in the adult males. Untargeted metabolomic analysis of a ML-susceptible isolate and a ML-resistant *D. immitis* isolate also found that the most significant differences in metabolite profiles were in tryptophan catabolism (Kumar, et al. forthcoming). The analysis of additional USA laboratory-maintained *D. immitis* isolates, as they become available to academic laboratories, will provide clarity as to whether the differential expression of *Dim*KYNU-1 and 3HA are associated with ML resistance and the differences in *Dim*KYNU-1 SNP frequencies, or are found in the JYD-34 isolate but are not specifically associated with resistance.

Conclusion

*Dim*KYNU-1 is a necessary precursor to the biosynthesis of RQ, an electron carrier essential to anaerobic metabolism in helminths. The presence of a SNP molecular marker differentiating ML-susceptible and ML-resistant USA laboratory-maintained isolates, indicated *Dim*KYNU-1 is a gene of interest which warranted further investigation. The differential constitutive expression of *Dim*KYNU-1 and 3HA in the ML-susceptible Kentucky isolate and the ML-resistant JYD-34 isolate indicates a higher frequency of *Dim*KYNU-1 SNP may affect the efficiency of gene regulation and expression, particularly in the males. Further analysis of *Dim*KYNU-1, tryptophan catabolism, and RQ biosynthesis is warranted. The genetic changes and the differential constitutive expression point of *Dim*KYNU-1 is an important putative biological marker and upstream target for future development of anti-filarial pharmaceuticals.

Declarations

Ethics approval

All experimental procedures were approved by McGill University in accordance with relevant guidelines and regulations.

Availability of data and material

The data presented in this study is included within the article. RNASeq sequence files for the adult females and adult males JYD-34 and Kentucky isolates are openly available on the NCBI Sequence Read Archive as fastq files under BioProject PRJNA910938.

Competing interests

The authors declare that they have no competing interests.

Funding

This research was supported by grant to RP from the Natural Sciences and Engineering Research Council of Canada, Grant ID: RGPIN/2777-2017.

Author Contributions

Emily Curry: Conceptualization, Methodology, Formal analysis, Investigation, Writing – original draft. **Cristina Ballesteros**: Conceptualization, Methodology, Investigation. **Roger Prichard**: Conceptualization, Writing – review & editing, Supervision, Funding acquisition. **Anne Lespine**: Conceptualization, Writing – review & editing, Supervision.

Acknowledgements

We thank Kathy Keller for help with MiSeq and RNASeq sample preparation and submission to Génome Québec. We thank Ray Kaplan for providing the *Dirofilaria immitis* Metairie isolate. The following *Dirofilaria immitis* isolates: Berkeley, GCFL, Georgia II, JYD-34, and WildCat were provided by TRS lab Inc. The following reagent was provided by the NIH/NIAID Filariasis

Research Reagent Resource Center for distribution through BEI Resources, NIAID, NIH: *Dirofilaria immitis*, Strain Missouri, Microfilariae in Dog Blood (Live), NR-48907; Strain MP3, Microfilariae in Dog Blood (Live), NR-48908; and Strain Yazoo, Microfilariae in Dog Blood (Live).

Supplementary Information

Table S1 Top 25 significantly upregulated transcripts in the Kentucky females compared to Kentucky males, log fold change, false discovery rate, nematode orthologs, and description.

Transcript ID	logFC	FDR	Nematode Orthologs	Description
nDi.2.2.2.t09375	17.20	5.24E-08	No orthologs	No description
nDi.2.2.2.t02607	11.57	6.13E-08	9	No description
nDi.2.2.2.t12322	11.14	2.45E-06	5	Calcium-binding EGF domain[a,b,c]
nDi.2.2.2.t11576	11.01	3.27E-06	3	EFG-like domain[c]
nDi.2.2.2.t04777	10.71	2.09E-05	No orthologs	No description
nDi.2.2.2.t03637	10.64	4.32E-08	No orthologs	No description
nDi.2.2.2.t12453	10.63	3.89E-06	No orthologs	No description
nDi.2.2.2.t10950	10.63	3.57E-06	12	No description
nDi.2.2.2.t07447	10.61	2.82E-09	12	No description
nDi.2.2.2.t01708	10.56	1.68E-09	9	No description
nDi.2.2.2.t12067	10.45	1.69E-08	14	Chitin binding Peritrophin-A domain[a,c]
nDi.2.2.2.t05290	10.26	1.61E-05	99	Homobox Protein[a,b,c]
nDi.2.2.2.t03425	9.63	1.2E-08	102	Homobox Protein[a,b,c]
nDi.2.2.2.t10164	9.48	6.83E-05	No orthologs	No description
nDi.2.2.2.t11559	9.31	4.37E-08	6	Chitin binding Peritrophin-A domain[a,c]
nDi.2.2.2.t10775	9.13	5.1E-07	7	No description
nDi.2.2.2.t11197	9.12	8.56E-08	No orthologs	No description
nDi.2.2.2.t12579	9.04	7.1E-05	10	No description
nDi.2.2.2.t05146	8.93	1.87E-08	7	Collagen Helix[c]
nDi.2.2.2.t09956	8.84	9.4E-08	78	Knirps-related protein-related[a,b,c]
nDi.2.2.2.t05886	8.83	1.6E-09	13	No description
nDi.2.2.2.t08691	8.83	1.26E-07	19	Collagen Helix[c]
nDi.2.2.2.t11844	8.81	1.91E-06	2	No description
nDi.2.2.2.t11109	8.77	3.31E-09	10	Chitin binding Peritrophin-A domain[a,b,c]
nDi.2.2.2.05781	8.66	2.15E-07	No orthologs	No description

[a] Gene Ontology

[b] Panther ID

[c] Pfam Annotation

Table S2 Top 25 significantly downregulated transcripts in the Kentucky females compared to Kentucky males, log fold change, false discovery rate, nematode orthologs, and description.

Transcript ID	logFC	FDR	Nematode Orthologs	Description
nDi.2.2.2.t09931	-17.91	6.52E-09	9	No description
nDi.2.2.2.t08314	-17.35	5.17E-09	759	Major sperm protein[b,c]
nDi.2.2.2.t13857	-16.54	4.38E-09	29	No description
nDi.2.2.2.t08315	-16.19	7.9E-09	755	Major sperm protein[b,c]
nDi.2.2.2.t12501	-16.11	7.51E-08	13	No description
nDi.2.2.2.t10944	-16.11	8.16E-09	No orthologs	No description
nDi.2.2.2.t10947	-15.94	8.49E-09	119	Hydorlase 4 domain-containing protein[b]
nDi.2.2.2.t09019	-15.85	2.04E-08	8	No description
nDi.2.2.2.t07057	-15.74	1.08E-07	147	Peroxisomal membrnae protein 2, PXMP2 MPV17[a,b,c]
nDi.2.2.2.t10993	-15.71	4.89E-09	5	Collagen Helix[c]
nDi.2.2.2.t03778	-15.66	1.04E-08	13	No description
nDi.2.2.2.t09768	-15.56	9.47E-09	16	No description
nDi.2.2.2.t10435	-15.30	2.36E-08	8	No description
nDi.2.2.2.t16157	-15.29	1.23E-07	2	No description
nDi.2.2.2.t09126	-15.18	8.26E-09	5	No description
nDi.2.2.2.t08555	-15.08	6.51E-08	13	No description
nDi.2.2.2.t10429	-15.06	3.42E-07	5	No description
nDi.2.2.2.t01489	-15.03	6.45E-08	13	No description
nDi.2.2.2.t11720	-14.90	2.92E-07	8	No description
nDi.2.2.2.t08652	-14.76	4.25E-08	1	No description
nDi.2.2.2.t10483	-14.76	8.59E-08	31	No description
nDi.2.2.2.t10088	-14.76	4.36E-09	14	No description
nDi.2.2.2.t00294	-14.56	2.63E-07	2	No description
nDi.2.2.2.t10497	-14.46	2.52E-09	11	No description
nDi.2.2.2.t12403	-14.40	1.7E-07	136	Trehalase[a,b,c]

[a] Gene Ontology

[b] Panther ID

[c] Pfam Annotation

Table S3 Top 25 significantly upregulated transcripts in the JYD-34 females compared to JYD-34 males, log fold change, false discovery rate, nematode orthologs, and description.

Transcript ID	logFC	FDR	Nematode orthologs	Description
nDi.2.2.2.t03131	14.18	8.82E-08	8	No description
nDi.2.2.2.t07770	13.70	3.26E-06	20	Globin domain-containing protein[a,b,c]
nDi.2.2.2.t08138	13.46	3.06E-07	88	Zinc finger transcription faction family protein 30[a,b,c]
nDi.2.2.2.t09956	12.99	7.72E-08	78	Knirps-related protein-related[a,b,c]
nDi.2.2.2.t09953	12.99	4.05E-08	78	Knirps-related protein-related[a,b,c]
nDi.2.2.2.t11791	12.84	1.64E-07	No orthologs	No description
nDi.2.2.2.t12470	12.69	1.52E-06	22	Helix-loop-helix DNA-binding domain[a,b,c]
nDi.2.2.2.t11430	12.16	1.11E-06	19	MLT-10 related protein[b]
nDi.2.2.2.t11812	12.07	1.47E-07	No orthologs	structural constituent of cuticle[a,c]
nDi.2.2.2.t09375	11.98	9.09E-08	No orthologs	No description
nDi.2.2.2.t11513	11.35	9.89E-07	3	COA Ligase 1[b,c]
nDi.2.2.2.t11109	11.27	2.35E-09	10	Chitin binding Peritrophin-A domain[a,b,c]
nDi.2.2.2.t08126	11.19	9.36E-07	1	No description
nDi.2.2.2.t07447	11.14	2.62E-09	12	No description
nDi.2.2.2.t08868	11.10	6.57E-07	1	EGF-like domain[c]
nDi.2.2.2.t11559	11.08	3.68E-08	6	Chitin binding Peritrophin-A domain[a,c]
nDi.2.2.2.t11925	11.07	2.58E-06	128	Zinc finger[b,c]
nDi.2.2.2.t11112	11.06	2.68E-06	No orthologs	No description
nDi.2.2.2.t10950	10.93	3.08E-06	12	No description
nDi.2.2.2.t06566	10.77	1.67E-06	24	Receptor family ligand binding region[c]
nDi.2.2.2.t11168	10.75	2.98E-08	No orthologs	No description
nDi.2.2.2.t05785	10.73	8.8E-09	No orthologs	No description
nDi.2.2.2.t11710	10.70	4.86E-06	3	No description
nDi.2.2.2.t12067	10.68	2.11E-08	14	Chitin binding Peritrophin-A domain[a,c]
nDi.2.2.2.t05784	14.18	5.57E-08	No orthologs	Collagen Helix[c]

[a] Gene Ontology

[b] Panther ID

[c] Pfam Annotation

Table S4 Top 25 significantly downregulated transcripts in the JYD-34 females compared to JYD-34 males, log fold change, false discovery rate, nematode orthologs, and description.

Transcript ID	logFC	FDR	Nematode Orthologs	Description
nDi.2.2.2.t08314	-18.55	4.09E-09	759	Major sperm protein[b,c]
nDi.2.2.2.t10088	-17.77	3.95E-09	14	No description
nDi.2.2.2.t08315	-17.70	6.26E-09	755	Major sperm protein[b,c]
nDi.2.2.2.t09931	-17.13	7.84E-09	9	No description
nDi.2.2.2.t04611	-16.67	9.42E-09	19	No description
nDi.2.2.2.t12501	-16.60	5.74E-08	13	No description
nDi.2.2.2.t10993	-16.51	3.43E-09	5	Collagen Helix[c]
nDi.2.2.2.t09019	-16.30	1.58E-08	8	No description
nDi.2.2.2.t03339	-16.14	3.1E-09	4	No description
nDi.2.2.2.t06378	-15.93	2.17E-09	333	Small heat shock protein[b,c]
nDi.2.2.2.t10435	-15.86	1.68E-08	8	No description
nDi.2.2.2.t10736	-15.80	2.97E-08	26	SH2 domain[c]
nDi.2.2.2.t10780	-15.71	4.39E-09	7	Trehalase[a,b,c]
nDi.2.2.2.t10944	-15.68	9.21E-09	No orthologs	No description
nDi.2.2.2.t10947	-15.67	9.05E-09	119	Hydrolase 4 domain-containing protein[b]
nDi.2.2.2.t10429	-15.66	2.3E-07	5	No description
nDi.2.2.2.t15157	-15.48	8.89E-07	9	No description
nDi.2.2.2.t00367	-15.16	2.89E-09	123	Receptor tyrosine kinase[a,b,c]
nDi.2.2.2.t11720	-15.15	2.33E-07	8	No description
nDi.2.2.2.t08039	-15.07	7.96E-09	5	No description
nDi.2.2.2.t03267	-15.06	1.63E-09	68	Sperm meiosis PDZ domain containing protein[a,b,c]
nDi.2.2.2.t12004	-14.95	6.94E-09	1	No description
nDi.2.2.2.t08652	-14.83	3.81E-08	1	No description
nDi.2.2.2.t08586	-14.80	3.96E-09	247	HVA22-like protein[b,c]
nDi.2.2.2.t08316	-14.67	2.62E-09	755	Major sperm proteinb,c

[a] Gene Ontology

[b] Panther ID

[c] Pfam Annotation

Table S5 Top 25 significantly upregulated transcripts in the JYD-34 females compared to Kentucky females, log fold change, false discovery rate, nematode orthologs, and description.

Gene Transcript ID	logFC	FDR	Nematode orthologs	Description
nDi.2.2.2.t09768	5.50	3.56E-02	16	No description
nDi.2.2.2.t12338	4.75	4.45E-02	No orthologs	No description
nDi.2.2.2.t12786	4.34	4.76E-04	No orthologs	No description
nDi.2.2.2.t07732	3.68	1.92E-02	5	No description
nDi.2.2.2.t09887	3.68	1.98E-06	15	Small heat shock protein[b,c]
nDi.2.2.2.t10654	3.57	1.98E-06	119	Small heat shock protein[b,c]
nDi.2.2.2.t09888	3.56	1.98E-06	15	Small heat shock protein[b,c]
nDi.2.2.2.t09890	3.52	1.98E-06	119	Small heat shock protein[b,c]
nDi.2.2.2.t09889	3.39	1.98E-06	15	No description
nDi.2.2.2.t12787	3.23	4.76E-04	No orthologs	No description
nDi.2.2.2.t10680	3.03	4.78E-03	No orthologs	No description
nDi.2.2.2.t03627	2.64	1.69E-02	22	Transducer of ERBB2- Isoform A[b]
nDi.2.2.2.t09317	2.58	9.38E-04	20	No description
nDi.2.2.2.t03191	2.40	5.22E-04	20	Serine/Threonine-kinase UNC-51 related protein[b]
nDi.2.2.2.t02996	2.39	1.97E-03	No orthologs	No description
nDi.2.2.2.t10141	2.32	2.91E-02	31	No description
nDi.2.2.2.t08672	2.25	3.06E-03	11	No description
nDi.2.2.2.t03766	2.18	6.14E-03	9	No description
nDi.2.2.2.t10026	2.17	2.68E-02	No orthologs	No description
nDi.2.2.2.t08317	2.16	1.11E-02	No orthologs	No description
nDi.2.2.2.t07759	2.14	7.27E-03	102	Protein binding activity[a]
nDi.2.2.2.t11101	2.12	3.95E-02	No orthologs	No description
nDi.2.2.2.t06731	1.95	1.39E-02	153	Protein kinase domain-containing protein[b]
nDi.2.2.2.t08120	1.91	2.52E-03	5	Protein CBG05606[b]
nDi.2.2.2.t05422	1.89	3.89E-03	No orthologs	Nuclear-transcribed mRNA catabolic process[a]

[a] Gene Ontology

[b] Panther ID

[c] Pfam Annotation

Table S6 Top 25 significantly downregulated genes in the JYD-34 females compared to Kentucky females, log fold change, false discovery rate, nematode orthologs, and description.

Gene Transcript ID	logFC	FDR	Nematode orthologs	Description
nDi.2.2.2.t04611	-6.37	2.55E-02	19	No description
nDi.2.2.2.t11995	-6.32	1.97E-03	1	No description
nDi.2.2.2.t10909	-5.82	2.30E-02	2	No description
nDi.2.2.2.t10736	-5.81	4.47E-02	26	SH2 domain containing protein[c]
nDi.2.2.2.t07464	-5.44	2.31E-04	10	MLT-4[b]
nDi.2.2.2.t07211	-4.94	2.10E-03	121	Acyl-CoA oxidase[c]
nDi.2.2.2.t10020	-4.35	3.11E-04	5	Stichodactyla toxin[c]
nDi.2.2.2.t12092	-4.20	8.36E-03	1	No description
nDi.2.2.2.t10989	-4.06	2.69E-02	109	Serine-type peptidase[a,b]
nDi.2.2.2.t11928	-3.68	2.69E-02	11	Integral component of membrane[a]
nDi.2.2.2.t03886	-3.26	7.71E-06	438	Vitellogenin related protein[b,c]
nDi.2.2.2.t09344	-3.15	2.97E-02	No orthologs	No description
nDi.2.2.2.t04750	-3.06	1.04E-02	4	No description
nDi.2.2.2.t01863	-3.05	1.65E-04	16	Vimentin-type intermediate filament-associated coiled-coil protein[b]
nDi.2.2.2.t04518	-3.00	9.38E-04	127	Nucleur hormone receptor[a,b,c]
nDi.2.2.2.t09408	-2.93	3.55E-02	26	No description
nDi.2.2.2.t11882	-2.88	1.47E-03	2	No description
nDi.2.2.2.t12160	-2.84	9.38E-04	No orthologs	No description
nDi.2.2.2.t11466	-2.80	3.05E-02	7	No description
nDi.2.2.2.t11721	-2.79	3.29E-03	17	Cell adhesion molecule[b]
nDi.2.2.2.t11556	-2.76	2.24E-03	10	insulin-like growth factor binding protein[a]
nDi.2.2.2.t07151	-2.70	8.06E-03	No orthologs	No description
nDi.2.2.2.t07987	-2.68	2.01E-03	170	Cell adhesion molecule[b.c]
nDi.2.2.2.t10864	-2.65	2.02E-02	4	G-protein coupled receptor[a,b]
nDi.2.2.2.t12266	-2.63	5.34E-03	6	No description

[a] Gene Ontology

[b] Panther ID

[c] Pfam Annotation

Table S7 Top 25 significantly upregulated transcripts in the JYD-34 males compared to Kentucky males, log fold change, false discovery rate, nematode orthologs, and description.

Gene Transcript ID	logFC	FDR	Nematode orthologs	Description
nDi.2.2.2.t12453	4.91	4.36E-02	No orthologs	No description
nDi.2.2.2.t11886	4.30	3.69E-04	No orthologs	Zinc Finger Protein[b]
nDi.2.2.2.t11013	3.74	2.83E-04	14	Zinc Finger Protein[b]
nDi.2.2.2.t03749	3.63	2.21E-04	No orthologs	No description
nDi.2.2.2.t10680	3.57	1.40E-03	No orthologs	Collagen Helix[c]
nDi.2.2.2.t03760	3.04	3.73E-02	161	Rig-3[b]
nDi.2.2.2.t10775	2.95	3.90E-02	7	No description
nDi.2.2.2.t03637	2.78	3.31E-02	No orthologs	No description
nDi.2.2.2.t10163	2.70	3.54E-02	No orthologs	No description
nDi.2.2.2.t09941	2.66	1.26E-02	19	No description
nDi.2.2.2.t03625	2.64	5.82E-04	20	No description
nDi.2.2.2.t09235	2.46	2.68E-03	119	Creatinase[c]
nDi.2.2.2.t06423	2.44	2.58E-02	37	Serpin[b,c]
nDi.2.2.2.t05389	2.40	1.89E-03	No orthologs	No description
nDi.2.2.2.t11214	2.38	1.49E-03	14	Zinc Finger Protein[b]
nDi.2.2.2.t06054	2.28	4.48E-04	15	SKN-1 dependant zygotic transcript related[b]
nDi.2.2.2.t06930	2.24	3.92E-02	14	Adenosine deaminase[b,c]
nDi.2.2.2.t09399	2.23	9.09E-03	1	RPI-1[b]
nDi.2.2.2.t11939	2.19	4.22E-03	11	Sedolisin[c]
nDi.2.2.2.t11383	2.18	3.85E-02	14	No description
nDi.2.2.2.t10848	2.17	3.74E-02	2	Nucleic acid binding[a]
nDi.2.2.2.t11164	2.16	3.75E-03	21	Aspartate aminotransferase[b,c]
nDi.2.2.2.t09049	2.16	5.63E-03	74	Zinc Finger Protein[b,c]
nDi.2.2.2.t04910	2.13	1.15E-03	No orthologs	No description
nDi.2.2.2.t04353	2.07	2.02E-03	18	Serine protease inhibitor 1

[a] Gene Ontology

[b] Panther ID

[c] Pfam Annotation

Table S8 Top 25 significantly downregulated transcripts in the JYD-34 males compared to Kentucky males, log fold change, false discovery rate, nematode orthologs, and description

Gene Transcript ID	logFC	FDR	Nematode Orthologs	Description
nDi.2.2.2.t10949	-8.32	5.44E-04	20	Collagen Helix[c]
nDi.2.2.2.t11357	-7.57	3.19E-03	18	Membrane protein[a]
nDi.2.2.2.t11395	-7.47	6.46E-03	4	CBG16264[b]
nDi.2.2.2.t10310	-7.25	1.82E-03	82	MLT-10 related protein[b]
nDi.2.2.2.t08138	-7.1	4.16E-03	88	Zinc finger transcription factor family protein 30[b]
nDi.2.2.2.t09104	-7.07	2.21E-04	215	Structural constituent of cuticle[a]
nDi.2.2.2.t11791	-7	2.19E-03	No orthologs	No description
nDi.2.2.2.t11710	-6.82	5.33E-03	3	No description
nDi.2.2.2.t12406	-6.81	1.12E-02	7	Transmembrane cell adhesion receptor MUA-3[b]
nDi.2.2.2.t11991	-6.76	2.23E-03	12	No description
nDi.2.2.2.t07951	-6.67	2.82E-05	No orthologs	No description
nDi.2.2.2.t11430	-6.65	7.34E-03	19	MLT-10 related protein[b]
nDi.2.2.2.t11832	-6.54	2.34E-04	5	No description
nDi.2.2.2.t11513	-6.53	4.22E-03	3	Long-chain-fatty-acid COA Ligase 1[b]
nDi.2.2.2.t08868	-6.26	3.89E-03	1	EGF-like domain[c]
nDi.2.2.2.t12504	-6.26	1.16E-02	1	Selectin[c]
nDi.2.2.2.t08006	-6.25	1.49E-02	17	Guanyl-nucleotide exchange factor[b]
nDi.2.2.2.t11112	-6.19	1.06E-02	No orthologs	No description
nDi.2.2.2.t11404	-6.1	3.98E-02	7	Calcium-binding EGF domain[c]
nDi.2.2.2.t12377	-6.09	1.01E-02	8	No description
nDi.2.2.2.t12790	-6.01	1.75E-02	1	Calcium-binding EGF domain[c]
nDi.2.2.2.t10765	-5.87	1.31E-05	7	No description
nDi.2.2.2.t11721	-5.77	1.21E-04	17	Pikachurin-like protein[b]
nDi.2.2.2.t11737	-5.72	7.51E-03	1	No description
nDi.2.2.2.t03131	-5.71	1.85E-02	8	No description

[a] Gene Ontology

[b] Panther ID

[c] Pfam Annotation

Table S9 Quantitative PCR forward and reverse primer sequences(5' → 3') of the six significantly differentially expressed genes, two shared in the females and males: nhr-48 and Let-2, two in the females: rpl-19 and C32D5.12; two in the males: sul-2 and nid-1 used to validate the RNASeq analysis

Gene		**Primer Sequence**
nhr-48	Forward	TATGGTGATCGTGCTATTGG
	Reverse	CTCTTGCCGATTAGCATTTC
let-2	Forward	TAATGAGCAAGGTATCGAGC
	Reverse	TGTACCGCAATAACATTTGC
rpl-19	Forward	ATCGACAAGATTTAGCACGA
	Reverse	TTGACCAGTAATAGAACGCC
C32D5.12	Forward	TTGTCAATTGTTGGACGGTA
	Reverse	TTGCGATACCAGCATAATGA
nid-1	Forward	AATACCACCAGAACTTGGTC
	Reverse	CATTCACCGTGCGATTAAAA
sul-2	Forward	GTCGATGACTTAGGCTATGG
	Reverse	CTCGACTTGGTGAACACATA

Table S10 Statistical summary of alignment to the *D. immitis* reference genome nDi.2.2 of the Kentucky isolate and JYD-34 isolate female and male adult worms.

Sample ID	JYD-34 F1	JYD34 F2	Kentucky F1	Kentucky F2	JYD-34 M1	JYD-34 M2	Kentucky M1	Kentucky M2
Raw total sequences:	86704828	88120846	85586394	76175998	76767544	82864990	95413420	87533322
Sequences:	86704828	88120846	85586394	76175998	76767544	82864990	95413420	87533322
Reads mapped:	86213446	87497131	85120744	75777424	76170027	82139136	94849924	87048608
Reads mapped and paired:	85950106	87142230	84906674	75575572	75846082	81719188	94534416	86759088
Reads properly paired:	82293004	83492454	81514276	72534274	71416772	76155640	89354160	81771334
Reads paired:	86704828	88120846	85586394	76175998	76767544	82864990	95413420	87533322
Bases mapped:	8707558046	8837210231	8597195144	7653519824	7693172727	8296052736	9579842324	8791909408
Error rate:	5.40E-03	6.77E-03	4.27E-03	4.50E-03	4.49E-03	5.15E-03	3.87E-03	3.77E-03
Average quality:	35.9	35.5	36	36	36.1	36	36	36
Properly paired reads (%):	94.9	94.7	95.2	95.2	93	91.9	93.6	93.4

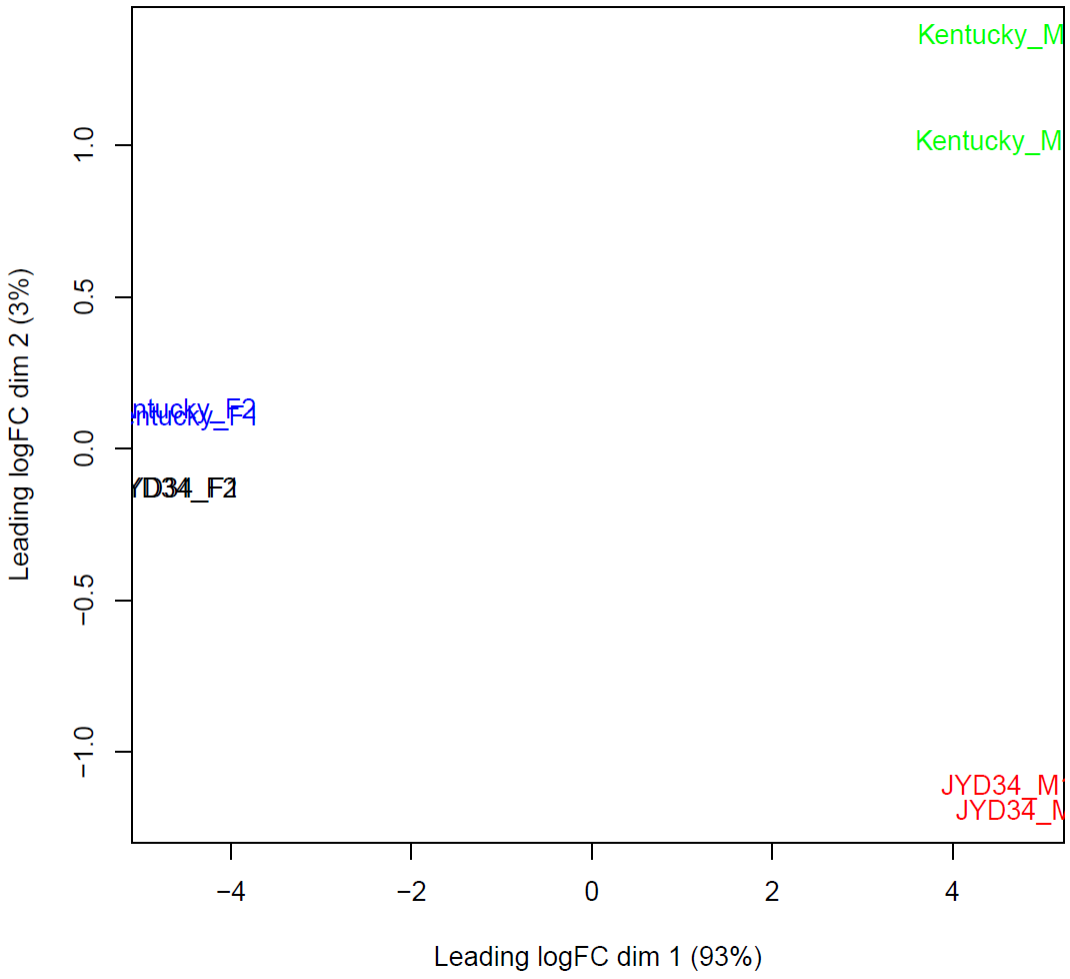

Figure S1 Principal component analysis constructed from the adult females and males of the *D. immitis* Kentucky isolate and JYD-34 isolate. Kentucky females are indicated in blue; Kentucky males are indicated in green, JYD-34 females are indicated in black. And JYD-34 males are indicated in red.

Chapter 5.

Discussion and Conclusion

Discussion

The widespread use of macrocyclic lactone (ML)-based chemoprophylactics for the preventative treatment of dirofilariosis has led to the development of ML-resistant *Dirofilaria immitis* isolates. To date the genetic mechanisms of ML resistance are unclear. It is undetermined whether ML resistance in *D. immitis* is a complex mechanism which depends on several factors or a simple single factor mechanism. Nevertheless, there are numerous genetic changes associated with the ML-resistant phenotype; however, their potential phenotypic and / or genotypic role in chemoprophylaxis failure are not fully understood (Bourguinat et al. 2011c, 2015, 2017, Mani et al. 2017, Ballesteros et al. 2018, Sanchez et al. 2020 Kumar et al. forthcoming). The use of ML chemoprophylaxis at a single proposed dose rate, may not be a clear indication of a population's genetic ML-susceptibility status. There may be *D. immitis* populations which appear susceptible at a given ML dose rate but may show a shift in susceptibility and be on the way to developing resistance, particularly if ML resistance is multigenic. These potential "developing resistance" populations may show changes in their genetic profile and behave similarly to ML-resistant or ML-susceptible isolates, depending on the assay, the ML drug, and drug concentration used. By considering the possible complexity of multigenic ML resistance, the thesis aimed to assess the phenotypic and genotypic variability which may help to distinguish ML-susceptible and ML-resistant populations.

Chapter 2 describes the development of an *in vitro* biological assay to differentiate ML-susceptible and ML-resistant *D. immitis* isolates. The rationale of the *in vitro* biological assay was that MLs act on the microfilariae (mf) lifestage by paralyzing the excretory-secretory pore

(ESP), inhibiting the release of metabolites, enzymes, and immunomodulatory molecules. The metabolic enzyme, triosephosphate isomerase (TPI), was analyzed due to its abundance in the *D. immitis* secretome and the commercial availability of highly sensitive colorimetric enzyme activity assays. I optimized the ML drug concentrations and incubation conditions of the TPI colorimetric enzymatic activity assay described in Chapter 2. It measured the effects of 24 hours ivermectin (IVM) exposure on TPI enzyme activity in the *D. immitis* mf at 0 nM and 25 nM.

The *in vitro* TPI colorimetric enzymatic activity assay was tested in eight USA laboratory-maintained isolates. The phenotypic data collected was consistent with concurrently published genetic analysis for ML resistance. The known ML-susceptible isolates Missouri and Berkeley had statistically significant decreases in TPI enzymatic activity when exposed to 25 nM IVM for 24 hours compared to the untreated control. The three known ML-resistant isolates, JYD-34, Metairie, and WildCat had consistently lower levels of TPI enzymatic activity, which did not respond to IVM treatment. Interestingly, the three remaining ML-susceptible or putative ML-susceptible isolates, Georgia II, Georgia III, and Big Head showed low levels of TPI enzymatic activity at 0 nM and 25 nM IVM. These three isolates shared a similar phenotype with the known ML-resistant isolates in this *in vitro* assay. These results corroborated recent MiSeq, ddPCR duplex, and microsatellite genotyping analyses which showed Georgia II, Georgia III, and Big Head do not have genotypes consistent with their claimed in *vivo* ML chemoprophylaxis response profiles (Sanchez et al. 2020, Curry et al. 2022a, Kumar et al. forthcoming).

The *in vitro* TPI colorimetric enzymatic activity assay may not be the optimal basis for a robust *in vitro* assay to differentiate genetically mixed populations from isolates which are clearly resistant *in vivo*. The apparent phenotypic susceptibility of these isolates, at a given ML dose rate proposed in registration trials may not correlate perfectly with true genotypic ML-

susceptibility. This *in vitro* biological assay is one of the first to document a differential phenotypic response to MLs in genetically mixed populations, which warrants further validation with additional *D. immitis* isolates as they become available. The *in vitro* TPI colorimetric enzymatic activity assay may have utility for the selection of truly susceptible populations for use in academic or pharmaceutical research. The phenotypic results discussed in Chapter 2 also corroborated the ESP as the likely putative target of ML activity in the mf lifestage, and I posited genetic changes in proximity to the ESP may affect drug efflux.

Importantly, genetic changes on the *D. immitis* P-glycoprotein 11 (DimPgp-11) gene have been proposed as markers of resistance. The *Dim*Pgp-11 (A11G) single nucleotide polymorphism (SNP) was one of the 42 nodes used to assess the genetic profiles of ten USA laboratory-maintained isolates and was one of the 10 molecular markers validated in US clinical samples in 2018 (Bourguinat et al. 2017, Ballesteros et al. 2018). Strong genetic evidence has linked *DimPgp*-11 with the ML-resistant phenotype; however, the expression and localization of this transporter have remained unexamined. It has been hypothesized, due to its homology with *C. elegans* P-glycoprotein 11 (*Cel*Pgp-11), that *Dim*Pgp-11 may be strategically located in proximity to the excretory-secretory system, where it may help regulate the response to MLs (Zhao et al. 2004).

Chapter 3 provides an extensive study on the genetic polymorphism, constitutive expression, and localization of *Dim*Pgp-11 in the *D. immitis* mf. I assessed the *Dim*Pgp-11 SNP in USA laboratory-maintained isolates using MiSeq sequencing primers previously described by Ballesteros et al. (2018). I noted the ML-resistant isolates had a higher frequency of the *Dim*Pgp-11 SNP alternate allele, ranging from 17 – 56 %. The ML-susceptible isolates had an alternate allele frequency ranging from 0 – 15 %. These results indicated an increased frequency of the

*Dim*Pgp-11 SNP alternate allele is still associated with ML resistance in the USA laboratory-maintained isolates despite multiple passages in a laboratory setting in the absence ML drug pressure.

Pgps are known ML transporters which are generally upregulated in ML-resistant nematodes (De Graef et al. 2013, Demeler et al. 2013, Janssen et al. 2013, Ménez et al. 2016). I assessed the constitutive expression of *Dim*Pgp-11 in the mf lifestage comparing ML-susceptible and ML-resistant *D. immitis* isolates using droplet digital PCR (ddPCR) technology. I designed and optimized all forward and reverse primers for *Dim*Pgp-11 and its reference genes, *Dim*Actin, *Dim*GAPDH, and *Dim*pmp-3, *de novo*. Surprisingly, the ML-resistant JYD-34 isolate expressed *Dim*Pgp-11 at a statistically significantly lower level compared to the ML-susceptible isolates. It is important to note, constitutive expression does not always correlate one-to-one with protein synthesis or the activity / efficiency of the transporter. Nevertheless, a decrease in constitutive expression may indicate potentially altered activity of *Dim*Pgp-11 in the ML-resistant isolates.

*Dim*Pgp-11 expression was localized using an antibody which targeted the first extracellular loop of the first transmembrane domain (TMD). I designed the antibody with GenScript® and validated it via Western blot and competitive binding assay. The *Dim*Pgp-11 expression sites localized to the cells surrounding the ESP, excretory cell, and more faintly along the body wall in the mf lifestage. The localization of *Dim*Pgp-11 and the differences in constitutive expression between the ML-resistant and ML-susceptible isolates analyzed suggest it may play a role in the regulation of MLs or in regulating the production of ESP products, including the secretion of immunomodulatory molecules. These results are in line with the differential phenotypic ML response profiles observed in Chapter 2.

In Chapter 4, the molecular biology protocols designed *de novo* and optimized to assess the impact of genetic polymorphisms on constitutive gene expression used in Chapter 3 are expanded upon to provide an extensive study on the newly identified SNP molecular marker. A highly differentially expressed indel on the intron between exons 9 and 10 of the *Dim*KYNU-1 gene was flagged as a region of interest in 2018 during comparison of the genomes of ML-resistant and ML-susceptible isolates (Ballesteros and Prichard unpublished). *Dim*KYNU-1 is an enzyme integral to tryptophan catabolism and a precursor to the biosynthesis of rhodoquinone (RQ). RQ is the electron carrier of an alternative anaerobic metabolism utilized by molluscs, annelids, and nematodes, including *D. immitis* adults. In eukaryotes, RQ is derived from the tryptophan catabolism L-kynurenine (KYN) pathway (Buceta et al. 2019, Del Borrello et al. 2019). KYNU-1 catalyzes the synthesis 3-hydorxyanthranilic acid (3HA) which provides the critical amine group to the RQ quinone ring (Buceta et al. 2019, Del Borrello et al. 2019, Salinas et al. 2020). Dysregulation of the KYN pathway leads to altered or abolished RQ production (Buceta et al. 2019, Del Borrello et al. 2019).

I designed MiSeq primers to assess the intron between exons 9 and 10 and subsequently identified a SNP at position 4740. I noted distinct genotypic differences of the *Dim*KYNU-1 SNP between ML-susceptible and ML-resistant *D. immitis* isolates. The *Dim*KYNU-1 SNP alternate allele was more abundant in the ML-resistant isolates, ranging from 9 – 62 %. The Georgia II isolate expressed an alternate allele frequency of 16 %. Georgia II, as previously observed, does not have a genotype consistent with its claimed *in vivo* ML-susceptible profile and has genotypic characteristics more aligned with a mixed or developing resistance population (Ballesteros et al. 2018, Sanchez et al. 2020, Curry et al. 2022a, Kumar et al. forthcoming). In the remaining five ML-susceptible isolates analyzed the frequency of the alternate allele was < 5

%. Future analysis in additional laboratory-maintained isolates and clinically collected *D. immitis* samples will help to determine the predictive ability of the *Dim*KYNU-1 SNP as a marker of ML resistance.

The constitutive expression of *Dim*KYNU-1 was measured in the adult females and males of the ML-susceptible Kentucky isolate and the ML-resistant JYD-34 via ddPCR and RNASeq sequencing. I designed new ddPCR primers for *Dim*KYNU-1. The reference genes and primers designed and validated in Chapter 3 were also utilized in this analysis. Additionally, I prepared the UNIX code required to prepare and analyze the RNASeq sequencing results. I found the Kentucky isolate demonstrated a sex-specific differential constitutive expression with *Dim*KYNU-1 expressed at a higher level in the adult males. *Dim*KYNU-1 was equally expressed in the ML-resistant JYD-34 isolate adult females and males. Interestingly, the enzymes preceding *Dim*KYNU-1 demonstrated a consistent pattern of sex-specific differential expression between the adult females and the adult males in both isolates. Tryptophan hydrolase (*Dim*tph) was expressed at lower levels, and arylformamidase (*Dim*amfd), nematode kynurenine aminotransferase (*Dim*nkat), and tyrosine aminotransferase (*Dim*tatn) were all expressed at higher levels in the adult females of the Kentucky and JYD-34 isolates. These results indicated that among the tryptophan catabolism genes assessed a difference in the pattern of constitutive expression between the Kentucky isolate and JYD-34 isolate was specific to *Dim*KYNU-1. The potential downstream impact of the sex-specific differences in *Dim*KYNU-1 constitutive expression seen in the Kentucky isolate, but not the JYD-34 isolate, was assessed by measuring the relative expression of its downstream product, 3HA. There is limited commercial availability for assays measuring the concentration and / or expression of 3HA. As a result, I designed and validated an indirect enzyme-linked immunosorbent assay (ELISA) to measure the relative

expression of 3HA. The Kentucky isolate showed no statistically significant change in the relative expression of 3HA between the adult females and males. The JYD-34 adult males had a statistically significantly greater relative expression of 3HA compared to the JYD-34 adult females and Kentucky adult females. The differential constitutive expression of *Dim*KYNU-1 and 3HA in the Kentucky and JYD-34 isolates appears to indicate a higher frequency of *Dim*KYNU-1 SNP may affect the efficiency of gene regulation and expression, particularly in the adult males.

It is essential to build a foundational understanding of the biological changes associated with the development of ML resistance in *D. immitis*, both phenotypic and genotypic. Throughout my thesis, I have investigated previously undescribed aspects of *D. immitis* biology, this includes the potential roles of the ESP, the *Dim*Pgp-11 ABCB transporter, and the tryptophan catabolism KYN pathway in ML resistance. The differential phenotypic response via the ESP to 24 hours IVM exposure between the ML-susceptible and ML-resistant isolates characterized in Chapter 2, as well as the localization of *Dim*Pgp-11 in proximity to the ESP described in Chapter 3, indicate the ESP is an ideal putative target for the development of new anti-filarial therapeutics. The optimized molecular biology protocol and preliminary data collected in the mf lifestage are the foundation for future analysis in the infective L3 larvae and adult life stages.

The *Dim*KYNU-1 SNP molecular marker, as well as the differential constitutive expression of *Dim*KYNU-1 and 3HA described in Chapter 4 highlight the necessity for further analysis of *Dim*KYNU-1, tryptophan catabolism, and RQ biosynthesis. *Dim*KYNU-1 and its downstream products may have importance as nematode specific biological markers and / targets. My thesis research provides valuable information on these new putative targets for the

development of future anti-filarial pharmaceuticals, as new therapeutics are urgently needed to maintain companion animal welfare in the face of this potentially fatal disease.

One of the major limitations of working with *D. immitis* was the availability of samples. It is very expensive and raises ethical questions regarding the use of animal to maintain the *D. immitis* isolates and their life cycles. Over the course of my thesis research, many of the isolates initially available to academic laboratories were removed from circulation and are no longer available. Similarly new ML-resistant isolates are currently unavailable. As a result, definitive conclusions cannot be made on associations with ML resistance. As more *D. immitis* isolates become available additional studies can be undertaken based on the research presented in this thesis. Firstly, the analyses of constitutive gene expression versus ML-induced gene expression, ideally in the adult females and males, infective L3 larvae, and mf of > 5 *D. immitis* isolates per *in vivo* ML phenotypic response profile. ddPCR and RNASeq analyses of this scale would allows us to validate the expression of genes already associated with ML resistance, such as *Dim*Pgp-11 and *Dim*KYNU-1, as well as identify new genes which may be significantly differentially expressed across life stages or following ML exposure. Secondly, the next steps of the *Dim*KYNU-1 analyses could include the targeted lipidomics of the *Dim*KYNU-1 and 3HA downstream product, RQ. Recent protocols developed for *C. elegans* would allow us to compare the expression ratio of the ubiquinone (UQ) and RQ electron carriers in ML-susceptible and ML-resistant *D. immitis* isolates (Del Borrello et al. 2019).

Conclusion

The work undertaken as part of my thesis has combined biochemistry, molecular biology, confocal imaging, and bioinformatic protocols. This has allowed me to identify enzyme secretion via the ESP as a phenotypic measure to differentiates ML-susceptible isolates from genetically

mixed and ML-resistant isolates. In parallel, I have confirmed and dissected two known markers of ML resistance. (i) I localized *Dim*Pgp-11 in proximity to the ESP as a strategic putative player in exchanging molecules from the parasite to the environment or vice versa; (ii) I identified a potential new player, *Dim*KYNU-1, in the development and modulation of multigenic ML resistance in *D. immitis*. The characterization of these phenotypes and genotypic markers facilitates a better understanding of the development of ML resistance and lays the foundations for future molecular analyses of ML resistance in the parasitic filarial nematode *D. immitis*.

Connecting Statement III

The Appendix analyzed three USA laboratory-maintained isolates: Berkeley, Georgia II, and WildCat; and 11 randomly selected European clinical samples using the top 9 clinically validated single nucleotide (SNP) molecular markers associated with macrocyclic lactone (ML) resistance. The samples tested were fresh microfilaria (mf) in blood and adult worms preserved in ethanol. The Berkeley isolate displayed slight allele alteration in comparison to the reference genome at three SNP sites ranging from 8 – 17 %. The Georgia II isolate displayed low levels of the alternate alleles ranging from 5 – 14 % at five SNP sites. The WildCat isolate is genotypically ML-resistant and displayed high levels of the alternate allele at all SNP sites ranging from 22 – 61 %. On the other hand, the 11 European clinical samples displayed genotypes consistent with ML-susceptibility based on the 9 SNP. The results of the Appendix provided the first genotypic analysis of these three USA laboratory-maintained isolates and any European samples.

The works conducted in the Appendix provided the genetic background for the Berkeley, Georgia II, and WildCat isolates, which aided in the assessment of phenotypic and genotypic ML resistance within the thesis manuscript. Additionally, the bioinformatic analyses and tools optimized in the Appendix provided the foundational skills required for the large data analyses undertaken in Chapters 3 and 4 to characterize the *Dim*Pgp-11 and *Dim*KYNU-1 SNP molecular markers.

Appendix.

Dirofilaria immitis: Genotyping randomly selected European clinical samples and USA laboratory isolates with molecular markers associated with macrocyclic lactone susceptibility and resistance.

Emily Curry[1*], Donato Traversa[2], Elena Cárreton[3], Laura Kramer[4], Heinz Sager[5], Lisa Young[6], Roger Prichard[1]

[1]Institute of Parasitology, McGill University, Sainte Anne-de-Bellevue, QC, Canada

[2]Faculty of Veterinary Medicine, Località Piano d'Accio snc, 64100, Teramo, Italy

[3]Faculty of Veterinary Medicine, IUIBS, University of Las Palmas de Gran Canaria, Spain

[4]Dipt. Scienze Medico-Veterinarie, Università di Parma, 43126 Parma, Italy

[5]Elanco Tiergesundheit AG, CH-4058 Basel, Switzerland

[6]Elanco Animal Health, Greenfield, IN 46140, USA

EC*: emily.curry@mail.mcgill.ca

DT: dtraversa@unite.it

RP: roger. prichard@mcgill.ca

EC: elena.carreton@ulpgc.es

LK: laurahelen.kramer@unipr.it

HS: heinz.sager@elancoah.com

LY: lisa.young@elancoah.com

Published in Pathogens (Curry et al. 2022)

Abstract

Dirofilaria immitis is a parasitic nematode and causes dirofilariosis, a potentially fatal pulmonary infection which primarily infects canids. Dirofilariosis infections are controlled via prophylactic macrocyclic lactone (ML) regimens. Recent evidence has confirmed the development of ML-resistant isolates in the USA, which are genetically distinct from wildtype populations. Single nucleotide polymorphism (SNP) associated with ML-resistant phenotypes were clinically validated in USA populations. In this study, three USA laboratory-maintained isolates: Berkeley, Georgia II, and WildCat; and 11 randomly selected European clinical samples from 7 hosts were analyzed. The samples tested were fresh microfilaria (mf) in blood or adult worms preserved in ethanol. The samples underwent MiSeq sequencing of the top 9 SNP associated with ML resistance. The results provide the first genotypic analysis of the three USA laboratory-maintained isolates and any European samples. The European clinical samples show no genomic evidence of ML resistance based on the 9 SNP. The early adoption of genotyping of clinical *D. immitis* samples could provide an early indication of the potential development of ML resistance and aid to distinguish clinical cases of heartworm infection due to ML resistance from those due to a lack compliance with the recommended treatments, as has been seen in North America.

Keywords: *Dirofilaria immitis*, Dirofilariosis, Macrocyclic Lactones, Susceptibility, Resistance, Molecular Markers, Single Nucleotide Polymorphism

1. Introduction

Dirofilaria immitis is a veterinary parasitic filarial nematode and the cause of dirofilariosis, a potentially fatal pulmonary infection which primarily affects canids, with humans occasionally acting as an incidental host. Macrocyclic lactones (MLs) were first approved as a monthly prophylactic treatment for dirofilariosis in 1987 and remain the standard of care (Chabala et al.

1980, Campbell 1981, Campbell et al. 1983, Ohishi et al. 1987a, 1987b). The MLs are used at extremely low dose rates, in *D. immitis* the MLs target and kill the infective L3 and developing L4 larvae. At slightly higher concentrations the MLs can reduce the fecundity of adults for up to 6 months and help clear blood-circulating microfilariae (mf). This class of drugs has been used as an effective and generally safe prophylactic treatment for preventing dirofilariosis. Complaints of heartworm preventive product ineffectiveness were brought to the USA FDA Center for Veterinary Medicine (FDA / CVM) as early as 1998, only 11 years after being placed on the market. In 2005, ML drug loss of efficacy (LOE) cases, documented in known dirofilariosis hotspots throughout the southern USA, were brought to public attention (Hampshire 2005). The heritability of ML resistant isolates was established in 2014 by experimentally infecting laboratory dogs with *D. immitis* field LOE isolates (Pulaski et al. 2014).

Whole genome analysis elucidated single nucleotide polymorphisms (SNPs) associated with a resistant phenotype (Bourguinat et al. 2015, Bourguinat et al. 2017a , 2017b). The 10 SNPs which best differentiated the ML-resistant phenotype from the ML-susceptible phenotype were selected for analysis in clinical dirofilariosis infections collected from the continental USA (Ballesteros et al. 2018). A significant correlation of the SNP loci frequencies and the moxidectin microfilaricidal response phenotype was observed in 9 of the 10 SNPs (Ballesteros et al. 2018). The clinical validation of the molecular markers for ML resistance in *D. immitis* provides the first genetic test to confirm the development of ML-resistant isolates which are genetically distinct from wildtype populations. These markers can be used to differentiate between ML-resistant *D. immitis* isolates versus cases of opportunistic infections caused by lack of compliance, inadequate administration, or no history of ML use.

Figure 1 a) Distribution of USA laboratory-maintained isolates received from TRS Laboratories b) Distribution of European clinical samples received from Italy, Hungary, Spain, and the Canary Islands. The maps were created using Google Maps, accessed May 2nd and August 26th, 2021.

The prevalence of *Dirofilaria* infections is on the rise in Europe (Genchi and Kramer, 2020). The rise in dirofilariosis infections is likely the result of increased temperatures due to climate change and increased movement of companion animals across borders (Genchi et al. 2005, Genchi et al. 2009, Traversa et al. 2010). Hundreds of thousands of dogs are relocated internationally each year in Europe, with more than 300,000 entering the United Kingdom via the EU Pet Travel Scheme (PETS) alone (Norman et al. 2020). Large numbers of dogs are also relocated throughout North America, with a recent report from Canada demonstrating that dogs originating in USA are positive for heartworm at double the frequency of Canadian dogs (Jacobson et al. 2020). *D. immitis* infections were reported in 109 dogs in Austria, with the dogs originating from Hungary, Greece, the western Balkans, the Iberian Peninsula, Romania, USA, or Bulgaria (Sonnberger et al. 2020). As temperatures continue to rise *D. immitis* infections are expected to spread north from the Mediterranean (Montoya-Alonso et al. 2016). Autochthonous transmission of canine dirofilariosis has encroached on regions previously untouched by naturally occurring infections such as Hungary and Balkan countries (Bacsadi et al. 2016, Ionică

et al. 2017, Farkas et al. 2020, Savić et al. 2020). Given the geographical expansion of dirofilariosis it will be important to monitor the effectiveness of MLs in Europe and the possible emergence of resistance. To date there is minimal published information on the genetic makeup and diversity of European isolates, with (Laidoudi et al. 2022) finding a single common haplotype present in European samples analyzed. In the current study we analyze the prevalence of the validated North American SNP markers associated with susceptibility and resistance to MLs in European clinical samples.

2. Results

The alternate allele frequencies were calculated from the read frequencies using BVAtools in comparison to the *D. immitis* reference genome nDi.2.2 (Dataset S1). The SNP markers were ordered based their individual performance identified with MetaboAnalyst using the Random Forest algorithm as defined by Ballesteros et al. (2018). The average alternative allele frequency for each of the 9 SNP positions were plotted in a heatmap for the three USA laboratory-maintained isolates and the 11 European sample (Figure 1). The WildCat isolate carried higher frequencies of the alternate nucleotide for all SNP markers ranging from 22 – 61 %, with a genotype comparable to previously characterized ML-resistant USA laboratory-maintained isolates, such as JYD-34 and Metairie (Figure 2) (Bourguinat et al. 2017a).

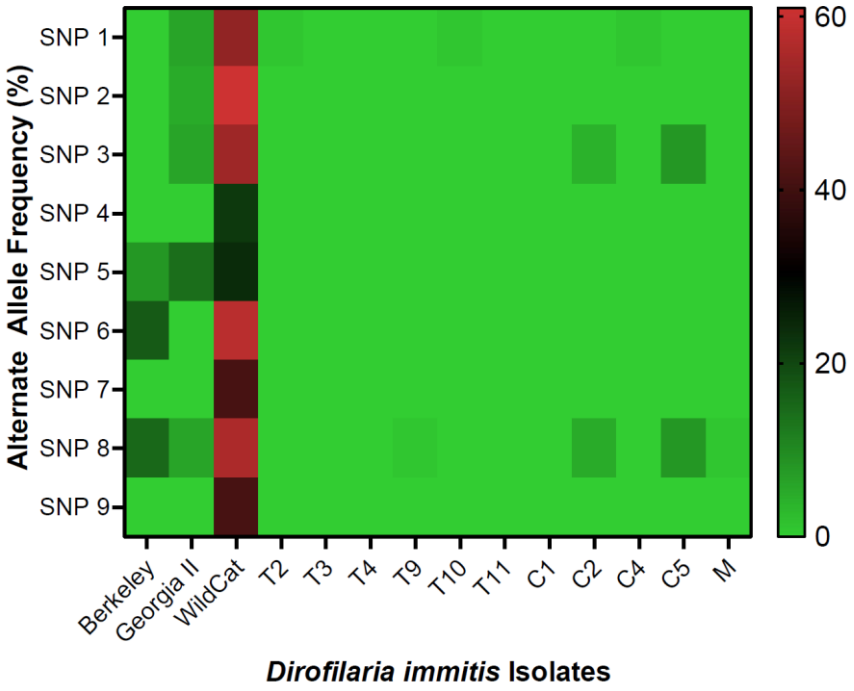

Figure 2 Heat map of the alternate allele frequency of the 9 SNP molecular markers, for the three USA laboratory-maintained isolates Berkeley, Georgia II, and WildCat; and the 11 European clinical samples, T2, T3, T4, T9, T10, T11, C1, C2, C4, C5, and M. The alternative allele frequencies for the 9 SNP molecular markers were prepared in comparison to the *D. immitis* reference genome nDi.2.2.

The Berkeley isolate displayed some allele alteration in comparison to the reference genome at SNPs 5, 6, and 8 ranging from 8 – 17 % at these three sites (Figure 2). The Georgia II isolate displayed low levels of alternate alleles from 5 – 14 % at 5 SNP sites, specifically: 2, 4, 5, 6, and 8 (Figure 2). The 11 European samples displayed genotypes consistent with ML-susceptibility. Two European samples C2 and C5 each showed a low-level presence of an alternate allele at two SNP sites. Sample C2 had an alternate allele frequency of 4 % at SNP 3 and 5 % at SNP 8 (Figure 2). Sample C5 had an alternate allele frequency of 8 % at SNP 3 and 8

% at SNP 8. Despite these slight alterations in samples C2 and C5 when compared to the reference genome nDi.2.2, the European samples were closely aligned to the reference genome.

3. Discussion

Previous research indicates an increase in *D. immitis* infections in the USA (AHS, 2014, Drake and Wiseman 2018). ML-resistant isolates, genetically distinct from the wildtype population, have been confirmed and documented in the southern USA during the last decade. This is not unexpected after long-term and widespread use of prophylactic MLs (Pulaski et al. 2014, Bourguinat et al. 2015, Bourguinat et al. 2017a, 2017b, Ballesteros et al. 2018). The current study completed the first genomic analysis of the USA laboratory-maintained Berkeley and Georgia II, and WildCat isolates; as well as 11 European clinical samples collected from seven canine hosts which were randomly selected from dirofilariosis endemic regions.

The Berkeley, Georgia II, and WildCat isolates were three isolates used to validate the efficiency of the milbemycin oxime based Credelio Plus™ in *in vivo* chemoprophylactic studies. The Berkeley and Georgia II isolates demonstrated a ML-susceptible phenotype with 100 % parasite clearance as defined by the FDA / CVM and the European Medicines Agency (EMA). The WildCat isolate demonstrated an efficacy rate ranging from 81.7 – 90 %; however, due to the lack of 100 % parasite clearance the WildCat isolate is defined as having an ML-resistant phenotype. The phenotypic ML-susceptibility categorisations were upheld in the current genomic SNP analysis.

D. immitis populations are heterologous and can have a high degree of genetic variability within a population of an isolate within an individual host. ML resistance, as it is currently defined is less than 100 % ML efficiency rate in *in vivo* chemoprophylactic studies. When *in vivo* clinical trials are run only one dose rate is usually tested; that proposed for the commercial

product. Therefore, it is not easy to pick up early evidence of resistance selection. To date USA laboratory-maintained isolates are characterized as ML susceptible due to their elimination at the commercial dose rate of treatment or proposed lack of ML-drug exposure. A lack of history of prophylactics in a particular dog does not necessarily mean that the ancestors of the challenged worms had not been exposed to repeated ML chemoprophylaxis. In fact, the American Heartworm Society (AHS) recommendation that all dogs in the USA be treated 12 months of the year. As a result, *D. immitis* populations whose ancestors were truly naïve to ML prophylaxis, are becoming increasingly rare.

The current definitions used to define "ML-susceptible", and "ML-resistant" isolates do not reflect the potential for genetically mixed populations and may not be a clear indication of an isolate's ML-susceptibility status (Sanchez et al. 2020, Curry and Prichard 2022). There may be *D. immitis* populations which appear susceptible at a given ML dose rate but may show a shift in susceptibility if a dose response curve is investigated (Prichard 2021). Phenotypic ML-susceptibility may not correlate directly with genotypic ML-susceptibility. The criteria utilized to define ML resistance in *D. immitis* may require revision to signal the genotypic variability within ML-susceptible, genetically mixed, and ML-resistant isolates and how these heterologous populations can produce variability in phenotypic assessments.

Genomic level testing, via the SNP molecular markers, provides key background information on the *D. immitis* isolates currently being used in laboratory and pharmaceutical research. However, little information has been documented on the potential development of ML resistance in European *D. immitis* populations. The European samples showed allele frequencies closely aligned with the *D. immitis* reference genome nDi.2.2 at the 9 SNP markers tested (Figure 2). The genotype analysis of the randomly selected European clinical samples showed

that all 11 samples have genotypes consistent with ML susceptibility. The current study is a small random sampling of *D. immitis* clinical samples from a limited number of countries; however, the results of the study indicate no evidence for the development of ML resistance based on the North American SNP molecular markers in the samples tested. Following this gathering of preliminary data, a larger study across more geographical locations in canines with detailed treatment histories should be considered for conclusive evidence.

4. Materials and Methods

4.1 USA Samples

Three USA laboratory-maintained isolates were analyzed, Berkeley, Georgia II, and WildCat (Table 1). The Berkeley *D. immitis* isolate originated in Berkeley County, South Carolina, and has been maintained since April 2014. The Georgia II isolate originated in Vidalia, Georgia and has been maintained since April 2013. The WildCat isolate originated in West Liberty, Kentucky and has been maintained since August 2012. The three isolates were provided by TRS Lab Inc. Athens, GA, USA.

Table 1 *Dirofilaria immitis* sample identification, life stage, treatment history and origin for the US laboratory-maintained isolates and the European clinical samples which underwent MiSeq Illumina Sequencing.

Sample	Life Stage	Isolate	Dog Type	ML Treatment	Origin
USA laboratory-maintained isolates					
WildCat	Blood mf	WildCat	Unknown	Non treated	West Liberty, KY, USA
Berkeley	Blood mf	Berkeley	Unknown	Non treated	Berkeley County, SC, USA
Georgia II	Blood mf	Georgia II	Unknown	Non treated	Vidalia GA, USA
European clinical samples					
T2	Adult ♀	Unknown	Unknown	Unknown	Lombardy Region, Italy
T3	Adult ♀	Unknown	Unknown	Unknown	Lombardy Region, Italy
T4	Adult ♀	Unknown	Unknown	Unknown	Lombardy Region, Italy
T9	Adult ♀	Unknown	Unknown	Unknown	Hungary
T10	Adult ♀	Unknown	Unknown	Unknown	Hungary
T11	Adult ♀	Unknown	Unknown	Unknown	Hungary
C1	Blood mf	Unknown	Canary Mastiff	Non treated	Canary Island, Spain
C2	Blood mf	Unknown	Canary Mastiff	Non treated	Canary Island, Spain
C4	Blood mf	Unknown	Canary Hound	Non treated	Canary Island, Spain
C5	Blood mf	Unknown	Canary Mastiff	Non treated	Canary Island, Spain
M	Blood mf	Unknown	Spanish Greyhound	Ivermectin	ǂHuelva, Andalusia Spain

4.2 European Sample Details

The 11 randomly selected European clinical samples were collected from seven different canine hosts (Figure 1). Samples T2, T3, and T4 were collected from a single canine in Lombardy, Italy. The dog died of unrelated causes and ML treatment history is unknown. The adult female worm samples were collected at necropsy and preserved in ethanol. Samples T9, T10, and T11 were collected from a single dog in Hungary. The ML treatment history is unknown. The adult female worm samples were collected at necropsy and preserved in ethanol. Samples C1, C2, C4, and C5 originated in hunting and guard dogs that lived in rural areas Gran Canaria, in the Canary Islands, Spain (Table 1). The mf positive blood samples were collected at a large dog shelter and there was no history of ML prophylaxis in the documentation delivered with the animals. Hunting and guard dogs traditionally do not receive dirofilariosis chemoprophylactics and

several factors influence this, including low economic and socio-cultural level (Montoya-Alonso et al. 2016). The dogs, from which the Gran Canaria samples were obtained, almost certainly never received prophylaxis. Finally, sample M was collected from a Spanish Greyhound from Huelva, Andalusia, Spain adopted and relocated to Savona, Italy (Table 1). Following adoption M was placed on 24 months of monthly ivermectin (IVM) at the standard dose rate without suppression of mf and numbers at approximately 4,150 mf / ml at the time of the blood draw. However, the presence of mf is not unexpected as IVM is not a registered microfilaricidal.

4.3 Sample Processing and DNA Extraction

The canine venous blood samples of the three USA laboratory-maintained isolates and the five European clinical blood samples were shipped to McGill University for immediate processing. The mf were extracted from the blood by filtration (Bourguinat et al. 2015). The blood was diluted 1 : 1 with NaHCO3 solution and passed through polycarbonate membrane filters (3.0 μm; 25 mm; Sterlitech® Corporation, Kent, WA, USA) to isolate mf. The six adult worms from Italy and Hungary canine hosts were shipped to McGill University and rehydrated in PBS prior to genomic DNA extraction.

Genomic DNA from the mf samples and the rehydrated adult worms were extracted using the QIAamp® DNA Micro kit (Qiagen Inc. Toronto, ON). DNA concentrations were determined with the Quant-iT™ PicoGreen DNA Assay Kit (Invitrogen®, Life Technologies Inc. Burlington, ON, Canada). The 14 samples were stored at – 80 ° C prior to being sent to Génome Québec for sequencing.

4.4 SNP Markers

The 9 SNP markers used to analyse the status of ML resistance in the European samples were the top 9 markers clinically validated in 2018 to best differentiate ML-susceptible and ML-resistant

phenotypes (Table S1) (Ballesteros et al. 2018). The SNP 10 marker reported in the same study on nDi.2.2.scaf00597 at position 12915 was not chosen for further analysis as it was not considered a reliable indicator for susceptible versus resistant genotyping.

4.5 Sequencing

The regions encompassing the 9 SNPs of interest were sequenced on an Illumina MiSeq Platform, at a coverage of 2000X. The Fluidigm Access Array system performed target enrichment using array-based PCR amplification of the genomic target regions. The three USA samples and the 11 European samples underwent parallel amplification using custom primers with added CS1 and CS2 tails, as described in Ballesteros et al. (2018) (Table S1). The samples were barcoded during target enrichment which allowed for multiplexed sequencing, and adapter sequences were added during the PCR amplification reaction. The MiSeq high throughput sequencing data reported for the samples are available on the NCBI Sequence Read Archive as BAM files under the following accession numbers SAMN26854346, SAMN26854345, SAMN26854344, SAMN26854343, SAMN26854342, SAMN26854341, SAMN26854340, SAMN26854339, SAMN26854338, SAMN26854337, SAMN26854336, SAMN26854335, SAMN26854334, and SAMN26854333 in BioProject PRJNA818334.

4.6 Data Analysis

Trimmomatic was used to trim for minimal trailing quality (30 PHRED score) and filter for minimum read length by removing the Illumina sequencing adapters from read and adapter clippings (Bolger et al. 2014). The resulting read pairs were aligned to the *D. immitis* reference genome nDi.2.2 (http://www.nematodes.org/genomes/dirofilaria_immitis) using BWA-mem (http://bio-bwa.sourceforge.net/) resulting in binary alignment map files (BAM) (Li and Durbin, 2009). The alignments were processed with Picard (https://broadinstitute.github.io/picard) for the

realignment of indels, mate fixing, and marking of duplicate reads. BVATools (https://bitbucket.org/mugqic/bvatools/src) was used to extract base frequencies at each of the 9 SNP positions and the read frequencies were assimilated to the allele frequencies (Dataset S1). Alternate alleles frequencies for the 9 SNP molecular markers were compared as half the samples were individual adult worms, for which population fixation indexes (FST) could not be calculated.

5. Conclusions

Autochthonous transmission of canine *D. immitis* appear to be migrating from the Mediterranean and Iberian Peninsula, moving further into Central and Northern Europe, likely, a result of the movement of dogs around Europe, and possibly a result of increasing mosquito populations. To date, no case of ML-resistant *D. immitis* infection has been documented in Europe. As the number of *D. immitis* infections continues to rise and spread throughout Europe, the early adoption of genotyping of clinical *D. immitis* samples could provide an early indication of the potential development of ML resistance and aid to distinguish clinical cases of heartworm infection due to ML resistance from those due to a lack of prevention or inadequate compliance, as has been seen in North America. Epidemiological surveys of *D. immitis* samples collected across Europe with diverse chemoprophylactic treatment histories from historically endemic regions of the Mediterranean, newly endemic regions such as the Balkans and Austria, and previously non-endemic regions of Northern Europe can provide insight into the genetic makeup and genetic diversity of European clinical samples.

Declarations

Author Contributions

Emily Curry: Methodology, Formal analysis, Investigation, Writing- Original Draft. Donato Traversa: Resources, Writing - Review & Editing. Elena Cárreton: Resources, Writing - Review & Editing. Laura Kramer: Resources, Writing - Review & Editing. Heinz Sager: Conceptualization, Writing - Review & Editing, Funding Acquisition. Lisa Young: Conceptualization, Writing - Review & Editing, Funding Acquisition. Roger Prichard: Conceptualization, Writing - Review & Editing, Supervision, Funding Acquisition

Funding

This research was funded by Elanco Animal Health (Greenfield, IN, USA).

Institutional Review Board Statement

Not applicable.

Informed Consent Statement

Not applicable.

Data Availability Statement

The data presented in this study are openly available on the NCBI Sequence Read Archive as BAM files under accession numbers SAMN26854346, SAMN26854345, SAMN26854344, SAMN26854343, SAMN26854342, SAMN26854341, SAMN26854340, SAMN26854339, SAMN26854338, SAMN26854337, SAMN26854336, SAMN26854335, SAMN26854334, and SAMN26854333 in BioProject PRJNA818334.

Acknowledgments

We thank Génome Québec Innovation Centre for the preparation of the alignment files. We thank TRS Lab Inc. for providing the USA *D. immitis* isolates. EC* thanks Kathy Keller for her

help in sample preparation and submission. EC* thanks Cristina Ballesteros for her guidance in the analysis of the sequencing data. DT thanks Antonio Frangipane di Regalbono for the help in recovering the Italian *Dirofilaria immitis* specimens. LK thanks Luigi Venco for reporting the sample M as a possible resistant.

Conflicts of Interest

The research was supported by Elanco Animal Health. LY and HS are employees of the sponsor. However, the sponsor of the research exercised no influence over the conduct of the research. The other authors declare no conflicts of interest that could influence the conduct or results of this study.

Supplementary Information

Table S1 The allele count and alternative allele frequencies for the 9 SNP molecular markers when compared to the *D. immitis* reference genome nDi.2.2.for the US laboratory-maintained isolate WildCat, originating from West Liberty, Kentucky. Data collected from genomic DNA of *D. immitis* microfilaria submitted for MiSeq Illumina sequencing and calculated using BVAtools.

Scaffold	Position	Allele Counts				Allele Frequency				RefBase
WildCat		C	A	T	G	C	A	T	G	
nDi.2.2.scaf00046	76278	16914	32	15786	92	0.52	0	0.48	0	T
nDi.2.2.scaf00046	22857	19932	3	12818	2	0.61	0	0.39	0	T
nDi.2.2.scaf00046	222254	3	15258	16	17624	0	0.46	0	0.54	A
nDi.2.2.scaf00185	10639	27	8	20292	5680	0	0	0.78	0.22	T
nDi.2.2.scaf00185	62174	21126	4	6727	5	0.76	0	0.24	0	C
nDi.2.2.scaf00140	30919	15936	15029	13	14	0.51	0.58	0	0	C
nDi.2.2.scaf00005	662854	12156	63	17757	28	0.41	0	0.59	0	T
nDi.2.2.scaf00004	79766	17491	12	13709	4	0.56	0	0.44	0	T
nDi.2.2.scaf00001	466197	21	15565	10737	22	0	0.59	0.41	0	A

Table S2 The allele count and alternative allele frequencies for the 9 SNP molecular markers when compared to the *D. immitis* reference genome nDi.2.2.for the US laboratory-maintained isolate Berkeley, originating from Berkeley County, South Carolina. Data collected from genomic DNA of *D. immitis* microfilaria submitted for MiSeq Illumina sequencing and calculated using BVAtools.

Scaffold	Position	Allele Counts				Allele Frequency				RefBase
Berkeley		C	A	T	G	C	A	T	G	
nDi.2.2.scaf00046	76278	107	12	32683	147	0	0.99	0	0	T
nDi.2.2.scaf00046	22857	58	8	29550	4	0	0	1	0	T
nDi.2.2.scaf00046	222254	13	29617	22	87	0	1	0	0	A
nDi.2.2.scaf00185	10639	28	2	17661	3	0	0	1	0	T
nDi.2.2.scaf00185	62174	20241	4	1648	0	0.92	0	0.08	0	C
nDi.2.2.scaf00140	30919	22101	4415	18	17	0.83	0.17	0	0	C
nDi.2.2.scaf00005	662854	85	59	27406	54	0	0	1	0	T
nDi.2.2.scaf00004	79766	3823	6	21182	54	0.15	0	0.85	0	T
nDi.2.2.scaf00001	466197	9	24228	23	48	0	1	0	0	A

Table S3 The allele count and alternative allele frequencies for the 9 SNP molecular markers when compared to the *D. immitis* reference genome nDi.2.2.for the US laboratory-maintained isolate Georgia II, originating from Vidalia, Georgia. Data collected from genomic DNA of *D. immitis* microfilaria submitted for MiSeq Illumina sequencing and calculated using BVAtools.

Scaffold	Position	Allele Counts				Allele Frequency				RefBase
Georgia II		C	A	T	G	C	A	T	G	
nDi.2.2.scaf00046	76278	1887	12	30690	159	0.06	0	0.94	0	T
nDi.2.2.scaf00046	22857	1680	5	29397	9	0.05	0	0.95	0	T
nDi.2.2.scaf00046	222254	8	29202	25	1726	0	0.94	0	0.06	A
nDi.2.2.scaf00185	10639	40	6	20972	2	0	0	1	0	T
nDi.2.2.scaf00185	62174	20971	6	3486	4	0.86	0	0.14	0	C
nDi.2.2.scaf00140	30919	27649	23	19	3	1	0	0	0	C
nDi.2.2.scaf00005	662854	79	58	27554	41	0	0	0.99	0	T
nDi.2.2.scaf00004	79766	1615	13	26037	6	0.06	0	0.94	0	T
nDi.2.2.scaf00001	466197	5	23841	19	57	0	1	0	0	A

Table S4 The allele count and alternative allele frequencies for the 9 SNP molecular markers when compared to the *D. immitis* reference genome nDi.2.2.for European clinical sample T2, originating from the Lombardy Region, Italy. Data collected from genomic DNA of *D. immitis* adult female submitted for MiSeq Illumina sequencing and calculated using BVAtools.

Scaffold	Position	Allele Counts				Allele Frequency				RefBase
T2		C	A	T	G	C	A	T	G	
nDi.2.2.scaf00046	76278	80	31	27479	147	0	0	0.99	0.01	T
nDi.2.2.scaf00046	22857	54	16	27125	3	0	0	1	0	T
nDi.2.2.scaf00046	222254	16	26194	25	77	0	1	0	0	A
nDi.2.2.scaf00185	10639	29	13	16373	2	0	0	1	0	T
nDi.2.2.scaf00185	62174	19972	6	18	3	1	0	0	0	C
nDi.2.2.scaf00140	30919	25084	16	21	3	1	0	0	0	C
nDi.2.2.scaf00005	662854	68	72	24346	41	0	0	0.99	0	T
nDi.2.2.scaf00004	79766	85	14	22694	4	0	0	1	0	T
nDi.2.2.scaf00001	466197	13	21079	9	59	0	1	0	0	A

Table S5 The allele count and alternative allele frequencies for the 9 SNP molecular markers when compared to the *D. immitis* reference genome nDi.2.2.for European clinical sample T3, originating from the Lombardy Region, Italy. Data collected from genomic DNA of *D. immitis* adult female submitted for MiSeq Illumina sequencing and calculated using BVAtools.

Scaffold	Position	Allele Counts				Allele Frequency				RefBase
T3		C	A	T	G	C	A	T	G	
nDi.2.2.scaf00046	76278	114	15	26392	127	0	0	0.99	0	T
nDi.2.2.scaf00046	22857	73	14	27048	2	0	0	1	0	T
nDi.2.2.scaf00046	222254	10	23364	14	82	0	1	0	0	A
nDi.2.2.scaf00185	10639	18	10	11827	5	0	0	1	0	T
nDi.2.2.scaf00185	62174	18757	5	10	3	1	0	0	0	C
nDi.2.2.scaf00140	30919	21713	10	18	5	1	0	0	0	C
nDi.2.2.scaf00005	662854	95	44	25257	54	0	0	0.99	0	T
nDi.2.2.scaf00004	79766	75	4	18803	4	0	0	1	0	T
nDi.2.2.scaf00001	466197	2	22252	21	55	0	1	0	0	A

Table S6 The allele count and alternative allele frequencies for the 9 SNP molecular markers when compared to the *D. immitis* reference genome nDi.2.2.for European clinical sample T4, originating from the Lombardy Region, Italy. Data collected from genomic DNA of *D. immitis* adult female submitted for MiSeq Illumina sequencing and calculated using BVAtools.

Scaffold	Position	Allele Counts				Allele Frequency				RefBase
T4		C	A	T	G	C	A	T	G	
nDi.2.2.scaf00046	76278	80	14	29237	125	0	0	0.99	0	T
nDi.2.2.scaf00046	22857	79	3	31371	8	0	0	1	0	T
nDi.2.2.scaf00046	222254	3	28493	30	88	0	1	0	0	A
nDi.2.2.scaf00185	10639	27	4	13618	7	0	0	1	0	T
nDi.2.2.scaf00185	62174	21689	7	53	0	1	0	0	0	C
nDi.2.2.scaf00140	30919	25533	30	14	2	1	0	0	0	C
nDi.2.2.scaf00005	662854	88	70	27343	40	0	0	0.99	0	T
nDi.2.2.scaf00004	79766	74	6	22054	2	0	0	1	0	T
nDi.2.2.scaf00001	466197	13	23673	32	47	0	1	0	0	A

Table S7 The allele count and alternative allele frequencies for the 9 SNP molecular markers when compared to the *D. immitis* reference genome nDi.2.2.for European clinical sample T9, originating from Hungary. Data collected from genomic DNA of *D. immitis* adult female submitted for MiSeq Illumina sequencing and calculated using BVAtools.

Scaffold	Position	Allele Counts				Allele Frequency				RefBase
T9		C	A	T	G	C	A	T	G	
nDi.2.2.scaf00046	76278	100	11	26435	127	0	0	0.99	0	T
nDi.2.2.scaf00046	22857	75	12	31584	3	0	0	1	0	T
nDi.2.2.scaf00046	222254	16	26722	17	102	0	0.99	0	0	A
nDi.2.2.scaf00185	10639	18	0	10045	1	0	0	1	0	T
nDi.2.2.scaf00185	62174	20368	7	11	0	1	0	0	0	C
nDi.2.2.scaf00140	30919	22804	14	8	4	1	0	0	0	C
nDi.2.2.scaf00005	662854	87	63	27962	51	0	0	0.99	0	T
nDi.2.2.scaf00004	79766	128	8	20933	5	0.01	0	0.99	0	T
nDi.2.2.scaf00001	466197	7	24316	18	31	0	1	0	0	A

Table S8 The allele count and alternative allele frequencies for the 9 SNP molecular markers when compared to the *D. immitis* reference genome nDi.2.2.for European clinical sample T10, originating from Hungary. Data collected from genomic DNA of *D. immitis* adult female submitted for MiSeq Illumina sequencing and calculated using BVAtools.

Scaffold	Position	Allele Counts				Allele Frequency				RefBase
T10		C	A	T	G	C	A	T	G	
nDi.2.2.scaf00046	76278	67	12	22664	123	0	0	0.99	0.01	T
nDi.2.2.scaf00046	22857	90	7	27415	2	0	0	1	0	T
nDi.2.2.scaf00046	222254	4	22890	27	110	0	0.99	0	0	A
nDi.2.2.scaf00185	10639	18	5	10640	2	0	0	1	0	T
nDi.2.2.scaf00185	62174	18442	2	23	2	1	0	0	0	C
nDi.2.2.scaf00140	30919	21654	23	13	2	1	0	0	0	C
nDi.2.2.scaf00005	662854	86	53	22887	45	0	0	0.99	0	T
nDi.2.2.scaf00004	79766	50	15	17788	6	0	0	1	0	T
nDi.2.2.scaf00001	466197	4	19642	9	46	0	1	0	0	A

Table S9 The allele count and alternative allele frequencies for the 9 SNP molecular markers when compared to the *D. immitis* reference genome nDi.2.2.for European clinical sample T11, originating from Hungary. Data collected from genomic DNA of *D. immitis* adult female submitted for MiSeq Illumina sequencing and calculated using BVAtools.

Scaffold	Position	Allele Counts				Allele Frequency				RefBase
T11		C	A	T	G	C	A	T	G	
nDi.2.2.scaf00046	76278	56	3	22645	111	0	0	0.99	0	T
nDi.2.2.scaf00046	22857	30	1	25528	4	0	0	1	0	T
nDi.2.2.scaf00046	22857	30	1	25528	4	0	0	1	0	T
nDi.2.2.scaf00185	10639	27	1	13540	1	0	0	1	0	T
nDi.2.2.scaf00185	62174	18542	3	15	1	1	0	0	0	C
nDi.2.2.scaf00140	30919	18340	11	15	1	1	0	0	0	C
nDi.2.2.scaf00005	662854	50	51	23208	35	0	0	0.99	0	T
nDi.2.2.scaf00004	79766	45	2	18282	1	0	0	1	0	T
nDi.2.2.scaf00001	466197	6	19183	11	31	0	1	0	0	A

Table S10 The allele count and alternative allele frequencies for the 9 SNP molecular markers when compared to the *D. immitis* reference genome nDi.2.2.for European clinical sample C1, originating from the Canary Islands, Spain. Data collected from genomic DNA of *D. immitis* microfilaria submitted for MiSeq Illumina sequencing and calculated using BVAtools.

Scaffold	Position	Allele Counts				Allele Frequency				RefBase
C1		C	A	T	G	C	A	T	G	
nDi.2.2.scaf00046	76278	80	9	20269	94	0	0	0.99	0	T
nDi.2.2.scaf00046	22857	63	15	21227	4	0	0	1	0	T
nDi.2.2.scaf00046	222254	6	19732	32	102	0	0.99	0	0	A
nDi.2.2.scaf00185	10639	12	7	9602	3	0	0	1	0	T
nDi.2.2.scaf00185	62174	15604	5	10	0	1	0	0	0	C
nDi.2.2.scaf00140	30919	19144	13	9	4	1	0	0	0	C
nDi.2.2.scaf00005	662854	47	43	20596	35	0	0	0.99	0	T
nDi.2.2.scaf00004	79766	59	8	16062	1	0	0	1	0	T
nDi.2.2.scaf00001	466197	3	17385	11	50	0	1	0	0	A

Table S11 The allele count and alternative allele frequencies for the 9 SNP molecular markers when compared to the *D. immitis* reference genome nDi.2.2.for European clinical sample C2, originating from the Canary Islands, Spain. Data collected from genomic DNA of *D. immitis* microfilaria submitted for MiSeq Illumina sequencing and calculated using BVAtools.

Scaffold	Position	Allele Counts				Allele Frequency				RefBase
C2		C	A	T	G	C	A	T	G	
nDi.2.2.scaf00046	76278	75	17	25099	122	0	0	0.99	0	T
nDi.2.2.scaf00046	22857	71	10	25172	0	0	0	1	0	T
nDi.2.2.scaf00046	222254	7	23996	29	983	0	0.96	0	0.04	A
nDi.2.2.scaf00185	10639	28	10	14837	9	0	0	1	0	T
nDi.2.2.scaf00185	62174	193170	22	0	0	1	0	0	0	C
nDi.2.2.scaf00140	30919	22151	28	14	4	1	0	0	0	C
nDi.2.2.scaf00005	662854	64	71	22511	39	0	0	0.99	0	T
nDi.2.2.scaf00004	79766	904	1	18802	5	0.05	0	0.95	0	T
nDi.2.2.scaf00001	466197	2	19345	12	54	0	1	0	0	A

Table S12 The allele count and alternative allele frequencies for the 9 SNP molecular markers when compared to the *D. immitis* reference genome nDi.2.2.for European clinical sample C4, originating from the Canary Islands, Spain. Data collected from genomic DNA of *D. immitis* microfilaria submitted for MiSeq Illumina sequencing and calculated using BVAtools.

Scaffold	Position	Allele Counts				Allele Frequency				RefBase
C4		C	A	T	G	C	A	T	G	
nDi.2.2.scaf00046	76278	36	8	7959	47	0	0	0.99	0.01	T
nDi.2.2.scaf00046	22857	29	0	12454	5	0	0	1	0	T
nDi.2.2.scaf00046	222254	0	8640	9	37	0	0.99	0	0	A
nDi.2.2.scaf00185	10639	8	2	2232	2	0	0	0.99	0	T
nDi.2.2.scaf00185	62174	6922	4	16	0	1	0	0	0	C
nDi.2.2.scaf00140	30919	9696	14	6	2	1	0	0	0	C
nDi.2.2.scaf00005	662854	59	25	12980	33	0	0	0.99	0	T
nDi.2.2.scaf00004	79766	21	5	4362	1	0	0	0.99	0	T
nDi.2.2.scaf00001	466197	3	9370	5	23	0	1	0	0	A

Table S13 The allele count and alternative allele frequencies for the 9 SNP molecular markers when compared to the *D. immitis* reference genome nDi.2.2.for European clinical sample C5, originating from the Canary Islands, Spain. Data collected from genomic DNA of *D. immitis* microfilaria submitted for MiSeq Illumina sequencing and calculated using BVAtools.

Scaffold	Position	Allele Counts				Allele Frequency				RefBase
C5		C	A	T	G	C	A	T	G	
nDi.2.2.scaf00046	76278	49	10	19675	80	0	0	0.99	0	T
nDi.2.2.scaf00046	22857	27	4	19946	3	0	0	1	0	T
nDi.2.2.scaf00046	222254	4	18179	17	1576	0	0.92	0	0.08	A
nDi.2.2.scaf00185	10639	45	7	14279	10	0	0	1	0	T
nDi.2.2.scaf00185	62174	15735	0	16	1	1	0	0	0	C
nDi.2.2.scaf00140	30919	18567	15	19	3	1	0	0	0	C
nDi.2.2.scaf00005	662854	51	47	18298	25	0	0	0.99	0	T
nDi.2.2.scaf00004	79766	1351	2	16119	5	0.08	0	0.92	0	T
nDi.2.2.scaf00001	466197	3	15783	13	31	0	1	0	0	A

Table S14 The allele count and alternative allele frequencies for the 9 SNP molecular markers when compared to the *D. immitis* reference genome nDi.2.2.for European clinical sample M, from Huelva, Andulusia, Spain , adopted and relocated to Savona, Italy. Data collected from genomic DNA of *D. immitis* microfilaria submitted for MiSeq Illumina sequencing and calculated using BVAtools.

Scaffold	Position	Allele Counts				Allele Frequency				RefBase
M		C	A	T	G	C	A	T	G	
nDi.2.2.scaf00046	76278	116	17	27101	119	0	0	0.99	0	T
nDi.2.2.scaf00046	22857	61	8	28136	10	0	0	1	0	T
nDi.2.2.scaf00046	222254	8	25508	40	105	0	0.99	0	0	A
nDi.2.2.scaf00185	10639	28	5	13581	5	0	0	1	0	T
nDi.2.2.scaf00185	62174	20278	4	18	1	1	0	0	0	C
nDi.2.2.scaf00140	30919	23777	15	27	0	1	0	0	0	C
nDi.2.2.scaf00005	662854	72	45	26547	65	0	0	0.99	0	T
nDi.2.2.scaf00004	79766	118	5	20352	4	0.01	0	0.99	0	T
nDi.2.2.scaf00001	466197	5	22744	18	79	0	1	0	0	A

Table S15 SNP ID, position, and primer sequences (Ballesteros et al. 2018)

ID	Scaffold	Position	Primer Name & Sequence
SNP 1	nDi.2.2.scaf00001	466197	scaf00001-466197-CS1F ACACTGACGACATGGTTCTACATTCTATCGAAAACCTTCCAG scaf00001-466197-CS2R TACGGTAGCAGAGACTTGGTCTAGGTTGCAAAAGTTGCAATG
SNP 2	nDi.2.2.scaf00004	79766	scaf00004-79766-CS1F ACACTGACGACATGGTTCTACACGTGACTAAAAGAATAGTG scaf00004-79766-CS2R TACGGTAGCAGAGACTTGGTCTCAATTTAGGGATATGACACAG
SNP 3	nDi.2.2.scaf00005	662854	scaf00005-662854-CS1F ACACTGACGACATGGTTCTACAGTTATTTGCACTACTCTCCC scaf00005-662854-CS2R TACGGTAGCAGAGACTTGGTCTTGGCGTACTGATCACATTGG
SNP 4	nDi.2.2.scaf00046	22857	scaf00046-22857-CS1F ACACTGACGACATGGTTCTACACGAGGTAAAGCACACAGAAG scaf00046-22857-CS2R TACGGTAGCAGAGACTTGGTCTCAACAAAATGCCGCAGATGG
SNP 5	nDi.2.2.scaf00046	76278	scaf00046-76278-CS1F ACACTGACGACATGGTTCTACAGGCCAATAAATAAAGGCTA scaf00046-76278-CS2R TACGGTAGCAGAGACTTGGTCTGTTTTCTGGAATTATCAGAC
SNP 6	nDi.2.2.scaf00046	222254	scaf00046-222254-CS1F ACACTGACGACATGGTTCTACACATCGTTGTCAACTTCCTGC scaf00046-222254-CS2R TACGGTAGCAGAGACTTGGTCTGAAATTTGAAAATGGGTACT
SNP 7	nDi.2.2.scaf00140	30919	scaf00140-30919-CS1F ACACTGACGACATGGTTCTACACGAAGAAGAAACTTTTCGGG scaf00140-30919-CS2R TACGGTAGCAGAGACTTGGTCTGTACAATTAATTGCTGTTCGC
SNP 8	nDi.2.2.scaf00185	10639	scaf00185-10639-CS1F ACACTGACGACATGGTTCTACAACGCAGGAAAGCTTTAATGG scaf00185-10639-CS2R TACGGTAGCAGAGACTTGGTCTATCATCATTTTATCAATTCC
SNP 9	nDi.2.2.scaf00185	62174	scaf00185-62174-CS1F ACACTGACGACATGGTTCTACATCGATCATTTAGTAACAACG scaf00185-62174-CS2R TACGGTAGCAGAGACTTGGTCTTTGCGTTACAGCGCCAAATC

Bibliography

AHS 2018. Current Canine Guidelines for the Prevention, Diagnosis, and Management of Heartworm (*Dirofilaria immitis*) Infection in Dogs. https://www.heartwormsociety.org/veterinary-resources/american-heartworm-society-guidelines

Ballesteros, C., Pulaski, C.N., Bourguinat, C., Keller, K., Prichard, R.K., Geary, T.G., 2018. Clinical validation of molecular markers of macrocyclic lactone resistance in *Dirofilaria immitis*. Int J Parasitol. Drugs Drug Resist. 8(3), 596-606.

Bacsadi, Á., Papp, A., Szeredi, L., Tóth, G., Nemes, C., Imre, V., Tolnai, Z., Széll, Z., Sréter, T., 2016. Retrospective study on the distribution of *Dirofilaria immitis* in dogs in Hungary. . Vet. Parasitol, 220, 83-86.

Bolger, A.M., Lohse, M., Usadel, B., 2014. Trimmomatic: a flexible trimmer for Illumina sequence data. Bioinformatics 30, 2114-2120.

Bourguinat, C., Keller, K., Bhan, A., Peregrine, A., Geary, T., Prichard, R., 2011a. Macrocyclic lactone resistance in *Dirofilaria immitis*. Vet. Parasitol. 181, 388-392.

Bourguinat, C., Keller, K., Blagburn, B., Schenker, R., Geary, T.G., Prichard, R.K., 2011b. Correlation between loss of efficacy of macrocyclic lactone heartworm anthelmintics and P-glycoprotein genotype. Vet. Parasitol. 176, 374-381.

Bourguinat, C., Keller, K., Prichard, R.K., Geary, T.G., 2011c. Genetic polymorphism in *Dirofilaria immitis*. Vet. Parasitol. 176, 368-373.

Bourguinat, C., Lee, A.C.Y., Lizundia, R., Blagburn, B.L., Liotta, J.L., Kraus, et al., 2015. Macrocyclic lactone resistance in *Dirofilaria immitis*: Failure of heartworm preventives and investigation of genetic markers for resistance. Vet. Parasitol. 210, 167-178.

Bourguinat, C., Che, H., Mani, T., Keller, K., Prichard, R.K., 2016. ABC-B transporter genes in *Dirofilaria immitis*. Int J Parasitol-Drug. 6, 116-124.

Bourguinat, C., Keller, K., Xia, J., Lepage, P., McTier, T.L., Woods, D.J., Prichard, R.K., 2017a. Genetic profiles of ten *Dirofilaria immitis* isolates susceptible or resistant to macrocyclic lactone heartworm preventives. Parasites Vectors 10, 504.

Bourguinat, C., Lefebvre, F., Sandoval, J., Bondesen, B., Moreno, Y., Prichard, R.K., 2017b. *Dirofilaria immitis* JYD-34 isolate: whole genome analysis. Parasites Vectors 10, 494.

Bowman, D.D., Atkins, C.E., 2009. Heartworm Biology, Treatment, and Control. Vet. Clin. North Am. Small Anim. Pract. 39, 1127-1158.

Bowman, D.D., McTier, T.L., Adams, E.L., Mahabir, S.P., Login, J.A., Bidgood, T., Woods, D.J., 2017. Evaluation of the efficacy of ProHeart(®) 6 (moxidectin) against a resistant isolate of *Dirofilaria immitis* (JYD-34) in dogs. Parasites Vectors 10, 502.

Brajcich, B.C., Iarocci, A.L., Johnstone, L.A., Morgan, R.K., Lonjers, Z.T., Hotchko, M.J., Muhs, J.D., Kieffer, A., Reynolds, B.J., Mandel, S.M., 2010. Evidence that ubiquinone is a required intermediate for rhodoquinone biosynthesis in *Rhodospirillum rubrum*. J. Bacteriol. 192, 436-445.

Bryant, C., 2018. The biochemistry of *Dirofilaria immitis*, In: Dirofilariasis. CRC Press, pp. 47-60.

Buceta, P.M.R., Romanelli-Cedrez, L., Babcock, S.J., Xun, H., VonPaige, M.L., Higley, T.W., Schlatter, T.D., Davis, D.C., Drexelius, J.A., Culver, J.C., 2019. The kynurenine pathway is essential for rhodoquinone biosynthesis in *Caenorhabditis elegans*. J. Biol. Chem. 294, 11047-11053.

Campbell, W.C., 1981. An introduction to the avermectins. N. Z. Vet. J. 29, 174-178.

Campbell, W.C., Fisher, M.H., Stapley, E.O., Albers-Schönberg, G., Jacob, T.A., 1983. Ivermectin: a potent new antiparasitic agent. Science 221, 823-828.

Campbell, A.R., Titus, B.R., Kuenzi, M.R., Rodriguez-Perez, F., Brunsch, A.D., Schroll, M.M., Owen, M.C., Cronk, J.D., Anders, K.R., Shepherd, J.N., 2019. Investigation of candidate genes involved in the rhodoquinone biosynthetic pathway in *Rhodospirillum rubrum.* Plos one 14, e0217281.

Carithers, D.S., 2017. Examining the role of macrolides and host immunity in combatting filarial parasites. Parasites Vectors 10, 1-13.

Chabala, J.C., Mrozik, H., Tolman, R.L., Eskola, P., Lusi, A., Peterson, L.H., Woods, M.F., Fisher, M.H., Campbell, W.C., 1980. Ivermectin, a new broad-spectrum antiparasitic agent. J. Med. Chem. 23, 1134-1136.

Curry, E., Traversa, D., Carretón, E., Kramer, L., Sager, H., Young, L., Prichard, R., 2022a. *Dirofilaria immitis*: Genotyping Randomly Selected European Clinical Samples and USA Laboratory Isolates with Molecular Markers Associated with Macrocyclic Lactone Susceptibility and Resistance. Pathogens 11.

Curry, E., Prichard, R., 2022b. Development of rapid *in vitro* colorimetric enzymatic activity assay to differentiate macrocyclic lactone susceptible and resistant *Dirofilaria immitis* isolates. Vet Parasitol. 304, 109696.

Curry, E., Prichard, R., Lespine, A., 2022c. Genetic polymorphism, constitutive expression, and tissue localization of *Dirofilaria immitis* P-glycoprotein 11: a putative marker of macrocyclic lactone resistance. Parasites Vectors 15, 482.

David, M.A., Orlowski, S., Prichard, R.K., Hashem, S., André, F., Lespine, A., 2016. In silico analysis of the binding of anthelmintics to *Caenorhabditis elegans* P-glycoprotein 1. Int J Parasitol-Drug. 6, 299-313.

David, M., Lebrun, C., Duguet, T., Talmont, F., Beech, R., Orlowski, S., André, F., Prichard, R.K., Lespine, A., 2018. Structural model, functional modulation by ivermectin and tissue localization of *Haemonchus contortus* P-glycoprotein-13. Int J Parasitol-Drug. 8, 145-157.

De Graef, J., Demeler, J., Skuce, P., Mitreva, M., Von Samson-Himmelstjerna, G., Vercruysse, J., Claerebout, E., Geldhof, P., 2013. Gene expression analysis of ABC transporters in a resistant *Cooperia oncophora* isolate following *in vivo* and *in vitro* exposure to macrocyclic lactones. Parasitology 140, 499-508.

Del Borrello, S., Lautens, M., Dolan, K., Tan, J.H., Davie, T., Schertzberg, M.R., Spensley, M.A., Caudy, A.A., Fraser, A.G., 2019. Rhodoquinone biosynthesis in *C. elegans* requires precursors generated by the kynurenine pathway. Elife 8, e48165.

Demeler, J., Krücken, J., AlGusbi, S., Ramünke, S., De Graef, J., Kerboeuf, D., Geldhof, P., Pomroy, W.E., von Samson-Himmelstjerna, G., 2013. Potential contribution of P-glycoproteins to macrocyclic lactone resistance in the cattle parasitic nematode *Cooperia oncophora*. Mol. Biochem. Parasitol. 188, 10-19.

Diakou, A., Prichard, R.K., 2021. Concern for *Dirofilaria immitis* and macrocyclic lactone loss of efficacy: current situation in the USA and Europe, and future scenarios. Pathogens, 10, 1323.

Doyle, S.R., Bourguinat, C., Nana-Djeunga, H.C., Kengne-Ouafo, J.A., Pion, S.D.S., Bopda, J., Kamgno, J., Wanji, S., Che, H., Kuesel, A.C., Walker, M., Basáñez, M.-G., Boakye,

D.A., Osei-Atweneboana, M.Y., Boussinesq, M., Prichard, R.K., Grant, W.N. 2017. Genome-wide analysis of ivermectin response by *Onchocerca volvulus* reveals that genetic drift and soft selective sweeps contribute to loss of drug sensitivity. PLoS Negl. Trop. Dis., p. e0005816.

Drake, J., Wiseman, S., 2018. Increasing incidence of *Dirofilaria immitis* in dogs in USA with focus on the southeast region 2013–2016. Parasites Vectors 11, 1-7.

Elanco GmbH. Credelio Plus. EMEA/V/C/005325/0000. European Medicines Agency. 2021.

Erabi, T., Higuti, T., Sakata, K., Kakuno, T., Yamashita, J., Tanaka, M., Horio, T., 1976. Polarographic studies in presence of triton X-100 on oxidation-reduction components bound with chromatophores from *Rhodospirillum rubrum*. J. Biochem. 79, 497-503.

Evans, C.C., Moorhead, A.R., Storey, B.E., Wolstenholme, A.J., Kaplan, R.M., 2013. Development of an *in vitro* bioassay for measuring susceptibility to macrocyclic lactone anthelmintics in *Dirofilaria immitis*. IJP-DDR 3, 102-108.

Evans, C.C., Moorhead, A.R., Storey, B.E., Blagburn, B.L., Wolstenholme, A.J., Kaplan, R.M., 2017. Evaluation of the larval migration inhibition assay for detecting macrocyclic lactone resistance in *Dirofilaria immitis*. Vet. Parasitol. 246, 76-81.

Farkas, R., Mag, V., Gyurkovszky, M., Takács, N., Vörös, K., Solymosi, N., 2020. The current situation of canine dirofilariosis in Hungary. Parasitol. Res. 119, 129-135.

Gasteiger E., Gattiker A., Hoogland C., Ivanyi I., Appel R.D., Bairoch A., 2003. ExPASy: the proteomics server for in-depth protein knowledge and analysis. Nucleic Acids Res. 3, 3784-3788.

Geary, J., Satti, M., Moreno, Y., Madrill, N., Whitten, D., Headley, S.A., Agnew, D., Geary, T., Mackenzie, C., 2012. First analysis of the secretome of the canine heartworm, *Dirofilaria immitis*. Parasites Vectors 5, 140.

Genchi, C., Rinaldi, L., Cascone, C., Mortarino, M., Cringoli, G., 2005. Is heartworm disease really spreading in Europe? Vet. Parasitol. 133, 137-148.

Genchi, C., Rinaldi, L., Mortarino, M., Genchi, M., Cringoli, G., 2009. Climate and *Dirofilaria* infection in Europe. Vet. Parasitol. 163, 286-292.

Genchi, C., Kramer, L.H., 2020. The prevalence of *Dirofilaria immitis* and *D. repens* in the Old World. Vet. Parasitol. 280, 108995.

Godel C., Kumar S., Koutsovoulos G., Ludin P., Nilsson D., Comandatore F., et al., 2012. The genome of the heartworm, *Dirofilaria immitis*, reveals drug and vaccine targets. FASEB J. 26(11), 4650-4661.

Hampshire, V.A., 2005. Evaluation of efficacy of heartworm preventive products at the FDA. Vet. Parasitol. 133, 191-195.

Harischandra, H., Yuan, W., Loghry, H.J., Zamanian, M., Kimber, M.J., 2018. Profiling extracellular vesicle release by the filarial nematode *Brugia malayi* reveals sex-specific differences in cargo and a sensitivity to ivermectin. PLOS Negl. Trop. Dis. 12, e0006438.

Hewitson, J.P., Rückerl, D., Harcus, Y., Murray, J., Webb, L.M., Babayan, S.A., et al., 2014. The secreted Triose Phosphate Isomerase of *Brugia malayi* is required to sustain microfilaria production *in vivo*. PLOS Pathog. 10, e1003930

Hibbs, R.E., Gouaux, E., 2011. Principles of activation and permeation in an anion-selective Cys-loop receptor. Nature 474, 54-60.

Hilmas, C., Pereira, E.F., Alkondon, M., Rassoulpour, A., Schwarcz, R., Albuquerque, E.X., 2001. The brain metabolite kynurenic acid inhibits α7 nicotinic receptor activity and increases non-α7 nicotinic receptor expression: physiopathological implications. J. Neurosci. 21, 7463-7473.

Hoch, H., Dillion, R., 2006. Canine Dirofilariasis. Standards of Care: Emergency and Critical Care Medicine 8.3.

Hoogewijs, D., Houthoofd, K., Matthijssens, F., Vandesompele, J., Vanfleteren, J.R., 2008. Selection and validation of a set of reliable reference genes for quantitative sod gene expression analysis in *C. elegans*. BMC Mol. Biol. 9, 9.

Howe K.L., Bolt B.J., Cain S., Chan J., Chen, W.J., Davis P., et al., 2016. WormBase 2016: expanding to enable helminth genomic research. Nucleic Acids. 44, 774-780.

Howe K.L., Bolt B.J., Shafie M., Kersey P., Berrimen M., 2017. WormBase ParaSite – a comprehensive resource for helminth genomics. WormBase ParaSite – a comprehensive resource for helminth genomics. Mol. Biochem. Parasitol. 215, 2-10.

Hunt-Newbury, R., Viveiros, R., Johnsen, R., Mah, A., Anastas, D., Fang, et al., 2007. High-throughput *in vivo* analysis of gene expression in *Caenorhabditis elegans*. PLoS Biol 5, e237-e237.

Ionică, A.M., Matei, I.A., D'Amico, G., Ababii, J., Daskalaki, A.A., Sándor, A.D., Enache, D.V., Gherman, C.M., Mihalca, A.D., 2017. Filarioid infections in wild carnivores: a multispecies survey in Romania. Parasites Vectors 10, 332.

Issouf, M., Guégnard, F., Koch, C., Le Vern, Y., Blanchard-Letort, A., Che, H., Beech, R.N., Kerboeuf, D., Neveu, C., 2014. *Haemonchus contortus* P-Glycoproteins Interact with

Host Eosinophil Granules: A Novel Insight into the Role of ABC Transporters in Host-Parasite Interaction. PLOS One 9, e87802.

Iwata, F., Shinjyo, N., Amino, H., Sakamoto, K., Islam, M.K., Tsuji, N., Kita, K., 2008. Change of subunit composition of mitochondrial complex II (succinate–ubiquinone reductase/quinol–fumarate reductase) in *Ascaris suum* during the migration in the experimental host. Parasitol. Int. 57, 54-61.

Jacobson, L.S., Ward, K.A., Lacaden, A.B., Hornak, T.A., 2020. Prevalence of heartworm in relocated, local and outreach clinic dogs: A Canadian sheltering perspective. Vet. Parasitol. 283, 109081.

Jaffe, J., Doremus, H., 1970. Metabolic patterns of *Dirofilaria immitis* microfilariae *in vitro*. The J. Parasitol., 254-260.

James C.E., Davey M.W., 2009. Increased expression of ABC transport proteins is associated with ivermectin resistance in the model nematode *Caenorhabditis elegans*. Int. J. Parasitol. 39(2), 213-20.

Janssen, I.J.I., Krücken, J., Demeler, J., Basiaga, M., Kornaś, S., von Samson-Himmelstjerna, G., 2013. Genetic variants and increased expression of *Parascaris equorum* P-glycoprotein-11 in populations with decreased ivermectin susceptibility. PloS one 8, e61635-e61635.

Janssen, I.J.I., Krücken, J., Demeler, J., von Samson-Himmelstjerna, G., 2015. Transgenically expressed *Parascaris* P-glycoprotein-11 can modulate ivermectin susceptibility in *Caenorhabditis elegans*. Int J Parasitol-Drug. 5, 44-47.

Köhler, P., 1991. The pathways of energy generation in filarial parasites. Parasitol. Today 7, 21-25.

Kumar, S., Prichard, R., Long, T., In Preparation. Droplet Digital PCR as a tool to detect resistant *D. immitis* isolates.

Laidoudi, Y., Bedjaoui, S., Latrofa, M.S., Fanelli, A., Dantas-Torres, F., Otranto, D., 2022. Genetic and geographical delineation of zoonotic vector-borne helminths of canids. Sci. Rep.12, 1-11.

Langeland, A., Jetter, H., O'Halloran, D.M., 2021. The diversity of ABC transporter genes across the Phylum Nematoda. Parasitol. Int. 83, 102357.

Lau, D.C.-W., McLeod, S., Collaery, S., Peou, S., Tran, A.T., Liang, M., Šlapeta, J., 2021. Whole-genome reference of *Dirofilaria immitis* from Australia to determine single nucleotide polymorphisms associated with macrocyclic lactone resistance in the USA. CRPVBD 1, 100007.

Lespine, A., Martin, S., Dupuy, J., Roulet, A., Pineau, T., Orlowski, S., Alvinerie, M., 2007. Interaction of macrocyclic lactones with P-glycoprotein: Structure–affinity relationship. Eur J Pharm Sci. 30, 84-94.

Lespine, A., Alvinerie, M., Vercruysse, J., Prichard, R.K., Geldhof, P., 2008. ABC transporter modulation: a strategy to enhance the activity of macrocyclic lactone anthelmintics. Trends Parasitol. 24, 293-298.

Lespine, A., Ménez, C., Bourguinat, C., Prichard, R.K., 2012. P-glycoproteins and other multidrug resistance transporters in the pharmacology of anthelmintics: Prospects for reversing transport-dependent anthelmintic resistance. Int. J. Parasitol.: Drugs Drug Resist. 2, 58-75.

Lespine, A., 2013. Lipid-like properties and pharmacology of the anthelmintic macrocyclic lactones. Expert Opin Drug Metab Toxicol . 9, 1581-1595.

Li, B.-W., Rush, A.C., Tan, J., Weil, G.J., 2004. Quantitative analysis of gender-regulated transcripts in the filarial nematode *Brugia malayi* by real-time RT-PCR. Mol. Biochem. Parasitol. 137, 329-337.

Li, H., Durbin, R., 2009. Fast and accurate short read alignment with Burrows–Wheeler transform. Bioinformatics 25, 1754-1760.

Liao, Y., Smyth, G.K., Shi, W., 2014. featureCounts: an efficient general purpose program for assigning sequence reads to genomic features. Bioinformatics 30, 923-930.

Lints, R., Emmons, S.W., 2002. Regulation of sex-specific differentiation and mating behavior in *C. elegans* by a new member of the DM domain transcription factor family. Genes Dev. 16, 2390-2402.

Lipton, J., 2004. Mate Searching in *Caenorhabditis elegans*: A Genetic Model for Sex Drive in a Simple Invertebrate. J. Neurosci. 24, 7427-7434.

Loer, C., Kenyon, C., 1993. Serotonin-deficient mutants and male mating behavior in the nematode *Caenorhabditis elegans*. J. Neurosci. 13, 5407-5417.

Maclean, M.J., Savadelis, M.D., Coates, R., Dzimianski, M.T., Jones, C., Benbow, C., et al., 2017. Does evaluation of *in vitro* microfilarial motility reflect the resistance status of *Dirofilaria immitis* isolates to macrocyclic lactones? Parasites Vectors 10, 480.

Manfredi, M.T., Cerbo, A.d., Genchi, M. 2007. Biology of filarial worms parasitizing dogs and cats (Naples, Veterinary Parasitology and Parasitic Diseases), pp. 39-45.

Mani, T., Bourguinat, C., Keller, K., Ashraf, S., Blagburn, B., Prichard, R.K., 2016. Interaction of macrocyclic lactones with a *Dirofilaria immitis* P-glycoprotein. Int. J. Parasitol. 46, 631-640.

Mani, T., Bourguinat, C., Prichard, R.K., 2017. Polymorphism in ABC transporter genes of *Dirofilaria immitis*. Int J Parasitol-Drug. 7, 227-235.

McCall, J.W., Genchi, C., Kramer, L.H., Guerrero, J., Venco, L., 2008. Chapter 4 Heartworm Disease in Animals and Humans, In: Advances in Parasitology. Academic Press, 193-285.

McCulloch, D., Gems, D., 2003. Evolution of male longevity bias in nematodes. Aging Cell 2, 165-173.

McTier, T.L., Six, R.H., Pullins, A., Chapin, S., McCall, J.W., Rugg, D., Maeder, S.J., Woods, D.J., 2017. Efficacy of oral moxidectin against susceptible and resistant isolates of *Dirofilaria immitis* in dogs. Parasites Vectors. 10, 482.

Ménez, C., Alberich, M., Kansoh, D., Blanchard, A., Lespine, A., 2016. Acquired Tolerance to Ivermectin and Moxidectin after Drug Selection Pressure in the Nematode 26.

Merola, V.M., Eubig, P.A., 2012. Toxicology of avermectins and milbemycins (macrocylic lactones) and the role of P-glycoprotein in dogs and cats. Vet. Clin. North Am. Small Anim. Pract. 42, 313-333, vii.

Molento M.B., Prichard R.K., 1999.The effects of the multidrug-resistance-reversing agent verapamil and CL347,099 on the efficacy of ivermectin or moxidectin against unselected and drug-selected strains of *Haemonchus contortus* in jirds (*Meriones unguiculatus*). Parasitol. Res. 85, 1007-1011.

Molento M.B., Prichard R.K., 2001. Effect of multidrug resistance modulators on the activity of ivermectin and moxidectin against selected strains of *Haemonchus contortus*. Pesqui. Vet. Bras. 21, 117-121.

Mónica, R.-B., Ruy, P.-M. 2019. Medical and Veterinary Importance of the Moonlighting Functions of Triosephosphate Isomerase. Curr. Protein Pept. Sci., 304-315.

Montoya-Alonso, J.A., Carretón, E., Morchón, R., Silveira-Viera, L., Falcón, Y., Simón, F., 2016. The impact of the climate on the epidemiology of *Dirofilaria immitis* in the pet population of the Canary Islands. Vet. Parasitol. 216, 66-71.

Moreno, Y., Geary, T.G., 2008. Stage- and Gender-Specific Proteomic Analysis of *Brugia malayi* Excretory-Secretory Products. PLOS Negl. Trop. Dis. 2, e326.

Moreno, Y., Nabhan, J.F., Solomon, J., Mackenzie, C.D., Geary, T.G., 2010. Ivermectin disrupts the function of the excretory-secretory apparatus in microfilariae of *Brugia malayi*. PNAS 107, 20120-20125.

Moreno, Y., Geary, T.G., Tritten, L., 2021. When Secretomes Meet Anthelmintics: Lessons for Therapeutic Interventions. Trends Parasitol. 37, 468-475.

Müller, M., Mentel, M., van Hellemond, J.J., Henze, K., Woehle, C., Gould, S.B., Yu, R.-Y., van der Giezen, M., Tielens, A.G., Martin, W.F., 2012. Biochemistry and evolution of anaerobic energy metabolism in eukaryotes. Microbiol. Mol. Biol. Rev. 76, 444-495.

Noack, S., Harrington, J., Carithers, D.S., Kaminsky, R., Selzer, P.M., 2021. Heartworm disease–Overview, intervention, and industry perspective. Int. J. Parasitol.: Drugs Drug Resist. 16, 65-89.

Norman, C., Stavisky, J., Westgarth, C., 2020. Importing rescue dogs into the UK: reasons, methods and welfare considerations. Vet. Rec. 186, 248-248.

Ohishi, I., Katae, H., Hayasaki, M., Nakagaki, K., Tada, Y., 1987a. Prophylactic Activity of Ivermectin against *Dirofilaria immitis* Infection in Dogs: Establishment of Effective Dose and Administration Schedule. Jpn. J. Vet. 49, 439-445.

Ohishi, I., Katae, H., Hayasaki, M., Tada, Y., 1987b. Prophylactic Activity of Ivermectin against *Dirofilaria immitis* Infection in Dogs: Larvicidal Activity of Ivermectin against *D. immitis* Larvae 30 Days after Infection. Jpn. J. Vet. 49, 115-120.

Oliveira, P.L., Oliveira, M.F., 2002. Vampires, Pasteur and reactive oxygen species: Is the switch from aerobic to anaerobic metabolism a preventive antioxidant defence in blood-feeding parasites? FEBS lett. 525, 3-6.

Omasits U., Ahrens C.H., Müller S., Wollscheid B., 2014. Protter: interactive protein feature visualization and integration with experimental proteomic data. Bioinformatics. Mar 15; 30(6), 884-886.

Phillips, R.S., 2014. Structure and mechanism of kynureninase. Arch. Biochem. Biophys. 544, 69-74.

Platzer, E.G., 2009. Chapter 78 - Dog Heartworm, In: Resh, V.H., Cardé, R.T. (Eds.) Encyclopedia of Insects (Second Edition). Academic Press, San Diego, pp. 299-300.

Power, R.I., 2022. Exploration of the sensitivity to macrocyclic lactones in the canine heartworm (*Dirofilaria immitis*) in Australia using phenotypic and genotypic approaches. Int. J. Parasitol.: Drugs Drug Resist.

Prichard, R.K., Geary, T.G., 2019. Perspectives on the utility of moxidectin for the control of parasitic nematodes in the face of developing anthelmintic resistance. Int. J. Parasitol.: Drugs Drug Resist. 10, 69-83.

Prichard, R.K. 2021. Macrocyclic lactone resistance in *Dirofilaria immitis*: Risks for prevention of heartworm disease. Invited review Int. J. Parasitol. 51: 1121-1132.

Pulaski, C.N., Malone, J.B., Bourguinat, C., Prichard, R., Geary, T., Ward, D., et al., 2014. Establishment of macrocyclic lactone resistant *Dirofilaria immitis* isolates in experimentally infected laboratory dogs. Parasites Vectors 7, 494.

Raza, A., Kopp, S.R., Bagnall, N.H., Jabbar, A., Kotze, A.C., 2016. Effects of *in vitro* exposure to ivermectin and levamisole on the expression patterns of ABC transporters in *Haemonchus contortus* larvae. Int. J. Parasitol. Drugs Drug Resist. 6, 103-115.

Salinas, G., Langelaan, D.N., Shepherd, J.N., 2020. Rhodoquinone in bacteria and animals: Two distinct pathways for biosynthesis of this key electron transporter used in anaerobic bioenergetics. Biochim. Biophys. Acta Bioenerg.1861, 148278.

Sanchez, J., Dharmarajan, G., George, M.M., Pulaski, C., Wolstenholme, A.J., Gilleard, J.S., Kaplan, R.M., 2020. Using population genetics to examine relationships of *Dirofilaria immitis* based on both macrocyclic lactone-resistance status and geography. Vet. Parasitol. 283, 109125.

Savić, S., Stosic, M.Z., Marcic, D., Hernández, I., Potkonjak, A., Otasevic, S., Ruzic, M., Morchón, R., 2020. Seroepidemiological Study of Canine and Human Dirofilariasis in the Endemic Region of Northern Serbia. Front. Vet. Ssci. 7.

Schinkel A.H., Smit J.J.M., van Tellingen O., Beijnen J.H., Wagenaar E., van Deemter L., et al., 1994. Disruption of the mouse mdr1a P-glycoprotein gene leads to a deficiency in the blood-brain barrier and to increased sensitivity to drugs. Cell. 77(4), 491-502.

Simón, F., Siles-Lucas, M., Morchón, R., González-Miguel, J., Mellado, I., Carretón, E., Montoya-Alonso, J.A., 2012. Human and Animal Dirofilariasis: the Emergence of a Zoonotic Mosaic. Clin. Microbiol. Rev. 25, 507-544.

Sonnberger, K., Duscher, G.G., Fuehrer, H.-P., Leschnik, M., 2020. Current trends in canine dirofilariosis in Austria—do we face a pre-endemic status? Parasitol. Res. 119, 1001-1009.

Spencer, W.C., Zeller, G., Watson, J.D., Henz, S.R., Watkins, K.L., McWhirter, R.D., et al., 3rd, 2011. A spatial and temporal map of C. elegans gene expression. Genome Res. 21, 325-341.

Tielens, A.G., Van Hellemond, J.J., 1998. The electron transport chain in anaerobically functioning eukaryotes. Biochim. Biophys. Acta Bioenerg.1365, 71-78.

Traversa, D., Di Cesare, A., Conboy, G., 2010. Canine and feline cardiopulmonary parasitic nematodes in Europe: emerging and underestimated. Parasites Vectors 3, 62.

Tritten, L., Geary, T.G., 2018. Helminth extracellular vesicles in host–parasite interactions. Curr. Opin. Microbiol 46, 73-79.

Unden, G., Bongaerts, J., 1997. Alternative respiratory pathways of *Escherichia coli*: energetics and transcriptional regulation in response to electron acceptors. Biochim. Biophys. Acta Bioenerg.1320, 217-234.

Van Hellemond, J.J., Klockiewicz, M., Gaasenbeek, C.P., Roos, M.H., Tielens, A.G., 1995. Rhodoquinone and Complex II of the Electron Transport Chain in Anaerobically Functioning Eukaryotes (∗). J. Biol. Chem. 270, 31065-31070.

Vatta, A.F., Dzimianski, M., Storey, B.E., Camus, M.S., Moorhead, A.R., Kaplan, R.M., Wolstenholme, A.J., 2014. Ivermectin-dependent attachment of neutrophils and peripheral blood mononuclear cells to *Dirofilaria immitis* microfilariae *in vitro*. Vet. Parasitol. 206, 38-42.

Verhalen, B., Dastvan, R., Thangapandian, S., Peskova, Y., Koteiche, H.A., Nakamoto, R.K., Tajkhorshid, E., McHaourab, H.S., 2017. Energy transduction and alternating access of the mammalian ABC transporter P-glycoprotein. Nature. 543, 738-741.

Wierenga, R.K., Kapetaniou, E.G., Venkatesan, R., 2010. Triosephosphate isomerase: a highly evolved biocatalyst. Cell. Mol. Life Sci. 67, 3961-3982

Wolstenholme, A., 2012. Glutamate-gated Chloride Channels. J Biol Chem. 287, 40232–40238.

Wolstenholme, A.J., Evans, C.C., Jimenez, P.D., Moorhead, A.R., 2015. The emergence of macrocyclic lactone resistance in the canine heartworm, *Dirofilaria immitis*. Parasitology. 142, 1249-1259.

Xu, M., Molento, M., Blackhall, W., Ribeiro, P., Beech, R., Prichard, R., 1998. Ivermectin resistance in nematodes may be caused by alteration of P-glycoprotein homolog. Mol. Biochem. Parasitol. 91, 327-335.

Yamashita, T., Ino, T., Miyoshi, H., Sakamoto, K., Osanai, A., Nakamaru-Ogiso, E., Kita, K., 2004. Rhodoquinone reaction site of mitochondrial complex I, in parasitic helminth, *Ascaris suum*. Biochim. Biophys. Acta Bioenerg. 1608, 97-103.

Yin, Y., Martin, J., McCarter, J.P., Clifton, S.W., Wilson, R.K., Mitreva, M., 2006. Identification and analysis of genes expressed in the adult filarial parasitic nematode *Dirofilaria immitis*. Int. J. Parasitol. 36, 829-839.

Zhang, Y., Chen, D., Smith, M.A., Zhang, B., Pan, X., 2012. Selection of Reliable Reference Genes in *Caenorhabditis elegans* for Analysis of Nanotoxicity. PLOS ONE 7, e31849.

Zhao, Z., Sheps, J.A., Ling, V., Fang, L.L., Baillie, D.L., 2004. Expression Analysis of ABC Transporters Reveals Differential Functions of Tandemly Duplicated Genes in *Caenorhabditis elegans*. J. Mol. Biol. 344, 409-417.